Title

In Search of Greener Pastures: Advancements in Modeling for Vegetation Dynamics, Climate-Driven Human Migration, and Disaster Classification

Author

Green, Rachel Kayla

Publication Date

2024

Peer reviewed|Thesis/dissertation

University of California
Santa Barbara

In Search of Greener Pastures: Advancements in Modeling for Vegetation Dynamics, Climate-Driven Human Migration, and Disaster Classification

A dissertation submitted in partial satisfaction
of the requirements for the degree

Doctor of Philosophy
in
Geography

by

Rachel Kayla Green

Committee in charge:

Professor Kelly Caylor, Chair
Professor Kathy Baylis
Dr. Chris Funk, Senior Researcher

June 2024

The Dissertation of Rachel Kayla Green is approved.

Professor Kathy Baylis

Dr. Chris Funk, Senior Researcher

Professor Kelly Caylor, Committee Chair

June 2024

In Search of Greener Pastures: Advancements in Modeling for Vegetation Dynamics, Climate-Driven Human Migration, and Disaster Classification

To Rita Green, Harry Green, Sheila Lubell, and Michael Lubell

Acknowledgements

Over the last few years, on days when lines of code broke, or I was left puzzled with results, or had to scrap projects altogether, often the only thing that kept me going was thinking about writing this section of my dissertation. And yet, as I now sit down to share my acknowledgments, I know it will be impossible to encapsulate all the support I have received throughout this journey. I'll try my best.

First, to my committee. Kelly Caylor, while your analogies only make sense half of the time, I think I speak for all of the WAVES members when I say that I appreciate your dedication to the craft. One of the first analogies I remember you mentioning is that the PhD is like a pencil - first, you start out dull with broad research interests and then gradually sharpen over time as you ask better questions. I hope I have now become a pointy pencil at this point, or perhaps even three. Thank you for the years of homemade pizza and pep talks. Understanding the world of empirical dynamic modeling has been one of the most significant intellectual challenges I have faced. Thank you for introducing me to and trusting me to pursue this work, along with encouraging me to tap into the "galaxy brain" sometimes and find interesting connections across my research. Trying to find you on campus was always a quest on its own, but once I made it to the top floor of Ellison or Bren and caught my breath, I always knew we were in for a great discussion. I am so grateful for your patience, creativity, and humor.

Kathy Baylis, I am so glad you came to UCSB and am honored to have had the opportunity to work with you. It has been such a comfort and gift to have a fellow Canadian in my corner, but beyond that, your wisdom, brilliance, and guidance are unmatched. I'm amazed by your ability to attract some of the best students from all over the world to the EDGE lab, who have now become some of my closest friends. Cheers to more days ahead of sunny hikes, followed by trips out to Los Olivos, and I'll see you one day in BC. Thank you for always reminding me that my work is making a contribution in some small way.

Chris Funk, thank you for being the reason UCSB Geography came onto my radar. Your humble leadership of the Climate Hazards Center and eager passion for connecting agroclimatological satellite records to feeding people on the ground are inspiring. I credit much of my career trajectory thus far to an attempt to mimic your energy of using data for good to help others.

Funding for my work was made possible by the National Science Foundation, the UCSB Graduate Division, the UCSB Geography Department, and the Earth Research Institute. I am deeply grateful to have been able to pursue research according to my own interests, thanks to these organizations. Thank you also to Valerie Gonzalez for your dedicated assistance during this last year of research.

Next, to friends. Bryn Morgan, what can I say – we did it, together. I'll miss having you just a few doors down whenever either of us needs a hug, but I know we will continue to have many more two or more-hour phone calls. Thank you for continuously challenging me and lifting me up. I'm so excited to see all the places you'll go. Kaili Brande, a million voice messages later, I've made it, in large part thanks to your encouragement and companionship. Here's to a million more. I'll be rooting for you all through your last year and beyond. Molly Wolfson and Greta Koumarianou, over years of laughter and tears, we have come out the other end as doctors and, I believe, lifelong friends. Thank you for helping me find myself again in the midst of a pandemic. I'm so proud of you both and look forward to more good food and company for years ahead.

Devin Gamble, words cannot describe my admiration for your perseverance and love for life – in everything from music to flowers. We've both moved from UBC to UCSB, and you've been such a strong source of support for over a decade. Thank you deeply. Lívia Costa, thank you for making me tea on overcast days, teaching me hilarious Portuguese phrases, and wearing your heart on your sleeve. Zoe Sims, your warm bowls of lovely concoctions and flowing conversations have nourished my belly and soul time and time again. Anna Boser, your enthusiasm is infectious. Thank you for making me begrudgingly do improv when I was feeling my worst and always modeling incredible confidence. Pratyush Tripathy, your ability to have everyone cracking up with laughter at a table is remarkable. I greatly applaud your "work hard, play hard" spirit. Katie McMahon, I am constantly impressed by your intelligence, kindness, and silliness and couldn't have asked for a better office mate. Fatiq Nadeem, I truly appreciate having deep discussions on life with you and having fun while at it. To my favorite geographer from across the pond, Jordan Lafayette. I am touched by your commitment to sending me funny videos every day these past few months. They have really cheered me up in the depths of writing. Nakoa Farrant, I'm so glad we both ended up at UCSB. Thank you so much for your patience as we got through the first year of coursework together. To my former WAVES lab members — Natasha Krell, Cascade Tuholske, and Ryan Avery – thank you for paving the path and offering your mentorship. I greatly admire your wonderful accomplishments.

Sally Raymond, thank you immensely for welcoming me into your home and making me feel at home for the last few years. I have learned so much from you each and every day. Thank you, Jean and Deniz, for listening to me and walking by my side as I grew into my full self.

So many others have been a part of the core memories I formed during my time here. Maya Zayne Dentzel, Kenzie Wade, Kristina Rodriguez, Ari Goldstein, Noa Cykman, Mariah Rivero, Stephanie Goldstein, Fernanda Ribeiro, and many more – thank you wholeheartedly. To those who live far away yet have cheered me on – Anna Weixelman, MJ Holec, Naomie Herpin, Erin Fitz, Kelley Lin, Helin Dura, Mischa Milne, Shalini Vadalia, Justin Santos, and Jen Goldshtein – you remain near and dear to my heart.

To everyone at Direct Relief, especially the Research and Analysis team, thank you for your support and patience while I have been completing this dissertation. I am so excited to continue living in Santa Barbara and doing meaningful work with you all.

To my family. Thank you to my parents, Brenda and David, for giving me a globe at a young age, showing me the far corners of the Earth, and encouraging me to become a scientist and a geographer. And to my brother, Josh, it is so cool to be doing our PhDs at the same time, let alone in similar fields. I was worried that you would beat me for a second, but alas, I had to finish first as the older sister.

Finally, I am profoundly grateful to have the opportunity to live in Santa Barbara, California – a beautiful place to call home and where I can think, discover, and create.

Curriculum Vitæ
Rachel Kayla Green

Professional Experience

2024 -	Data Scientist at Direct Relief, Santa Barbara, California

Education

2024	Ph.D. in Geography, University of California, Santa Barbara (UCSB) Committee: Kelly Caylor (chair), Kathy Baylis, Chris Funk
2018	B.S. in Natural Resources Conservation, University of British Columbia

Fellowships, Scholarships, and Grants

2023	Doctoral Student Travel Grant, *UCSB Academic Senate*
2018 - 2022	Jack and Laura Dangermond Travel Scholarship, *UCSB Dept. of Geography*
2018	National Science Foundation Graduate Research Fellowship
2018	University of California, Santa Barbara Central Fellowship
2018	Social Sciences and Humanities Research Council of Canada - Canada Graduate Scholarships - Master's Program (awarded but declined)
2017	Queen Elizabeth II Diamond Jubilee Green Leaders Scholarship Program Commonwealth Forests

Publications

In review	Hadunka, P., Baylis, K., **Green, R.**, Evans, T., Zimmer, A. The effect of invasive pests on food security: An understudied effect of climate change. *American Journal of Agriculture Economics.*
2022	Hannah, C., Davies, J., **Green, R.**, Zimmer, A., Anderson, P., Battersby, J., Baylis, K., Joshi, N., Evans, T. Persistence of Open-Air Markets in the Food Systems of Africa's Secondary Cities. *Cities, 124,* 103608.

2021 McCullum, A., McClellan, C., Daudert, B. Huntington, J., **Green, R.**, Ly, V., Marley, A., Tulley, N., Morton, C., Hegewisch, K., Abatzoglou, J., McEvoy, D. Satellite-Based Drought Reporting on the Navajo Nation. *Journal of the American Water Resources Association, 57(5)*, 675-691.

Oral and Poster Presentations

2023 **Green, R.**, Caylor, K. "Measuring the Sensitivity and Stability of Vegetation in Response to the Hydroclimate Across East Africa with an Empirical Dynamic Modeling Approach." European Geosciences Union General Assembly. Vienna, Austria.

2022 **Green, R.**, Baylis, K., Caylor, K. "Modeling Drivers of Internal Displacement from Climate in East Africa." American Geophysical Union Fall Meeting. Chicago, IL. Graduate Climate Conference. Seattle, WA.

2022 Tuholske, C., Latka, C., Baylis, K., Blekking, J., **Green, R.**, Kim, M., Anderson, P., Caylor, K., Funk, C. "Extreme heat impacts on food security in Africa." European Geosciences Union General Assembly. Vienna, Austria.

2021 **Green, R.**, Caylor, K. "Coupled Vegetation-Hydroclimate Dynamics Across East Africa, Drivers of Prediction Skill in Cropland Regions, and Implications for Drought Early Warning." American Geophysical Union Fall Meeting. New Orleans, LA.

2020 **Green, R.**, Caylor, K., Funk, C., Roberts, D. "Seasonal Vegetation-Hydrological Coupling across Land Covers in East Africa." American Geophysical Union Fall Meeting." Virtual.

2019 **Green, R.**, Caylor, K., Funk, C., Roberts, D., McNally, A. "Drought Projection and Modeling Causal Feedbacks with Earth Observations in East Africa." American Geophysical Union Fall Meeting. San Francisco, CA.

2018 McCullum, A., **Green, R.**, McClellan, C., Schmidt, C. "Satellite-based Drought Reporting on the Navajo Nation: Utilizing Ground Measurements and NASA Earth Observations to Inform Management Decisions." NASA Applied Sciences Water Resources Meeting. Boulder, CO.

Invited Workshops

2022	Environmental Justice and Interventions Workshop, University of California, Santa Barbara (co-organizer)
2021	Complexity Interactive Program - Santa Fe Institute
2020	Complex Systems Summer School - Santa Fe Institute (postponed)
2018	NASA Summer School on Satellite Observations and Climate Models - NASA Jet Propulsion Center for Climate Sciences and the Keck Institute for Space Studies
2017	Indigenous Communities: Promoting Social and Ecological Sustainability in the Face of Climate Change - National Socio-Environmental Synthesis Center

Research Positions

2022-2024	**Graduate Student Researcher,** Earth Research Institute, UCSB Mentor: Dr. Kelly Caylor
2022-2023	**Graduate Student Researcher,** Environment Markets Lab, UCSB Mentor: Dr. Tamma Carleton
2018 - 2024	**Associate Researcher,** Climate Hazards Center, UCSB Mentor: Dr. Chris Funk
2017 - 2018	**Associate Researcher,** Bay Area Environmental Research Institute, NASA Ames Research Center, Moffett Field, CA Mentors: Dr. Amber Jean McCullum and Dr. Cindy Schmidt
2017	**Affiliate Researcher,** Spatial Informatics Group, LLC/University of San Francisco, San Francisco, CA Mentor: Dr. David Saah
2017	**Researcher and Team Lead,** NASA DEVELOP National Program, NASA Ames Research Center, Moffett Field, CA
2017	**Affiliate Researcher,** Department of Forest and Wood Science, Stellenbosch University, Stellenbosch, South Africa

Mentor: Dr. Pierre Ackermann

2016 - 2017 **Research Assistant,** Belowground Ecosystem Group/Mother Tree Project, Department of Forest and Conservation Sciences, University of British Columbia, Vancouver, Canada
Mentor: Dr. Suzanne Simard

Teaching

Summer 2022 **Teaching Assistant,** Land, Water, and Life, UCSB

Summer 2022 **Teaching Assistant,** Maps and Spatial Reasoning, UCSB

Spring 2022 **Teaching Assistant,** Research Methods in Geography, UCSB
Professor: Dr. Dan Montello

Fall 2021 **Teaching Assistant,** World Regions, UCSB
Professor: Dr. David Lopez-Carr

Community Outreach and Service

2022 - 2023 **Graduate Mentor,** Graduate Scholars Program, UCSB

2018 - 2023 **Representative,** University Center Governance Board, UCSB

2018 - 2021 **Editorial Board Member,** Journal of Environment and Development

Field Experience

2019 Urban food security survey, Kenya

Languages and Software

Spoken French (intermediate)

Computational Python, R, ArcGIS, QGIS, MATLAB, Git, LaTeX

Abstract

In Search of Greener Pastures: Advancements in Modeling for Vegetation Dynamics, Climate-Driven Human Migration, and Disaster Classification

by

Rachel Kayla Green

Climate change and its associated environmental impacts pose immense challenges that require innovative approaches to address. This dissertation presents three distinct studies that showcase the application of advanced modeling and machine learning methods to investigate critical issues at the intersection of changing human and natural systems. In Chapter 2, I employ a novel modeling framework to analyze the complex relationship between vegetation dynamics and hydroclimate variability across East Africa. Empirical dynamic modeling is a data-driven approach for studying state-dependent dynamics and interactions within complex systems, enabling the identification of key driving variables and the prediction of future system behaviors. Adopting this method, the study provides insights into how the stability and vulnerability of ecosystems vary with environmental conditions, land cover type, and seasonality. In Chapter 3, I explore how various factors contribute to human displacement, focusing on the environmental drivers and mechanisms of migration in Somalia. Gravity models are a class of spatial interaction models that estimate the flow or movement between locations based on the attractiveness of the destinations and the impedance between the origin and destination. I use these models to examine the connections between climate, socio-economic, and political factors influencing population movements. Notably, I find that livelihood is an important differentiating factor in determining whether the climate strongly impacts individuals' migration patterns. In Chapter 4, I implement advanced natural language processing

techniques to develop an automated system for classifying global multi-hazard disaster events from humanitarian news articles and reports. Large language models are a form of artificial intelligence and deep learning that can process, understand, and generate human language by learning from vast amounts of textual data, enabling them to perform a wide range of natural language processing tasks. By employing these models, the study demonstrates the potential of emerging technologies in improving the efficiency of disaster information retrieval and response. With a geographical framework that unifies perspectives from environmental, social, and computer science, these chapters collectively contribute to developing data-driven solutions for understanding environmental stressors.

Contents

Chapter 1

Introduction

The escalating impacts of climate change and the rapid advancement of technology are transforming the world as we know it, presenting both challenges and opportunities for natural systems and human societies. As we face increasingly volatile climate patterns and their cascading effects, there is a pressing need to think creatively, beyond traditional disciplinary boundaries, to meet extraordinary future uncertainties. Mitigating unprecedented challenges requires adopting new analytical tools and innovative methods to deepen our understanding of the complex mechanisms governing the interactions between environmental and human dynamics. In this dissertation, I explore critical aspects of this understanding: how dynamical models can provide new perspectives on how vegetation responds to environmental fluctuations, how push-and-pull factors such as extreme weather patterns can compel certain human populations to migrate, and how emerging technologies like large language models can aid in disaster informatics.

This dissertation is structured into three main chapters, each dedicated to addressing a unique aspect of the connections between environmental changes and their broader impacts. Chapter 2 explores the complexities of vegetation dynamics in East Africa, Chapter 3 examines human displacement drivers in Somalia, and Chapter 4 applies advanced artificial intelligence (AI) technologies to classify and manage disaster-related data.

I begin my research on the African continent, which is recognized as one of the regions most susceptible to climate change, resulting in droughts, agricultural losses, and limited water resources (Pricope et al., 2013). In East Africa, temperature, evapotranspiration, and hydrological extremes are anticipated to continue increasing into the future (Gebrechorkos et al., 2023). These shifting patterns will deeply impact the livelihoods of the approximately 80% of East Africans who depend on rain-fed agriculture (Kalisa et al., 2019). Yet, the extent to which hydroclimatic characteristics influence the spatiotemporal heterogeneity of vegetation dynamics is a contested area of research. In Chapter 2, I take on this debate by comparing the sensitivity and stability of East African croplands to other vegetation types with respect to land surface temperature, precipitation, evapotranspiration, and soil moisture. Ecosystems exhibit state dependency, or non-linearity, which means that their response to environmental factors is not always directly correlated or predictable. This aspect can make it challenging to comprehend and model ecosystem behavior using traditional statistical methods, which often assume linear relationships between variables (Chang et al., 2017). Instead, I interpret vegetation-hydroclimate dynamics using Empirical Dynamic Modeling (EDM), an alternative equation-free approach that can accommodate interdependent effects (Ye et al., 2015). Introducing this new method for measuring vegetation predictability, this study investigates the characteristics of ecosystems that exhibit strong resilience. I also consider the underlying mechanisms that enable these systems to maintain stability in the face of environmental perturbations.

Narrowing the scope of my analysis to Somalia, my next study shifts attention toward environmental impacts on human well-being. In this arid country, environmental changes such as water scarcity, land degradation, aridity, soil constraints, and changes in cropland

and pasture areas play consequential roles in influencing livelihood adaptive strategies, which in certain cases manifest as migration (Neumann et al., 2015). In Chapter 3, I tie the diverse patterns of migration motivations with time and location-specific environmental, socio-economic, and political conditions. I use a gravity model approach to understand the various drivers of historical migration flows in Somalia. My contribution to the growing literature on environmentally induced displacement lies in my approach to investigating the mechanistic processes that drive migration decisions. By examining livelihoods as important pathways that differentiate individuals' decisions and abilities to migrate, I offer new insights into the relationship between environmental factors and human mobility (Griffith et al., 2023).

In Chapter 4, I zoom out to the global landscape, focusing on how we can better detect and build contextual knowledge around extreme disaster events. When disasters strike, emergency responders must quickly search vast amounts of media to find crucial information, which can delay and complicate their response (Imran et al., 2020). Monitoring and gaining situational awareness can be challenging, particularly when multiple disaster events occur simultaneously or in sequence (Tamagnone et al., 2023). In these cases, it is essential to treat events not as isolated incidents but as intertwined within a broader system of instability and damage. Large language models (LLMs), which are AI-powered systems trained on extensive amounts of text data to understand language, can expedite disaster information synthesis and serve as a tool for emergency decision support (Chen et al., 2023). I test the ability of LLMs to perform a multi-label classification task of identifying multiple disaster types from humanitarian news articles. In doing so, I examine the prospects and shortcomings of AI-led information retrieval for the disaster risk management field.

Chapter 2

Measuring the Sensitivity and Stability of Vegetation in Response to the Hydroclimate Across East Africa with an Empirical Dynamic Modeling Approach

Abstract Hydroclimatic factors influence vegetation growth in East Africa, but the nature of this relationship varies by land cover type. Using approximately 20 years of satellite records, this study investigates the differences in vegetation dynamics between croplands and other land cover types. Employing Empirical Dynamic Modeling (EDM), a data-driven approach that uses observational time series data to model and predict complex systems by capturing their interconnected relationships, I evaluate the predictability of vegetation dynamics. This is achieved by analyzing the Normalized Difference Vegetation Index (NDVI) in relation to fluctuations in precipitation, soil moisture, evapo-

transpiration, and land surface temperature across different land cover types, including croplands, shrublands, grasslands, and woodlands.

The findings reveal spatial differences in NDVI predictability, with regions near the equator showing less predictability due to erratic rainfall and high aridity. Woodlands exhibit the strongest predictability across the region among the land cover types, while grasslands show the most variable outcomes. Croplands and shrublands are closely aligned in their predictability on average, though there is wide variation across the region. The study emphasizes that both physiological features (uptake and storage capabilities) and environmental conditions (rainfall seasonality and aridity) play a crucial role in determining the consistency of vegetation within and across types on an interannual basis.

Short-term vegetation dynamics (one-month lead) can be predicted with high accuracy from multi-year records, but predictability diminishes as the lead time is extended to four or six months, at which point seasonality becomes the dominant influence. A key insight from this study is the enhanced understanding of the interaction between vegetation and land surface temperatures, which has implications for effective agriculture production and efficient water management.

This research contributes to the growing application of EDM in biogeosciences and lays the groundwork for using historical satellite observations to anticipate future environmental shifts, particularly in light of East Africa's vulnerability to climate change and increasing agricultural demands.

2.1 Introduction

Drylands are critical ecosystems that cover approximately 41% of the Earth's land surface (Prăvălie, 2016). These regions support 38% of the world's population, encompass 44% of cropland areas, and host 20% of plant biodiversity hotspots (Huang et al., 2017;

Maestre et al., 2021), underscoring their significance in sustaining human well-being, agricultural production, and ecological diversity. However, drylands are also fragile environments that experience highly variable climates and low water availability. Under a changing climate, these regions are expected to face further challenges, with projections indicating a reduction in mean annual precipitation and an increase in the frequency of extreme precipitation events (Tietjen et al., 2010).

East Africa's drylands, in particular, have been identified as an area of heightened risk for experiencing the adverse effects of environmental change. This can be observed in the form of vegetation productivity decline, land degradation (Wei et al., 2018), intensified hydrological extremes (droughts and floods), and increasing temperatures (Gebrechorkos et al., 2023). According to the Shared Socioeconomic Pathways emission scenarios, most of East Africa is expected to experience increased precipitation in the coming decades. However, arid and semi-arid areas will likely receive less rainfall, while the highlands and lake regions are expected to receive more precipitation (Ayugi et al., 2022). The majority of people in East Africa (approximately 80%) depend on rain-fed agriculture for their livelihood (Kalisa et al., 2019). Short and long-term fluctuations in vegetation productivity driven by climate variability cause significant socioeconomic disruptions and affect the natural resource management strategies of farmers, fishers, and pastoralists (Conway et al., 2005). Understanding vegetation dynamics in East Africa, including stability, sensitivity, and predictability, or the degree to which behaviors can be anticipated, is essential for mitigating the impacts of environmental change on the region's ecosystems and livelihoods.

Increasing environmental pressures stress the importance of understanding how these shifts will alter the functioning of dryland vegetation. Numerous studies have sought to determine the relative influence of factors such as precipitation (Maurer et al., 2020), soil moisture (D'Odorico et al., 2007), and temperature (Chen et al., 2019) on vegetation sensitivity and variability. For instance, Chen et al. (2019) find that increasing interannual variability of global vegetation greenness is primarily driven by changes in temperature, solar radiation, and precipitation, leading to a decrease in vegetation stability and an increase in sensitivity to environmental disturbances, particularly in arid regions. In global drylands, interannual precipitation variability has been shown to have a negative effect on aboveground net primary production (ANPP), with dry years decreasing ANPP and wet years increasing ANPP (Gherardi and Sala, 2019).

These elements act differently in driving dryland vegetation dynamics depending on species composition, seasonality, and other localized factors. According to a study conducted in a semi-arid region of the United States by Thoma et al. (2016), water balance variables significantly influence vegetation greenness during most growing season months more than climate variables. The importance of certain factors on greenness shifts seasonally, with antecedent water input and storage being the primary factor in the spring, drought indicators in the summer, and antecedent soil moisture availability in the fall. In the arid to sub-humid zones of Sub-Saharan Africa, the productivity of vegetation is affected by climate variability. Higher temperatures and humidity, as well as less consistent rainfall, can impact the availability of water and nutrients for the vegetation, which affects their overall growth and physiological processes (Rishmawi et al., 2016).

There is a discrepancy, however, in vegetation response to environmental variability over time and space (Sohoulande Djebou et al., 2015; Measho et al., 2019). This may be due to non-linear feedbacks (Hsu et al., 2012), such as those between soil moisture recharge and increased precipitation (Rishmawi et al., 2016) or when critical thresholds of drought are crossed that impair vegetation functioning (Li et al., 2023b). Linear regression methods of describing the variability in precipitation or other hydroclimatic variables and vegetation production (e.g., Chamaillé-Jammes and Fritz (2009)) may mischaracterize and oversimplify these complex relationships. Furthermore, many studies on dryland vegetation dynamics are focused on particular vegetation types or make assumptions about functional relationships. Others follow conceptual and methodological designs that are too intellectually specialized, which can hinder the generalizability of their outcomes and approaches to other contexts.

Causal inference methods, such as structural equation modeling, can help identify key drivers or factors that influence the behavior of the Earth system. These techniques can also be used to evaluate the performance of physical models and their assumptions (Runge et al., 2019a). Several methods related to causal inference have been applied to Earth system sciences. First, Granger Causality (GC) relies on the predictability of one time series based on the past values of another, assuming linearity and stationarity in the data. The approach is applied by (Papagiannopoulou et al., 2017), who introduce a non-linear GC framework to investigate climate-vegetation dynamics, motivated by the limitations of traditional linear methods in capturing the complex relationships between climate and vegetation, particularly in water-limited regions. Tuttle and Salvucci (2016) also use GC to determine divergent patterns in the soil moisture-precipitation relationship over the contiguous United States, which could be attributed to regional aridity. Yet, one constraint of GC is the necessity for variables to be separable. Its applicability becomes less clear in deterministic systems that exhibit weak to moderate coupling, a trait frequently observed in ecosystem dynamics. This can lead to inconclusive results when examining interconnected systems (Sugihara et al., 2012).

Another method, the Peter-Clark Momentary Conditional Independence (PCMCI) algorithm, tests for causal relationships by examining conditional independence among variables. PCMCI is suitable for high-dimensional time series with potential non-linear relationships where the dependency structure is represented in a graphical model (Runge et al., 2019b). While the method has been applied to study the interactions and feedback between atmospheric and biospheric variables (Krich et al., 2019), understanding the PCMCI model outputs can be challenging due to its technical nature, which involves advanced statistical and information theory concepts.

In this study, I consider an alternative approach known as Empirical Dynamic Modeling (EDM), which is a method of viewing dynamic relationships between variables from data as part of a system without relying on theoretical assumptions (Chang et al., 2017; Fogarty and Collie, 2020). The "dynamical systems" view sees ecosystems as composted of interconnected variables such as species or environmental drivers, each represented in a changing "state space," where the ecosystem's condition is a moving point. This approach reveals that what appears as random "noise" may actually be predictable patterns influenced by overlooked factors, and the system's behavior is traced as a trajectory that eventually converges to a stable set of conditions known as the "attractor" (Munch et al., 2020). EDM avoids the need for a parametric model and observations of all variables in a system (Munch et al., 2023), presenting instead a more holistic perspective of ecosystems as being composed of inseparable state variables (otherwise known as coordinates or dimensions).

I use EDM to analyze vegetation productivity predictability (or the interannual consistency) and the strength of causal relationships driving dryland vegetation dynamics across East Africa. Utilizing two decades of remotely sensed observations, I explore the spatiotemporal differences in how hydroclimatic elements, including precipitation, land surface temperature, soil moisture, and evapotranspiration, influence vegetation greenness via the Normalized Difference Vegetation Index (NDVI). I conduct a detailed analysis of how NDVI predictability due to environmental conditions varies between different land cover types. In particular, I distinguish between managed vegetation (i.e., croplands) and unmanaged vegetation (i.e., woodlands, shrublands, and grasslands). I then focus on how different characteristics, including the prediction interval, latitude, rainfall seasonality, and aridity, affect cropland predictability.

Earth observation data are increasingly used to explore the interrelationships between environmental dynamics. For instance, Pérez-Suay and Camps-Valls (2019) propose a methodology for observational causal inference in bivariate scenarios within geoscience and remote sensing. They present a specific application for vegetation parameter modeling, emphasizing the significance of understanding complex interactions governing Earth's systems. Their approach utilizes regression models and dependence estimation to identify causal relationships from observational data.

This study contributes to the growing body of work in biogeosciences and hydrometeorology using the EDM framework. One extension of EDM is the Convergent Cross Mapping (CCM) approach, which infers causality by predicting one variable's state based on another. CCM assumes underlying dynamical and non-linear system interactions and requires time series data that capture the system's dynamics for state-space reconstruction (Sugihara et al., 2012). Wang et al. (2018) use CCM to detect causal and non-linear relationships between soil moisture, evapotranspiration, and precipitation. They find an optimal lag for the effect of soil moisture on precipitation of one month, which then substantially decreases in impact after four months, indicating the potential for sub-seasonal precipitation prediction, especially in semi-arid and semi-humid regions. Ombadi et al. (2020) apply CCM to analyze causal drivers of evapotranspiration rate in shrubland regions, including net radiation, vapor pressure deficit, soil water content, air temperature, soil temperature, and wind speed. The study also reveals the relative contributions of these drivers across seasons. Shi et al. (2022) present a novel approach to determine the propagation time of drought from meteorological to hydrological phases. The study challenges conventional correlation analyses, favoring CCM for assessing causality using observational data. Finally, Sasaki et al. (2023) study dryland sensitivity to climate change in Mongolia using EDM and CCM to detect causal effects on ANPP. They find that

ANPP is greatly influenced by annual precipitation, temperature, and aridity, including their variability. The study stresses the necessity of considering non-linear relationships to accurately predict biosphere feedback to the climate system.

I also build upon previous studies that have measured the predictability of NDVI signals using traditional, non-dynamical systems methods. Martiny et al. (2010) perform linear multiple regression models with ocean and atmospheric predictors to estimate and predict regional NDVI interannual variability in semi-arid African regions. Linear statistical models, though simple and interpretable, can face difficulties in capturing the complexities of climate-vegetation interactions. One of the main challenges is their assumption of linearity, which oversimplifies complex interactions. Additionally, identifying key predictors can be difficult. Linear models also have limited adaptability to changing conditions and assume predictor independence. Moreover, these models may not be adequate in interpreting mechanisms. To address these limitations and improve understanding of NDVI predictability, researchers have explored advanced modeling techniques such as non-linear models, machine learning algorithms, or integrated statistical-dynamical models to provide a more comprehensive representation of the relationships between climate variables and vegetation dynamics. For instance, Jiang et al. (2016) apply several methods, including Mann-Kendall, Thiel-Sen slope, correlation analysis, linear regression, and Artificial Neural Network-Genetic Algorithm (ANN-GA) to test the lag effects of climatic variables (precipitation and temperature) on vegetation productivity in Canada. They find the non-linear model (ANN-GA) performed better than using linear (regression) models and discover spatiotemporal variability in NDVI predictability. Mangiarotti et al. (2010) study the predictability of NDVI in West Africa, employing EDM-like methods of embedding the NDVI time series into a pseudo-phase space to reconstruct the local attractor of vegetation dynamics. By extracting various geometric parameters and statical estimates associated with the attractor, they estimate how the horizon of predictability for vegetation dynamics varies due to factors like local stability and land use practices. Mangiarotti et al. (2012) later conducted a similar study that tests the importance of resolution in predicting vegetation cycles, finding that longer prediction horizons and lower resolutions are needed to achieve higher accuracy.

While NDVI projections and forecasts are insightful and useful for applications in agriculture, food security, and water resource management, the objective of this study is not to improve them directly. Several authors have made progress in this pursuit. Funk and Brown (2006) use a statistical model that projects NDVI changes over short time scales (1 to 4 months) in semi-arid Africa by incorporating precipitation and relative humidity as environmental drivers. Using robust geostatistics to predict time-integrated NDVI in Australia, Pringle (2013) demonstrate a means of discriminating between cropping and grazing areas, quantifying prediction uncertainty, and addressing outliers. An experimental tool called VegOut-Ethiopia predicts NDVI conditions in Ethiopia through multiple linear regression equations with indices describing droughts, oceanic/atmospheric interactions, and biophysical characteristics (Tadesse et al., 2014). Asoka and Mishra (2015) developed a predictive multiple linear regression model with NDVI, soil moisture, and the El Niño-Southern Oscillation (ENSO) Index, which revealed good skill in forecasting NDVI anomalies in India at a 1-month lead time. Last, Tian et al. (2019) used NDVI data and an ecohydrological model to analyze arid to moderately humid regions globally. The findings reveal that larger accessible water storage leads to improved forecast skill decay, enabling three-month advance forecasts of vegetation conditions in global drylands, particularly in dry climatic zones with higher dryness values.

In the following sections, I will explain the EDM framework and its implementation more thoroughly. The findings demonstrate how vegetation predictability varies between and within land cover types. I will then discuss the possible mechanisms that can determine the spectrum of ecosystem responses to interannual climate variability. Finally, I reflect on the suitability of EDM as an approach for ecohydrological applications.

2.2 Methods

2.2.1 Study Area

East Africa, the region comprising the countries of Burundi, Djibouti, Eritrea, Ethiopia, Kenya, Rwanda, Somalia, South Sudan, Sudan, Tanzania, and Uganda, is home to 457 million people who are reliant on bimodal rainfall seasons – long rains (March-May) and short rains (October-December) (Palmer et al., 2023). These rainfall patterns in East Africa exhibit significant spatio-temporal heterogeneity, which has cross-sectoral impacts on agriculture, food security, water resources, energy production, and population health in the region (Funk et al., 2008; Palmer et al., 2023). Referred to as the "East African Climate Paradox," the decline in the long rains contrasts with climate projections of a wetter future for the region (Lyon and Vigaud, 2017; Walker et al., 2020). Rainfall season frequency, timing, intensity, and duration vary based on the interactions between the shifting movement of the Intertropical Convergence Zone, the Indian Ocean Dipole, and the El Niño Southern Oscillation (Palmer et al., 2023; Wei et al., 2018). During the long rains, which feed the main crop-growing season, the vegetation shows less interannual variability compared to the short rains (Kalisa et al., 2019). Semi-arid areas within the region experience an average annual rainfall of less than 800 mm compared to 800 to 1300 mm of rainfall per year in sub-humid areas (Kalisa et al., 2019). Agriculture is a major source of livelihood, with smallholder farmers relying mainly on rain-fed crops, accounting for upwards of 90% of the total production. (Adhikari et al., 2015). The dominant biomes in East Africa include forest, wet and dry miombo (deciduous woodland), bushland/thicket, and grassland/shrubland (Nicholson et al., 1990). Population pressure and increased land use activity have resulted in biodiversity decline, deforestation, and degradation (Pfeifer et al., 2013).

2.2.2 Data

To capture the complex interactions of the land-atmosphere system across East Africa, I examined five critical components: vegetation condition, land surface temperature, precipitation, evapotranspiration, and soil moisture. Looking at records between July 1, 2002, and July 31, 2021, I resampled each remotely sensed image to a spatial resolution of 0.05 degrees using bilinear interpolation and composited them to dekadal (∼10-day) periods.

Vegetation Condition

The Normalized Difference Vegetation Index (NDVI) is a widely used proxy measurement of photosynthetic activity as well as the greenness, condition, or density of vegetation (Cao et al., 2013; Hawinkel et al., 2016). NDVI is calculated from the near-infrared (NIR) and red bands of multispectral sensors with the formula NDVI = (NIR - RED)/(NIR + RED), and values range from -1 to 1. I use the U.S. Geological Survey's Earth Resources Observation and Science (EROS) Center Moderate Resolution Imaging Spectroradiometer (eMODIS) NDVI product, which was developed for operational land monitoring applications that necessitate near-real-time NDVI data as well as historical trend information for temporal anomaly detection (Brown et al., 2015). The NDVI maximum-value products are available at dekadal intervals at 250-meter resolution from 2002 to 2022. The eMODIS product is utilized by the Famine Early Warning Systems Network (FEWS NET) to monitor vegetation conditions across major food-insecure regions worldwide. NDVI and anomaly maps are generated with a temporal smoothing algorithm on raw MODVIS NDVI composites (Swets et al., 1999). A cloud and atmospheric contamination correction is also applied to the finalized product to ensure quality.

Land Surface Temperature

The MODIS/Aqua Land Surface Temperature/Emissivity version 6 product (MYD11C1) provides daily global land surface temperature (LST) and emissivity values in a 0.05-degree Climate Modeling Grid (CMG) (Wan, 2014). The MYD11C1 product is derived directly from the MODIS LST/Emissivity (MYD11B1) 6 km SIN Grid and are available from 2002 to the present.

Precipitation

The Climate Hazards Center InfraRed Precipitation with Station (CHIRPS) Precipitation dataset provides 30+ years of quasi-global rainfall data, available at monthly, dekadal, pentadal, and daily time intervals (Funk et al., 2015). CHIRPS spatial coverage spans from 50°S-50°N (over all longitudes), and the data record extends from 1981 to the near present. CHIRPS data have a 0.05-degree native spatial resolution. Satellite data are calibrated with in situ station data to create gridded rainfall time series appropriate for trend analysis and seasonal drought monitoring. The creation of CHIRPS has supported drought monitoring efforts by FEWS NET and organizations worldwide.

Evapotranspiration

The Global Reference Evapotranspiration (refET) product, developed by the National Oceanic and Atmospheric Administration (NOAA) primarily for the FEWS NET community, aims to improve drought and famine early warning in food-insecure countries (Hobbins et al., 2018). refET is estimated using the FAO model of the Penman-Monteith refET, driven by radiative and meteorological forcings from NASA's Modern-Era Retrospective Analysis for Research and Applications (MERRA-2) reanalysis dataset. The refET output is spatially downscaled to match subgrid variability provided by the International Water Management Institute (IWMI) monthly climatological refET grids. The resulting product covers the globe at a 0.125-degree spatial resolution and is available from 1980 to present.

Soil Moisture

The FEWS NET Land Data Assimilation System (FLDAS) Soil Moisture product is an output from a custom instance of the NASA Land Information System (LIS) framework (McNally et al., 2017). The FLDAS multi-model and multi-forcing estimates of hydro-climate conditions contribute to FEWS NET operations. Soil moisture percentiles are calculated using soil moisture outputs from the Noah Land Surface Model (Noah) and Variable Infiltration Capacity (VIC) simulations. In this study, I use the 0-10 cm depth soil moisture dataset. Data are available from 2000 to the present at 0.1-degree spatial resolution.

Land Cover

The European Space Agency Climate Change Initiative Land Cover (ESA-CCI LC) dataset is a 300 m global land cover product produced annually since 1992. The product merges multiple available Earth observation products based on the GlobCover products of the ESA (Defourny et al., 2017). There are 37 land cover types identified in the dataset, classified using the Land Cover Classification System developed by the Food and Agriculture Organization (FAO). In this analysis, I use the land cover map from 2016 and focus on the five dominant land cover types in East Africa: broadleaved open deciduous forest (15-40%) (referred to as woodland forest hereafter), cropland rainfed,

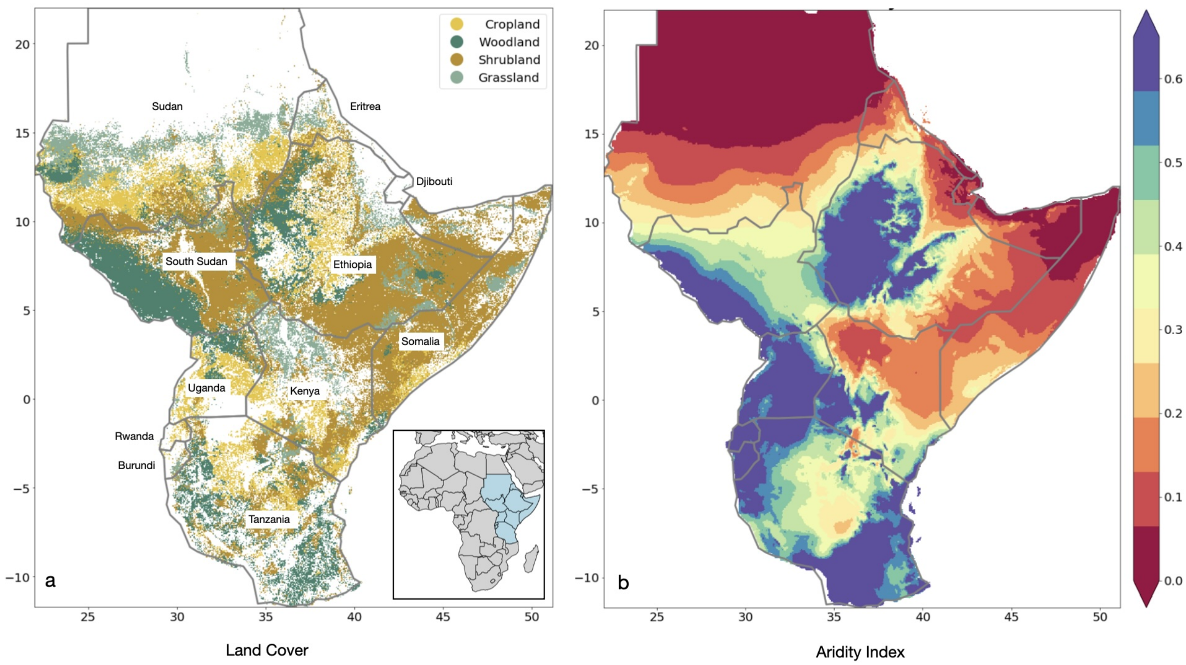

Figure 2.1: (a) Primary vegetation land covers in East Africa – cropland, woodland, shrubland, and grassland, with a subset map of the study countries highlighted within Africa. (b) Aridity Index values, where areas below 0.2 are classified as arid, 0.2 - 0.5 are semi-arid, 0.5 - 0.65 are dry sub-humid, and > 0.65 are humid.

cropland irrigated, grasslands and shrublands. The dataset was resampled to 0.05 degrees to match the spatiotemporal resolution of the environmental variables. The land cover distribution across East Africa is shown in Figure 2.1(a).

Aridity

I derive aridity measurements from the Global Aridity Index and Potential Evapotranspiration (PET) Climate Database-Version 2. The global high-resolution (30 arc-seconds) data represent the average aridity over the 1970-2000 period (Trabucco and Zomer, 2019). The aridity index is the ratio of mean annual precipitation to mean annual reference evapotranspiration. It measures moisture availability for the potential growth of reference crops or other vegetation types. As an index, the aridity can be interpreted across ecosystems. A map of the Aridity Index for East Africa is shown in 2.1(b).

2.2.3 Empirical Dynamic Modeling

Empirical Dynamic Modeling (EDM) is a data-driven approach for non-linear system analysis and prediction that can be used to study the behavior of such complex systems. The method uses time-series data to generate an attractor, or reconstructed state space known as the "shadow manifold" from one or more observable variables to represent a system's dynamic states over time. The applications of EDM span multiple disciplines. It has been shown that complex dynamics can be effectively detected and predicted in a wide range of disciplines, including neuroscience (Natsukawa and Koyamada, 2017; Schiecke et al., 2015), epidemiology (Deyle et al., 2016; Nova et al., 2019), and climate (van Nes et al., 2015). Within the field of ecology, researchers have implemented EDM to uncover phenomena including population abundance and recruitment (Nakayama et al., 2018; Ye et al., 2015), regime shifts (Scheffer et al., 2009), and spatial synchrony (Clark et al., 2015).

Time-Delayed Embedding

A foundational concept in EDM is time-delayed embedding, which is an advanced analytical technique for examining complex, non-linear systems. By reconstructing the state space, it becomes feasible to identify patterns, commonly known as attractors, which signify stable cycles within the system. With historical observations, it is possible to make predictions about a system's potential trajectories and anticipate future states. This technique draws from Takens' embedding theorem, which postulates that a scalar time series can be transformed into a multidimensional space from a sequence of time-delayed iterations as new dimensions (Takens, 1981). This reconstruction process retains the system's core properties and can provide valuable insights into its inherent dynamics and interactions that underlie its behaviors.

Simplex Projection

Simplex projection is a mathematical method of non-parametric analysis that can be used in ecological and environmental sciences to measure the predictability of complex systems from time series data (Sugihara and May, 1990; Sugihara et al., 2012). Following the concept of time-delayed embedding, the simplex projection algorithm rests on the notion that the behavior of a system can be predicted from the cycles and relationships observed in historical data. The approach avoids the need to model any core equations or processes explicitly. Instead, one constructs a high-dimensional state space manifold by embedding the time series of multiple variables hypothesized to influence a target variable. The embedding is typically done using time delay coordinates, which capture the temporal dependencies among the variables. From state space reconstruction, the simplex projection algorithm estimates the system's trajectory into a lower-dimensional simplex, representing a probabilistic estimate of the system's future states. The position of the target variable within the simplex reflects its predictability and relationships with the other variables. By comparing the observed and predicted positions of the target variable, it is then possible to evaluate the accuracy and skill of the projection.

Several steps are involved in the computation of predictability with simplex projection. The observed time series is first transformed into a reconstructed state space with time-delayed embedding in a single variate analysis. An alternative multivariate approach uses several variables that provide additional information that may improve the predictive skill of a target variable. In this case, the embedded state spaces of the target and candidate variables are combined into a single state space manifold. At each point in the manifold, the algorithm selects a set of nearest neighbors that exhibit similar positions and dynamics to the target prediction point. The embedding dimension defines the number of nearest neighbors. Next, the future value of a target variable is calculated with a weighted linear regression of the nearest neighbors, where the weight is determined by its distance to the target point to account for non-linear relationships that may exist in the system. Finally, the simplex projection's predictive skill is evaluated with a leave-one-out cross-validation. Performance is commonly measured with the correlation coefficient (ρ), root-mean-square error (RMSE), or mean absolute error (MAE). Figure A.1 demonstrates simplex projection with a singular time series in its original form (before time-delayed reconstruction), where historical trajectories can be used to predict future states.

Convergent Cross Mapping

Convergent Cross Mapping (CCM) extends the time-delay embedding paradigm, introduced by Sugihara et al. (2012) for observation-based causal exploration[1]. The theorem posits that one can reconstruct a dynamical system manifold M, using the lagged time series of a single variable, otherwise referred to as the shadow manifold, that is diffeomorphic (topologically equivalent) to the true manifold (Ombadi et al., 2020; Takens, 1981). Following Takens' theorem (Takens, 1981), this shadow manifold M_x can be constructed by creating three time-lagged copies of one variable, $X(t)$, $X(t-\tau)$, and $X(t-2\tau)$) where τ represents one time step. At each time interval, $m(t)$, there is a unique corresponding point from M and M_x. A complimentary "shadow manifold" can also be reconstructed from other dimensions or variables making up M. Multivariate CCM allows for three time series of distinct variables (X, Y, Z) to be cast into a manifold

[1] In the time-series literature, causality is often defined as a phenomenon "A" that consistently precedes another outcome, "B". This terminology does not mean 'causal' in the traditional sense that "A" 'causes' "B." In this paper, I will use the terminology common to the time-series literature.

whereby each time point, $m(t)$, is comprised of the coordinate values of the three time series: $m(t) = [X(t), Y(t), Z(t)]$ (Shi et al., 2022). If X and Y, for instance, produce a one-to-one mapping, meaning for each t, there is a singular point correlated between $Mx(t)$ and $My(t)$, they are known as mutual neighbors. The manifolds display topological isomorphism (correspondence) as the two shadow manifolds cross-map onto one another (Figure A.2). As demonstrated in Figure A.3, for bidirectional causality to occur, X and Y must share an original manifold, and at each t, both X and Y reflect one another. For a unidirectional causality, the information from Y, for instance, can only be retrieved from the information of X, but not vice versa (Shi et al., 2022).

To determine cross-mapping skill, the nearest neighbors of the shadow manifold of one variable, X, and their Euclidean distances to points on Mx_t are measured to locate each contemporaneous point between both manifolds (Ombadi et al., 2020). Sufficient samples (i.e., library length) of X and Y are necessary so that the manifolds are dense enough to detect corresponding nearest neighbors. As the number of samples increases, the correlation coefficient ρ between observed and estimated values will stabilize (Shi et al., 2022). If unidirectional causality is present, one of the variables is expected to converge close to zero. In contrast, in the case of bidirectional forcing, the two variables will converge faster or reach a higher plateau at a certain value (Schiecke et al., 2015). Relative causal strength of one variable over another can be resolved by the difference in cross-map skill (Sugihara et al., 2012).

2.2.4 Model Implementation

Cross-year examination of NDVI's cyclical consistency from a state space perspective

The variation in NDVI within and between years can be explored using time-delayed embedding. The two key parameters required when transforming a single-variable time series into a multi-dimensional phase space are the time delay (τ) and embedding dimension (E). Time delay refers to the intervals between points in the generated delayed copies that construct the phase space. The embedding dimension determines the dimensions in the reconstructed phase space (Chang et al., 2017).

When applying time-delayed embedding to NDVI time series, the change in magnitude of NDVI distributions per time interval over multiple years can be observed. Manifolds in EDM transform complex system structures into lower dimensions using state variables, retaining phase space topology. With one sample NDVI time series, I constructed a manifold with an embedding dimension (E) and time delay (τ) of one dekad, forming a three-dimensional structure of the original time series and two lagged copies.

I calculated the convex hull of the outermost points in the manifold to measure the variability in NDVI from year to year for any given dekad. I chose to use the convex hull as it provides a single metric that is easy to understand and is not affected by the specific structure created by the manifold. By comparing measurements associated with different dekads, it is possible to visualize how the consistency of NDVI influences the predictability of future behavior at different points in the year.

Measuring NDVI predictability between land covers

I applied the simplex projection algorithm to the time series of all vegetated land cover pixels in East Africa to evaluate NDVI's predictive capability under varying environmental conditions. All EDM analysis from this point was computed using the pyEDM Python package.

My approach – using a large cohort of time series data throughout the study region – marks a departure from prior research, which has predominantly relied on singular, aggregated time series to measure the dynamics of specific systems. By analyzing patterns across hundreds of thousands of pixels, my research reveals the spatial heterogeneity and variance in ecosystem dynamics across different land covers. I calculated the predictive skill of NDVI for each pixel, using a range of embedding dimensions (1 - 10 dekads) and prediction intervals (3 - 18 dekads) to identify the optimal configurations that best characterize the regional NDVI patterns. I then ran multivariate simplex projection with several model inputs consisting of historical NDVI time series data alongside two ancillary variables at a time out of the following: precipitation, temperature, reference evapotranspiration (refET), and soil moisture. Additionally, I applied a 50/50 train-test split for each model scenario to ensure robust model validation.

Quantifying causal relationships in ecohydrological systems

To identify the relevancy of the candidate hydroclimatic variables for generating robust and accurate NDVI predictions, I evaluated the relative importance of precipitation, LST, soil moisture, and refET on vegetation productivity with CCM. I computed the CCM skill (ρ) between combinations of each environmental variable paired with NDVI for every pixel's time series in the study region. Model parameters were set to the following levels – embedding dimension (E): 6, embedding time shift (τ): -1, prediction interval (T_p): 0, and the number of random samples: 10.

2.3 Results

2.3.1 Interannual variation of vegetation condition

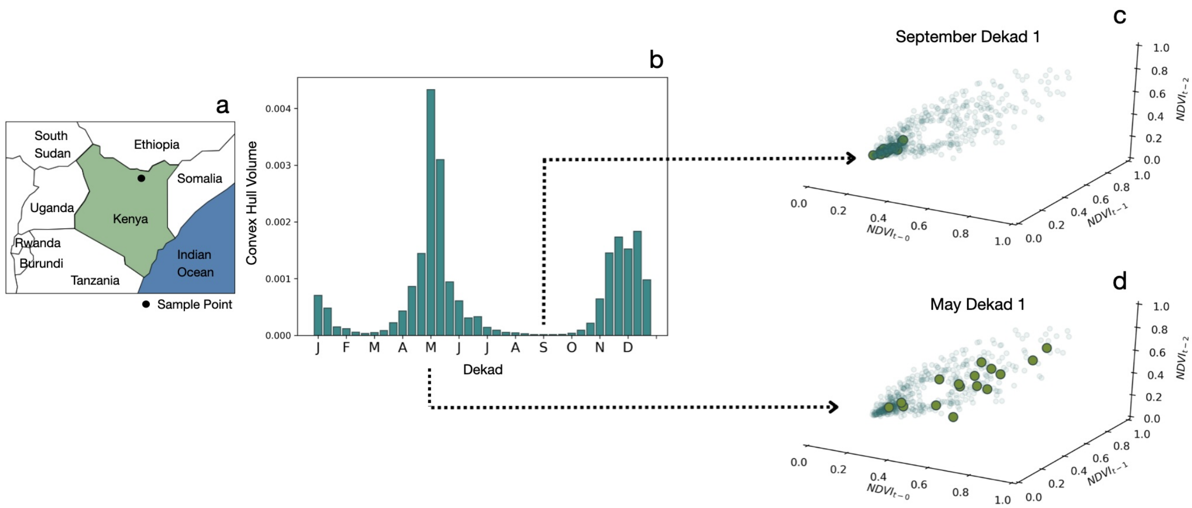

Figure 2.2: The NDVI of a given dekad can vary substantially from year to year. At an example location in Kenya (a), the NDVI time series is used to reconstruct a manifold with time-delayed embedding, and the convex hull volumes for each dekad across years (2002-2021) are measured in (b). The months where the convex hull of the manifold was the lowest (least dispersion) and highest (most dispersion) were in September and May, respectively, as shown in (c). The highlighted dots represent the time-delayed NDVI value for every year in that month.

Vegetation productivity (NDVI) is heteroscedastic within and across years. A reconstructed manifold made up of a single time series delayed with lagged versions of itself reveals how the dispersion of NDVI outcome for a given dekad can vary widely at different times of the year over multiple years. Figure 2.2 displays how, at a sample location selected within Kenya, the NDVI values within each dekad vary widely interannually. While it is an intuitive observation that such deviation occurs, particularly in drylands, I demonstrate how visualizing the topology of a time series' manifold and measuring the convex hull of each dekad's state space over multiple years reveals not only the locations of where the NDVI cycle may be more or less consistent but also when during the annual cycle to expect (in)consistency. Measurements of time-delayed manifolds are insightful for identifying regions or ecosystems that may be more or less resilient to changes in climate and land management practices. In practical application, this metric could be informative for agricultural operations, where farmers need precise knowledge of when and where the timing of planting and harvesting as well as yields will be most reliable.

2.3.2 NDVI predictability across lead times and land covers

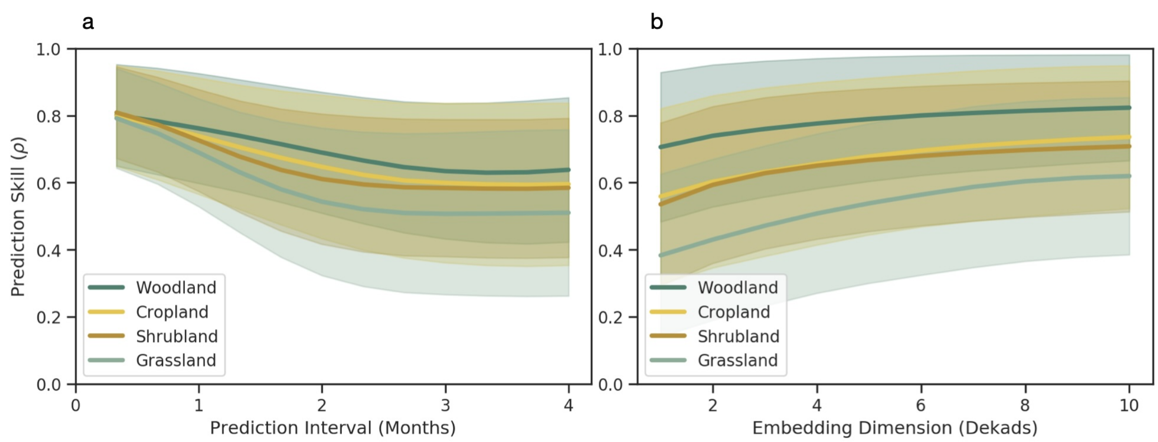

Figure 2.3: (a) With increasing lead time (prediction interval), the predictability will decrease until seasonality starts to dominate the cycle around 4 months. While there are noticeable differences between land covers on average, there is a wide variability within each land cover, shown in shaded areas that fill the range of skill values over all pixels for a given land cover type. (b) Increasing the embedding dimension offers greater memory with which to predict future states of NDVI. Prediction skill increases then plateaus by 10 dekads for all land covers.

NDVI predictability is highest at low lead times (prediction interval) within the first month across all land covers at a skill score (ρ) of approximately 0.8 (Figure 2.3). Subsequently, skill declines and later plateaus by the second month. On average, woodland ecosystems exhibit the highest predictability over a four-month prediction interval. In contrast, grasslands exhibit a trajectory of predictive skill that is consistently lower than other land cover types over the same period. Despite demonstrating the least overall predictive accuracy, the predictability of grasslands stabilizes after 2 months. By 4 months, the predictability of all land cover types stabilizes, suggesting the onset of rainfall seasonality as a predominant factor influencing vegetation conditions beyond this point. While there are noticeable differences between the average predictability of each land cover, there is wide variability across pixels, and the distributions overlap one another.

2.3.3 Distinct patterns of NDVI predictability among croplands

Figure 2.4 shows the spatial and temporal variability in predictive skill across croplands of East Africa. Using historical precipitation and LST data as ancillary variables for predictions one month ahead (left), the NDVI predictability is generally high across the region (ρ greater than 0.6), notably in the northern and southern extremities, as indicated by the darker shading. However, extending the prediction interval to four months (right) reveals a discernable decline in predictive skill throughout the region. The decline in predictability is significant within the equatorial zone, where the skill score hovers around 0.3. The trend depicted in Figure 2.5 shows how the predictability of croplands changes with respect to latitude. In the figure, pixels are categorized according to latitude bins. With longer lead times and in locations closer to the equator, the mean predictability and overall distribution of predictive skills decrease.

The predictability of vegetation conditions is tightly coupled to rainfall seasonality. Water availability, measured by rainfall's magnitude, distribution, and timing throughout the year, is a strong determinant of vegetation phenology, survival, and productivity. I calculated the rainfall Seasonality Index, *SI*, based on Walsh and Lawler (1981), for East Africa with the CHIRPS precipitation dataset. The index provides meaningful quantification and comparison of the relative seasonality of precipitation between different

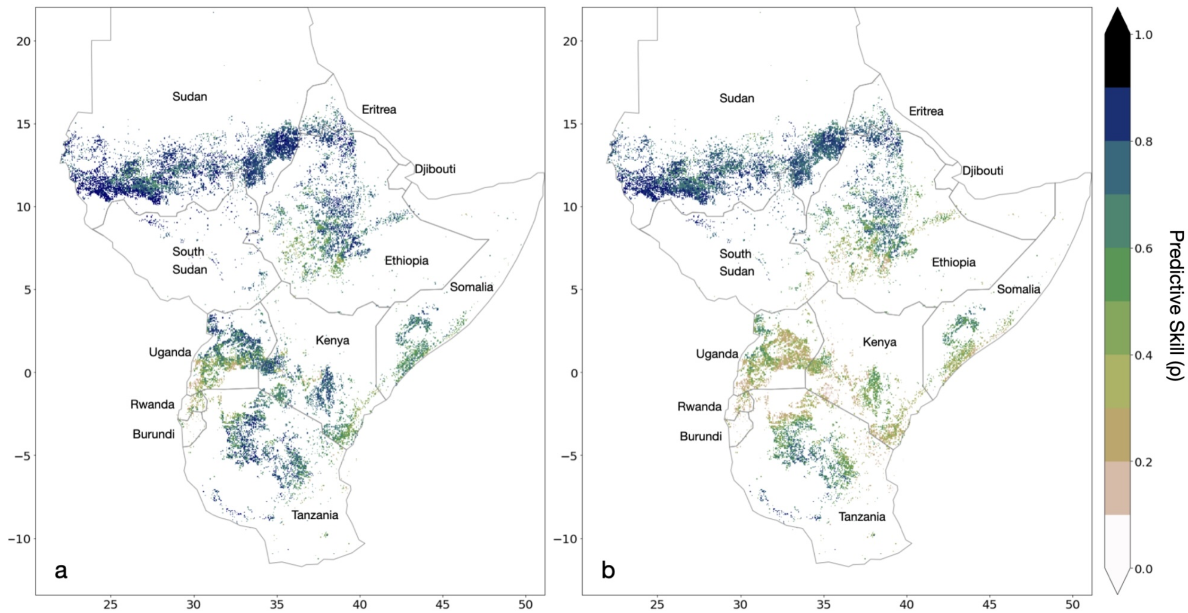

Figure 2.4: Predictive skill of NDVI from historical land surface temperature and precipitation across croplands in East Africa at a one-month lead time (a) compared to a fourth-month lead time (b). Predictability is estimated with multivariate Simplex Projection, and skill is determined by Pearson's correlation coefficient (ρ) between observed and predicted values.

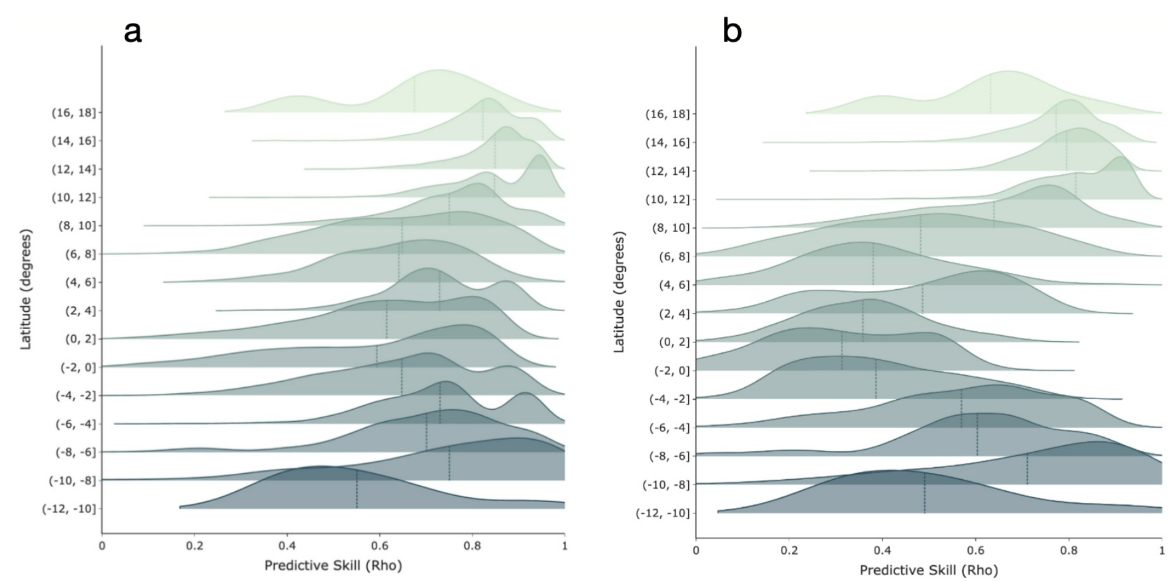

Figure 2.5: In latitudes within the equatorial zone of East Africa, where rainfall is more erratic and extreme, predictability is reduced from a one-month lead (a) to a four-month lead (b).

areas. It is determined by taking the absolute difference between the rainfall totals of the wettest summer month and the wettest winter month, divided by the total annual rainfall. The equation is as follows:

$$SI = \frac{1}{\bar{R}} \sum_{n=1}^{n=12} \left| \bar{x}_n - \bar{R}/12 \right| \tag{2.1}$$

where $\bar{x}_n$ = mean rainfall of month n and $\bar{R}$ = mean annual rainfall.

Table 2.1: Seasonality Index classes (when using mean monthly data) from Walsh and Lawler (1981).

Rainfall regime	SI class limits
Very equable	≤ 0.19
Equable but with a definite wetter season	$0.20 - 0.39$
Rather seasonal with a short drier season	$0.40 - 0.59$
Seasonal	$0.60 - 0.79$
Markedly seasonal with a long drier season	$0.80 - 0.99$
Most rain in 3 months or less	$1.00 - 1.19$
Extreme, almost all rain in 1 - 2 months	≥ 1.20

Higher values signify greater seasonality, meaning more annual rainfall is concentrated in a certain time of year, whereas lower values indicate areas where rainfall is distributed more evenly throughout the year. See Table 2.1 for seasonality classes and Figure 2.6 for the spatial distribution of seasonality across East Africa.

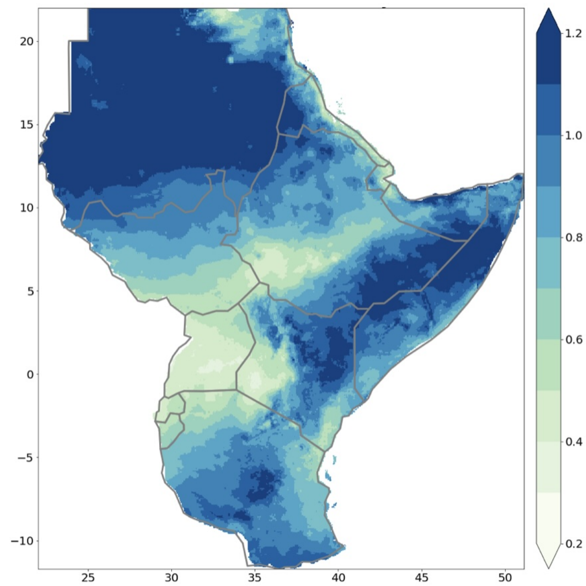

Figure 2.6: Average rainfall seasonality during the study period (2002-2021) in East Africa based on the index by Walsh and Lawler (1981). Lighter areas experience precipitation equably throughout the year, whereas darker areas experience a short, wet season.

Aridity also plays a critical role in determining vegetation productivity. Vegetation inhabiting highly arid climatic zones and distinct rain seasons generally outperform in predictability to those growing in more humid areas with more distributed rain throughout the year (Figure 2.7a). I also calculate the count of pixels existing along the continuum of aridity and seasonality, noting the sparse occurrence of croplands in humid regions of East Africa, which skews the perception of aridity's overall contribution to small changes in NDVI predictability for this region (Figure 2.7b). Within the study area, croplands are primarily present in a narrow band of aridity (0.24 to 0.36) and rainfall seasonality (0.96 to 1.12).

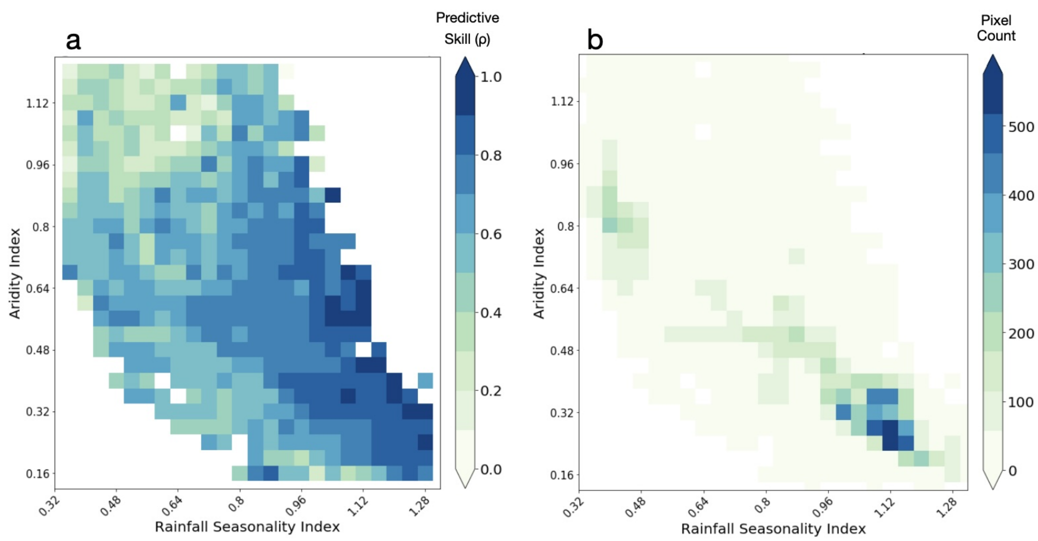

Figure 2.7: NDVI cropland prediction skill (a) and pixel count (b) by aridity and rainfall seasonality bins. Across croplands in East Africa, areas with higher NDVI predictability tend to be in arid and semi-arid regions with a high rainfall seasonality index, meaning the annual rainfall is concentrated within 1-3 months. However, when considering the number of pixels that fall within each bin of the two indices, there is a substantially greater cropland area (measured in number of pixels) that falls within a narrow range of approximately 0.96 to 1.12 the rainfall seasonality index (longer dry season and concentrated rains) and between 0.24 to 0.36 in the aridity index (arid/semi-arid). The remainder of the study region has minimal representation across the possible range of values.

2.3.4 Elucidating vegetation-hydroclimatic interrelationships

According to the cross-mapping assessment, each environmental variable combination converges as the number of observations (library length) increases, indicative of interconnected dynamics between each pair (Figure 2.8). It is possible to visually compare the differences in CCM skill of hydroclimatic variables imposed on NDVI by isolating the last value at the maximum library length or number of observations (Figure 2.9). The grouped bars for each pairing's end value show that both pairs converged beyond 0, with all values plateauing to a skill score (ρ) above 0.6. Yet for each pair, the hydroclimatic variable reaches a value above that of NDVI, where a greater gap between the lines suggests a stronger forcing of the top variable on NDVI. The difference in forcing or CCM skill between precipitation and NDVI is the largest among pairings, validating the importance of rainfall amount and timing in this water-limited region on the stability of vegetation growth. The NDVI and LST CCM skills have minimal differences in their final values, indicating high correspondence or coupling in the timing of their trajectories. Figure A.4 displays the converged skill value for all combinations of variables.

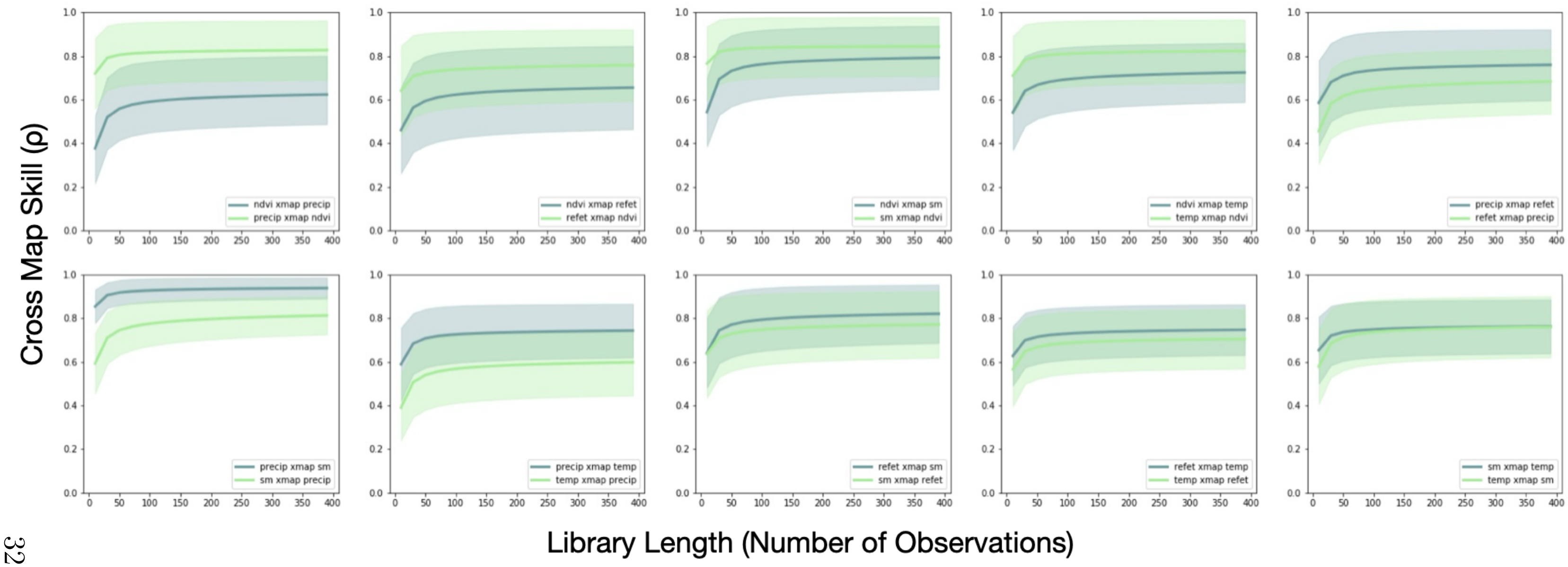

Figure 2.8: Cross mappings between each set of variable pairs (combinations of NDVI, precipitation, refET, soil moisture, and LST) across all cropland pixels in East Africa. Skill is measured by the Pearson's correlation coefficient (ρ) of the estimated and observed values of the target variable (e.g., in the first panel, the blue line 'ndvi xmap precip' means that NDVI is the candidate manifold cross-mapping onto the target, precipitation). Solid lines are the average cross-map skill for all pixels, and shaded areas show the range of results for all pixels. The two sets converge rapidly in each subplot, indicative of bidirectional causation. The gap in average lines can be interpreted as the relative strength of one variable forcing another. For instance, in the first panel, precipitation wields a strong effect on NDVI based on the relatively large vertical separation between the two compared to other combinations, particularly that of soil moisture and temperature, where the lines are nearly indistinguishable, suggestive of nearly identical historical signatures or immediate feedbacks.

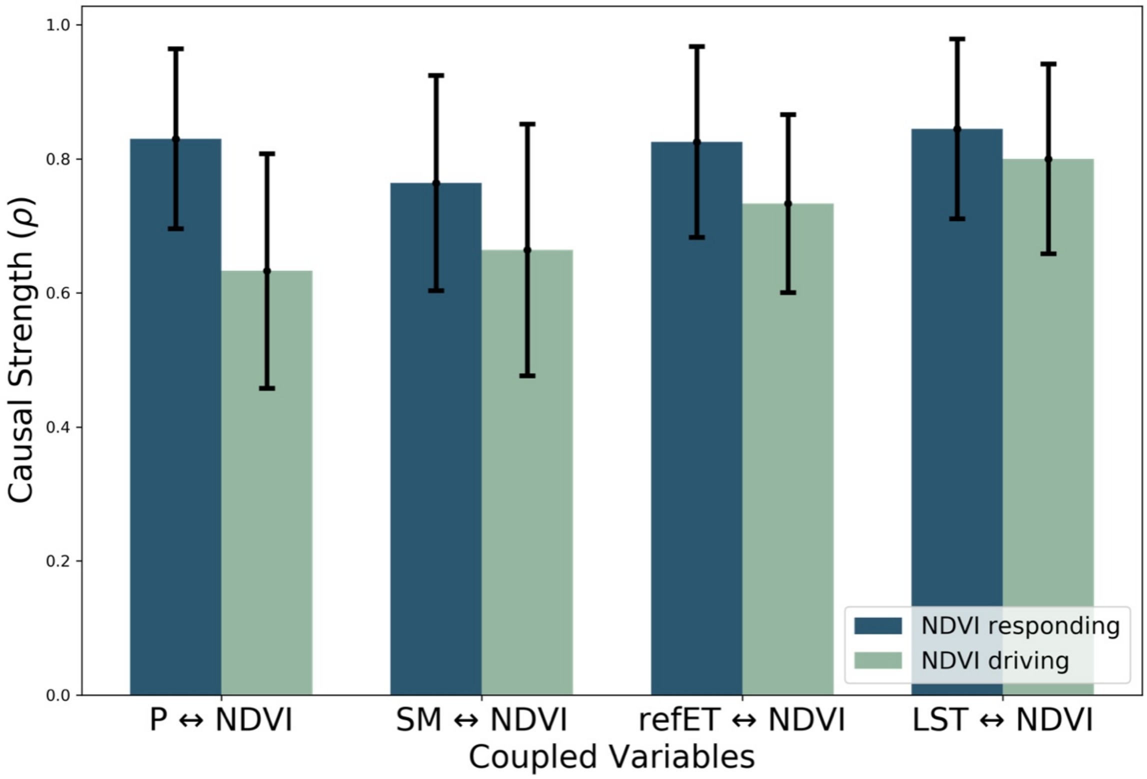

Figure 2.9: Cross mapping skill scores (labeled as 'Causal Strength') between NDVI and other hydroclimatic variables across East Africa's croplands reveal their feedback's importance and directionality. Causal strength is measured by the final scores (ρ) of each line from Figure 2.8 where they have converged or plateaued at the maximum library length or number of observations. Note, while the dataset has 687 dekads of observations, I cut off the library length in the figures at 400 observations, by which point each cross-mapping converged. Error bars mark the range of skill over all pixels. Higher bars with minimal height differences between forcing directions indicate strong bidirectional connections. The leading bar in a pair indicates the forcing direction with more causal influence.

2.4 Discussion

2.4.1 EDM as a tool for exploring dryland vegetation dynamics and its implementation with remote sensing data

In this study, I present an application of EDM using geospatial datasets to explore ecohydrological relationships. By adopting a spatially explicit EDM structure, I provide a new perspective on the linkages between climatic variables and vegetation productivity. East Africa's many climate zones and vegetation patterns make this spatial approach particularly useful. Given the region's propensity for pronounced climatic variation, even over short distances, I map the predictability thresholds of ecological responses to hydroclimatic conditions using real observations.

According to Olson et al. (2008), a multi-disciplinary approach that combines models and data is necessary to study the complex couplings between land use, land cover, and climate. The authors use East Africa as a case study to demonstrate the challenges in integrating diverse datasets, calibrating models, and quantifying differences in scale between environmental feedback loops. They discuss how livelihoods in East Africa are highly dependent on and responsive to climate variability and change. I contend that using EDM can be an innovative and useful technique to address these challenges. By utilizing long records of geospatial information to investigate complex dynamics in a region with diverse landscapes and important land use implications, EDM can provide valuable insights into the impacts of climate on vegetation productivity.

The spatial replication approach is a notable contribution to the field of EDM as it permits detailed interrogation and visualization of geographically explicit variability and predictability. Previous studies have referred to spatial replication in alternative contexts, so I will clarify how the technique I use in this study differs. Clark et al.

(2015) introduce "multispatial CCM" to detect causal relationships from ecological series shorter than 30 sequential observations by bootstrapping samples to create longer assemblages. Munch et al. (2023) also refer to spatially replicating short time series to improve EDM forecasts by concatenating delay vectors from time series across space that exhibit similar dynamics. While these methods prove beneficial for applications of EDM with moderately to very short time series, often from field collections of ecological species, the length of remote sensing environmental records I use is beyond sufficient (687 dekads of observations) to meet EDM criterion and each dekad can be treated as an individual instance. In this case, I refer to conducting spatial replication to compare the predictability of locations that may exhibit similar biogeographical characteristics but different dynamics and vice versa.

Using EDM with remote sensing time series data offers opportunities to uncover environmental dynamics at a broader yet also granular scale. Previous EDM studies have utilized single-point or spatially averaged data sources. These include research examining the relationship between sea surface temperatures and fish abundance (Deyle et al., 2013; Ye et al., 2015), climate and influenza (Deyle et al., 2016) or dengue infections (Nova et al., 2021), environmental drivers and algal blooms (McGowan et al., 2017), and temperature and greenhouse gases (van Nes et al., 2015). The use of EDM with satellite-derived observations offers several key benefits. These data cover various spatial and temporal scales, from local to global and daily to annual. Thus, they allow us to investigate how alterations in ecological and hydroclimatic conditions interact across scales.

2.4.2 Biophysical characteristics and mechanisms that influence vegetation predictability

In East Africa, vegetation density correlates strongly with the amount and timing of rainfall, which varies spatially and temporally. This study provides a detailed analysis of how different factors interact to regulate vegetation patterns. Factors like evapotranspiration rates, soil moisture, land surface temperature, and vegetation cover all play a role in shaping ecological dynamics at a local scale. The study's pixel-wise analysis offers a better understanding of how different types of vegetation, such as shrublands or grasslands, respond to environmental changes. The magnitude, rate, and time scales of these changes can affect each vegetation type differently, which suggests that customized models may be necessary for each type of vegetation. For instance, shrublands, primarily influenced by temperature and radiation, react at different time scales and magnitudes to climatic forcing than savannas, which rely primarily on precipitation.

Water availability is a crucial determinant of vegetation growth, accounting for the bulk of variability across biomes (Hawinkel et al., 2016). Deep-rooted vegetation, common in arid regions, tends to be highly resilient to erratic rainfall patterns and prolonged dry spells. The water storage capabilities of such vegetation types and their water use efficiency may explain the patterns of NDVI predictability observed. Areas with pronounced rainfall seasonality broadly exhibit high NDVI predictability overall. In future analysis, one could split the full-time series into wet and dry seasons and evaluate trends in how different factors play a more significant and immediate role in determining vegetation stability during each season. For instance, vegetative growth relies more on soil moisture content, rooting depth, and plant water-use efficiency during drier periods than in the wet seasons.

The predictability of NDVI varies significantly across different land covers in East

Africa. In regions that experience strong rainfall seasonality, NDVI predictability is quite high overall, with skill ranging between 0.6 and 0.8. When pronounced seasons have abundant rainfall, vegetation will green up rapidly and simultaneously. As such, there is an increased ability to foresee the course of vegetation productivity. During the dry season, however, vegetation browning is not as straightforward to predict due to additional influential factors such as soil moisture, rooting depth, and plant water-use efficiency. Thus, consideration of intraseasonal NDVI predictability in relation to rainfall seasonality warrants further inquiry, as vegetation dynamics may display considerable variation contingent upon the season.

The spatial distribution, annual cycle, and interannual variability of vegetation are highly related to spatial and temporal patterns of precipitation as well as other climate signals (Mangiarotti et al., 2012). Hawinkel et al. (2016) determine that mean annual precipitation explains the majority of variability in vegetation response across ecological zones in East Africa, while topographic and soil factors are also of some importance. In water-limited regions, the precipitation signal is tightly coupled with the inter-annual variability of ecosystem dynamics and thus is a useful measure for predicting NDVI (Funk and Brown, 2006). Variability in moisture availability between vegetation types is a function of structure, climate, water use efficiency, fractional cover, and soil conditions. Broadly, water use efficiency is highest in plants within the driest environments. Changes in annual species composition, functional types, and overall land cover characterization can also reduce predictability (Mangiarotti et al., 2012).

Woodland regions in East Africa exhibit more consistent interannual NDVI values, with distinct wet and dry seasons. The results also confirm that shorter and drier vegetation is more sensitive to erratic rainfall. These findings are supported by those of Nicholson et al. (1990), who observe that the phenology of East African woodlands is more stable compared to other forest types and that the minimum NDVI is longer and more distinct. In the bushland/thicket and grassland areas, the authors find that while NDVI and rainfall seasonal cycles are highly irregular, the two measures correspond closely in timing and magnitude, whereby the NDVI signal responds clearly and immediately to rainfall variability (Nicholson et al., 1990).

Rooting depth is also well-aligned with ecosystem functioning and varies with species composition and density, as well as soil characteristics (Canadell et al., 1996). Vegetation root distribution also dictates soil water-holding capacity and uptake rates from different layers (Zeng, 2001). In their global study of species rooting depth across various functional groups, (Canadell et al., 1996) find that woody species have the greatest maximum rooting depth, a prerequisite to strong water retention, followed by shrubs, herbaceous plants, and crop species.

My extensive analysis using remote sensing to assess the relative stability of NDVI in relation to water availability confirms findings from earlier small-scale, field-based studies. For example, Hesla et al. (1985) observed that shrubland species in Kenya have higher stomatal conductances and water potentials than grassland species. Higher predictive skill at longer lead times in shrublands than grasslands may be a product of superior transpiration regulation to limit water loss and consequently reduced response in the NDVI signal to rainfall variability.

Root-zone soil water strongly influences the prediction of vegetation conditions, as it has a memory that lasts for weeks to months. For instance, NDVI is shown to be forecastable with relative success across the majority of global drylands out to three months in advance based on water storage information (Tian et al., 2019). Wei et al. (2018) also conclude that a high correlation exists between NDVI and soil water across most of East Africa and that spatial patterns of soil water are more similar to NDVI than precipitation, likely because the lag between soil water uptake and greening is shorter.

While I used precipitation and temperature records equally to predict NDVI across land covers, the amount and way different vegetation types respond to these climate-driven factors differs. Wu et al. (2015) discuss how the growth of shrublands at middle and low latitudes is primarily dependent on temperature and radiation, whereas woody vegetation is more reliant on precipitation and temperature for their growth. Conversely, savannas are largely influenced by precipitation. Moreover, variation in grassland vegetation growth is predominantly determined by sufficient photosynthesis and precipitation, while cropland growth is driven by three main climatic factors – precipitation, radiation, and temperature Wu et al. (2015). Future analysis could implement an EDM with the addition of radiation and explore the predictive response when controlling for certain climate drivers or differentially weighting multiple factors over different land cover types.

Structural characteristics (e.g., leaf area) and physiological strategies (e.g., stomatal conductance and light use efficiency) also contribute to vegetation function (Li et al., 2023a). A given vegetation type's isohydric and anisohydric tendencies may influence differences in NDVI prediction accuracy. Notably, isohydric plants that strictly regulate their stomata tend to have more predictable NDVI patterns due to water conservation during periods of increasing dryness (Konings et al., 2017). On the other hand, anisohydric plants tend to use water more liberally, favoring aggressive growth and carbon uptake even in arid conditions, which may reduce predictability. This dichotomy is present in East Africa, where ecosystems with taller trees and broad leaves are generally more isohydric, while croplands tend to exhibit anisohydric behavior as crops are bred for rapid growth and increased carbon uptake, often at the expense of water conservation (Konings and Gentine, 2017).

2.4.3 Study Limitations and Future Directions

While satellite-based estimates offer the most homogenous quality over areas with limited ground observations (Hawinkel et al., 2016), the pre-processed and smoothed nature of the eMODIS NDVI data (Swets et al., 1999) may have augmented predictability outcomes. As EDM relies solely on the inherent patterns of time series, it does not require prior knowledge of ecological mechanisms as opposed to process-based approaches. While this affords flexibility in modeling complex dynamics, it comes at the cost of interpretability, as the model cannot explicitly reveal how hydroclimatic variables and vegetation physiological processes translate into productivity.

Regarding the specific methods of EDM, the primary advantage of simplex projection is that it allows researchers to analyze complex multivariate datasets with relationships that are difficult to discern using traditional statistical methods. Several challenges, however, include identifying the appropriate parameters, the sensitivity to data quality, and computational intensity when handling large geospatial data. In addition, while the algorithm can diagnose a system's predictive power and contributing elements, it may not explain the mechanisms underlying such patterns. Further, CCM has been noted to have several limitations when identifying causality in hydrology that can lead to high false positive rates (Bonotto et al., 2022; Ombadi et al., 2020). These include the role of seasonality, whereby cyclical patterns are deterministic and likely a confounding factor. While CCM is considered a bi-variable causal approach, the relationships observed may result from stronger external shared forcings and synchronization behavior (Bonotto et al., 2022).

Further refinements to better understand ecohydrological stability in diverse environments and test robustness could include training the EDM on a larger dataset covering a wider climatic gradient. Incorporating other remote sensing vegetation indices in the model may also improve the accuracy of predictability across different land covers as NDVI has been known to have saturation issues at high vegetation cover and precipitation levels (Huang et al., 2021).

Additionally, working with a static land cover year may not capture changes to boundaries and vegetation type due to land management or other anthropogenic influences over time. Non-stationary behavior due to shifts in cultivation practices or crop types planted could have also influenced the measured predictability scores. I recommend future research agendas that delve into crop-specific phenological patterns for applications in agricultural monitoring. Along these lines, conducting an attribution study and residual trend analysis could reveal which aspects of trends of vegetation productivity, specifically in cropland areas, are due to climate and environmental elements alone versus the influence of anthropogenic factors, thereby informing potential future sensitivity and drivers (Mechiche-Alami and Abdi, 2020). I also did not consider precipitation persistence (Tuttle and Salvucci, 2017) or self-propagation trends (Schumacher et al., 2022) due to soil moisture-precipitation positive cycling that either perpetuates droughts or leads to more precipitation. An area for continued inquiry could involve exploring how projected drying and expansion of drylands may further exacerbate land-atmosphere feedback.

Another potential concern is the prevalence of spatial autocorrelation. Gridded data of environmental variables or climatic factors often have similar values in areas that are close to each other due to, for instance, similar soil types, climate, or human interventions. If there is a strong spatial autocorrelation, the EDM may largely identify relationships based on spatial proximity rather than a genuine ecological phenomenon, which could inflate the model's perceived accuracy over the entire study region. This challenge is also present when distinguishing causality under synchronized dynamics where pixels are not wholly independent. One way to address the spatial autocorrelation among neighboring replicates would be to conduct diagnostic tests such as Moran's I, identify areas of strong autocorrelation, and filter out redundant pixels that elevate overall predictability or use a clustering procedure to group similar pixels together to reduce local scale overconfidence.

I also did not include oceanic phenomena (e.g., El Niño–Southern Oscillation and Indian Ocean Dipole) as a model variable because previous studies determined that the interannual response of vegetation greenness to precipitation variability is determined more by the structural characteristics of the vegetation itself rather than through climatic-oceanic or topographic features (Hawinkel et al., 2016). Local land feedback has also been found to substantially impact aridity more than remote oceanic warming (Berg et al., 2016). As hydroclimatic factors directly and immediately impact vegetation greenness, future work exploring long-term land management strategies could consider additional aspects.

While the dataset was suitable for CCM analysis regarding observation length and frequency, climate trends may have influenced the results over the nearly 20-year study period. CCM relies on a recurrence assumption, meaning causality is assessed by identifying the degree to which shadow manifolds consistently revisit similar states. If subperiods of the time series follow different trends, then the assumption could be violated, and the CCM skill could be artificially boosted by temporal autocorrelation rather than by recurrence (Bonotto et al., 2022). A Theiler window can omit neighboring points to control for this issue, though at the cost of ignoring real-world trends. Preprocessing data by detrending or removing seasonal components can avoid some artifacts that falsely detect causality but at the expense of important features necessary for CCM (Bartsev et al., 2021).

Climate projections suggest that the frequency and severity of concurrent soil drought and atmospheric aridity will worsen due to coupled land-atmosphere feedback (Zhou et al., 2019). While remote oceanic warming has been shown to significantly modulate terrestrial climate change, projected land surface processes, including decreasing soil moisture and the physiological effect of increasing atmospheric CO2 on vegetation, greatly intensify and contribute to continental aridity trends (Berg et al., 2016). Drylands rely heavily on moisture recycling and are especially constrained by water-limited evaporation. Coupled with the expansion of arid lands globally, these components make drylands highly vulnerable to cascading and self-reinforcing droughts (Schumacher et al., 2022).

In an era of accelerating global climate change, traditional models based on historical data may become less reliable. These static models are often predicated on the assumption that past patterns can inform future events, though as evolving patterns stray from historical cyclical outcomes, accuracy could wane. Climatic anomalies, more frequent extreme events, and non-linear changes to ecosystem behavior can lessen the efficacy of these models, especially in areas that are already sensitive to climate disturbances. EDM is an adaptive tool that can capture these emergent patterns, adjust to complex scenarios, and seamlessly recalibrate to new data.

2.5 Conclusion

I employ a multivariate state space reconstruction algorithm that accounts for hydroclimatic drivers, including land surface temperature, precipitation, soil moisture, and reference evapotranspiration, to estimate the predictability of vegetation conditions based on the knowledge of these related drivers. As the prediction horizon extends, the precision of the model diminishes because the trajectories of the nearest neighbors in the reconstructed manifold become increasingly dispersed. In addition, predictive skill varies spatially across East Africa and different biomes. Woodland forest leads with the highest predictive skill across embedding dimensions and prediction intervals, followed by croplands. This study presents a spatially explicit EDM approach that could be utilized as a blueprint for similar investigations in other regions.

Operating beyond a forecasting tool, EDM provides insight into the sensitivity and stability of ecosystems. It is a means by which one can measure the strength of the relationships between variables in a complex system with minimal *a priori* parameters compared to process-based models that place constraining assumptions on the mechanisms of dynamics. From an EDM perspective, state-dependent variables that collapse onto an attractor describe the fundamental characteristics of a system rather than predetermined functions based on equations. EDM can also help identify model misspecifications and improve their construction by identifying important components, such as forcing variables (Munch et al., 2020).

The approach has potential value for addressing land management, agricultural decision-making, and drought relief (Tian et al., 2019). The state space view of the inter- and intra-annual consistency in vegetation growth patterns has useful applications, from quantifying the impact of land use and land cover change on ecosystem health and biodiversity to monitoring crops and directing agricultural management practices. This method can assist in identifying regions or ecosystems that are more susceptible or less resilient to changes in environmental conditions or land management practices. Amidst a rapidly changing global climate, precise and predictive tools are needed to understand and anticipate ecological transitions. By identifying areas with high NDVI consistency and understanding the drivers behind them, this study highlights the potential of remote sensing data to capture the responsiveness of ecological systems.

Chapter 3

Gravity Model Estimation of the Drivers to Internal Human Displacement in Somalia

Abstract The drylands of Africa are increasingly vulnerable to the impacts of climate change, with cascading effects on livelihoods, food security, and human mobility. In Somalia, the confluence of recurrent droughts, extreme flooding, protracted armed conflict, and the disruption of traditional pastoral and agricultural livelihoods has arisen as a determinant that amplifies internal displacement. This study investigates the causal mechanisms through which climate shocks influence both out- and in-migration. Employing a gravity model framework, I estimate the relative influence of weather anomalies, conflict intensity, and livelihood factors on inter-regional displacement flows within Somalia. The analysis reveals that while climate does not play a strong role in all circumstances, it can be a critical driver for certain populations. Most notably, those who live in predominantly pastoralist or pastoralist and fishing areas are much more likely to migrate due to anomalous rainfall. Conversely, anomalous air temperatures do not serve as a primary

influence on migration as a short-run shock. Conflict severity, nevertheless, stands up to robust testing as a significant driver of migration. While this study adds to the growing literature examining displacement dynamics, particularly in Somalia, its novel contribution lies in the numerical modeling of how livelihood factors intersect with climate and conflict variables to shape mobility patterns.

3.1 Introduction

Human migration in response to a changing climate is emerging as one of the most urgent humanitarian challenges of the twenty-first century (Martínez-Zarzoso et al., 2023). Several factors contribute to this phenomenon. First, climate change is causing more frequent and intense extreme weather events, which force people to abandon their homes and livelihoods. Migration can also be seen as a form of adaptive strategy if individuals have the resources to move. Climate-related disasters, including droughts and floods, can cause severe damage to local livelihoods, compelling people to seek opportunities elsewhere. These economic shocks, along with conflicts exacerbated by climate-related disasters, further fuel human mobility (Ceola et al., 2023). Researchers predict that droughts will have a substantial impact on societies in Africa, in particular, due to an increase in precipitation deficits and durations under global warming scenarios. Moreover, populations living in African drylands are anticipated to double by 2050, while cities in these regions are projected to become risk hotspots for climate change and climate-induced human displacements, worsening pre-existing vulnerabilities (Ceola et al., 2023).

Given these issues, it is crucial to discern whether the effects of climate patterns alone can drive migration or if they amplify existing factors such as conflict and poverty resulting from the loss of income (Martínez-Zarzoso et al., 2023). In this chapter, I examine the drivers of internal displacement in Somalia, a country faced with numerous challenges that have led to widespread internal displacement, including protracted armed conflicts, severe flooding, prolonged droughts, and deep-rooted socio-political instability. The Internal Displacement Monitoring Center (IDMC) reported that there were 621,000 internal displacements as of 2022 due to conflict and violence and 1,152,000 associated with disasters in Somalia (IDMC, 2023a). Yet these figures, IDMC states, are underestimates as it is difficult to verify which movements are caused by singular versus mixed triggers. Accordingly, this situation has garnered significant attention from academic researchers and humanitarian organizations.

In this study, I contribute to the ongoing conversation around quantitative practices to understand the climate-conflict-migration nexus. The research expands upon previous work on whether out-migration can be attributed to climate shocks. I add insight into how certain livelihoods are specifically impacted, testing the extent to which weather extremes and short-run hazards can explain displacement for different populations. Further, I evaluate both in- and out-migration drivers. I use gravity model estimation, a method commonly used in trade and migration studies (Anderson, 2011), to test assumptions about the drivers of mobility in Somalia. The models are constructed in a manner to evaluate the importance of different factors in their influence on displacement, including distance, population size, livelihood type, weather conditions, and conflict severity. By estimating the impact of heterogeneous push and pull factors, this study offers a comprehensive, contextual perspective that dissects the role of various characteristics in shaping the enduring displacement crisis in Somalia.

To facilitate discussion around the concepts of environmental change and migration, I will first briefly lay out a few definitions. Climate mobility encompasses various forms of movement resulting from direct or indirect impacts of climate change and related environmental hazards. Various forms of mobility include migration, forced displacement, and relocation or evacuation in response to climatic stress and hazards (Rigaud et al., 2018). Displacement involves forced mobility, often due to sudden-onset disaster events, typically short-term and over short distances, with affected households returning to their original locations once the danger has passed. Climate migrants are defined as individuals or groups who are pushed to leave their homes over longer periods or permanently due to sudden or gradual changes in climatic conditions. Permanent migration can also result from initial displacement if the displaced individuals do not return to their original locations (Hoffmann, 2022). Individuals or communities may also become forcibly displaced when they are compelled to leave their homes because of armed conflict, disasters, and other disruptive events (Earney and Moreno Jimenez, 2019). Internal displacement, specifically, is the forced movement of individuals from their residence to another location within their country's borders due to various distressing events (Clement et al., 2021).

Year after year, the number of internally displaced people (IDPs) continues to rise. At the end of 2022, Internally Displaced People (IDPs) made up the majority of the global forcibly displaced population at 58 percent. Additionally, the number of IDPs protected/assisted by the United Nations High Commissioner For Refugees (UNHCR) reached 57.3 million, which is double the amount of the previous decade and represents a 12 percent increase from the previous year (UNHCR, 2022). According to IDMC, among those internally displaced due to disasters, by the end of 2022, the numbers jumped to 8.7 million people across 88 countries and territories. This was a 45 percent increase in the number of disaster-related IDPs since 2021 (IDMC, 2023b). Despite the meticulous efforts by organizations such as UNHCR and IDMC, recent research on monitoring and describing global migration trends has become more complex due to several evolving elements. These factors include the shift in historical migration patterns, the emergence of migration economies, the rising environmental migration driven by climate change, and the growing occurrence of conflict-driven migration in specific regions (Griffith et al., 2023).

In the following sections, I will discuss the research landscape around (1) environmental change and migration, (2) gravity modeling of migration, (3) the interaction between climate, conflict, and migration, (4) patterns of environmental migration in African drylands, and (5) specific literature pertaining to understanding displacement in Somalia.

3.1.1 Literature Review

Empirical Study of Environmental and Climate Effects on Migration

In recent years, there has been a growing interest in the scientific literature on the topic of environmental change and climate migration. This trend can be seen through the integration of semantic elements (e.g., vulnerability, social justice, security, and adaptability) that climate and environmental change research shares with that on migration (Maretti et al., 2019). With the strong connection between these themes, taking account of the socio-environmental context in understanding migration dynamics and integrating both quantitative and qualitative approaches is crucial.

Kaczan and Orgill-Meyer (2020) synthesize the literature on the impact of climate change on migration, concluding four key themes that disrupt common thinking on the topic: (1) climate-induced migration is not necessarily more common among poorer households, as wealthier households may have the means to migrate, (2) climate-induced migration tends to result in more long-distance domestic moves rather than local or international crossing, (3) slow-onset climate changes, such as droughts, are more likely to lead to increased migration than rapid-onset changes, such as floods, and (4) the severity of climate shocks affects migration in a non-linear way, depending on whether households have the resources to migrate or are vulnerable to the effects of climate change.

Two primary motivations differentiate empirical research on the environment-migration nexus: forecasting versus hindcasting. In other words, studies may focus on (1) predicting the numbers of people who will move due to climate change and where or (2) tracing the pathways by which previous environmental fluctuations or shocks have affected migration, often with the intention to inform future outcomes (Morrissey, 2014). One of the most prominent research efforts to project future environmental-induced internal migration, published in what is known as the "Groundswell" reports, estimates that by 2050, without climate change and development action, climate change could result in more than 216 million people migrating within their own countries in six regions – Latin America, North Africa, Sub-Saharan Africa, Eastern Europe and Central Asia, South Asia, and East Asia and the Pacific (Clement et al., 2021). Yet, while forecasts may be helpful in conceptualizing these enormous expected shifts and directing mitigating policies, we are not currently at a stage in which they are reliable and should only be considered as tools for exploring various possible futures (Schewel et al., 2024). Instead, developing models to understand the scenarios in which environmental change can modulate migration patterns using past observations is equally, if not more, important.

Research approaches that measure key indicators of climate-induced migration can significantly impact our understanding of the phenomenon. Quantitative evidence can be gathered from large-scale spatial and longitudinal analyses that monitor greater trends or from agent-based (Morrissey, 2014; Groen, 2018; Nelson et al., 2020) and system dynamics models (Ginnetti and Franck, 2014) that can simulate decision-making processes that may shift movement patterns in the future under different climate scenarios (Hoffmann et al., 2021). Other methods include machine learning (ML) algorithms such as random forests (RFs) and gradient boosting machines (GBMs) to predict the number of people displaced that coincided with historical hazards (floods, storms, or landslides). For instance, Ronco et al. (2023) incorporate a diverse set of socioeconomic and environmental variables on a national and disaster-specific scale, explainable AI, and causality measures to shed light on global human mobility's complex processes and drivers. In doing so, they find that displacements result from uneven vulnerabilities that can be largely attributed to the combination of poor household conditions and extreme precipitation.

Others have studied how economic development, political stability, and social networks are intertwined with environmental change and migration (Hoffmann et al., 2020, 2021). Risks to public health due to disease outbreaks or injuries and disruptions in healthcare services in areas affected by climate-related events also impact migrant decision-making and their well-being (Khalid et al., 2023; Issa et al., 2023b). Additionally, both rapid and slow-onset natural hazards impact movement patterns differently (Kaczan and Orgill-Meyer, 2020; Martínez-Zarzoso et al., 2023; Kabir et al., 2018; Zickgraf, 2021). Land degradation has also been shown to contribute to this critical problem (Hermans and McLeman, 2021; Hoffmann et al., 2022).

This is to say that migration decisions are not solely based on environmental changes but are influenced by multiple factors, and research on this topic must be approached with a contextual and multi-causal lens (Warner et al., 2010; Piguet, 2022). Black et al. (2011) classifies five families of drivers that affect migrant decision-making: economic, political, social, demographic, and environmental drivers. Under the wing of environmental drivers, migration may mainly be impacted through two direct pathways: availability and reliability of ecosystem services and exposure to hazards, as well as indirect mechanisms, for example, via loss of livelihoods or conflict over resources. Throughout this chapter, I will explore how to tease apart these mechanisms.

Gravity Modeling of Migration

In this study, I employ an analytical approach to examine internal displacement flows within Somalia. I measure the impact of key factors, including population dynamics, climatic conditions, and the prevalence of conflict on migration between different regions across the country. Multiple recent studies have similarly implemented gravity model analysis to investigate the extent to which climatic variations can explain migration flows. Progressing from a basic gravity model that includes population and distance to nested models that integrate supplementary explanatory variables may further explain how migration is impacted by socio-demographic and climate features.

Garcia et al. (2015) modeled internal migration flows in several countries of sub-Saharan Africa using census microdata and global climate variables. While the authors found high correlations in their models for predicting within-country migration, the contribution of climate variables was relatively low compared to the socio-demographic effects. They highlight several limitations of their method, however, including the inability to monitor circulatory movements when the census microdata tracks only permanent migration, the lack of consideration for other impacts such as conflict events, underlying data quality issues, and possible misalignment between the spatiotemporal scale of how climate drivers affect migration and data availability. Backhaus et al. (2015) focus on bilateral international migration, finding a positive correlation between migration and temperature and precipitation (though to a lesser extent). The authors have noted a correlation between countries that depend on agriculture and the out-migration rate. This correlation is more closely linked to temperature than precipitation. Additionally, they found that state fragility directly affects emigration but did not observe a significant interaction with climate.

Mastrorillo et al. (2016) study the effect of climate variability on internal migration flows in South Africa. They similarly conclude a relationship between temperature extremes (positive), excess rainfall (negative), and agricultural employment and production on out-migration, though the impact varied substantially by migrant socio-economic and demographic differences. Pirani et al. (2019) explore how inter-district migration in Tanzania is determined by adverse environmental conditions, including households that have been affected by droughts and floods, crop diseases or pests, or severe water shortages, while also accounting for socio-economic covariates and border contiguity in their model specifications. The authors find that crop-related shocks were significant factors in shaping internal migration and severe water shortage to a smaller degree. Levels of urbanization, education, and economic development in the destination areas were also highly relevant in the migration destination process, while distance and contiguity played an important role.

Concerning conflict as a driver of displacement, Saldarriaga and Hua (2019) take a comparable gravity modeling approach with the case of Colombia, studying the correlation between the intensity of violence in origin and destination municipalities and victims that are forcibly displaced. Since displaced people tend to cluster in space, the study also considers the level of community participation in each location and the strength of social networks at the destination. Abel et al. (2019) study the climate, conflict, and migration nexus with global bilateral refugee flows data and gravity-type models. Their findings suggest that climate conditions, especially severe droughts, are consequential in explaining asylum-seeking flows, though this varies across regions and periods. The Arab Spring and the Syrian war are examples, for instance, of where the interaction between political transformation, drought, and armed conflict significantly elevated asylum-seeking migrants (Abel et al., 2019; Kelley et al., 2015).

Notably, each of these studies analyzes migration patterns from panel data at the annual or multi-year scale, which may not pick up on the impact of rapid-onset shocks (e.g., flash floods) and seasonal labor migration patterns. In this chapter, I use a unique dataset with frequently and continuously reported estimates of displaced populations within Somalia, which offers a deepened understanding of mobility pathways. On the other hand, as I did not have access to individual or community-level socio-demographic information, as well as high-resolution records of those at risk but unable to move, I inevitably miss populations that are "trapped" and highly vulnerable (Borderon et al., 2019; Zickgraf, 2019). Nawrotzki and DeWaard (2018) implement gravity models to estimate inter-district migration flows in Zambia, combining climate data with aggregated census microdata of socio-demographic factors to predict not only characteristics that would enable populations to migrate but also those that cause immobility. Poverty, the steep costs of migration, and the further degradation of already weakened livelihoods under climate change all contribute to specific groups being susceptible to becoming trapped in place.

Climate, Conflict, and Migration

While climate-related migration poses a legitimate concern, I would be remiss to exclude conflict as an important component that greatly magnifies internal displacement. The relationship between conflict, climate, and migration has been a topic of growing interest in academic research. Numerous studies have explored the linkages between these factors, revealing the potential causal pathways with empirical evidence supporting these associations.

Across Eastern Africa, countries are contending with difficult repercussions of more frequent and severe droughts, which have exacerbated food insecurity and economic losses, prompting greater tensions and pervasive conflicts between herders and farmers. The resulting resource-based conflicts and large-scale displacement disproportionately affect pastoralists and rural smallholder farmers in highly drought-prone areas. While rural-to-urban migration in the region is largely driven by livelihood diversification, it also serves as an emergency response to drought (Adaawen et al., 2019).

Climate-induced resource scarcity, such as water and arable land, can trigger competition and conflict, particularly in regions already experiencing socio-political tensions (Helman and Zaitchik, 2020; Raleigh and Kniveton, 2012). Droughts, extreme weather events, and other climate-related hazards can lead to forced displacement and migration.

As a result, this displacement can engender social and political tensions in the areas of origin and destination (Mach et al., 2019).

Changes in agricultural productivity, livelihoods, and employment opportunities due to climate variability can influence migration patterns and cause conflict over resources (Freeman, 2017; Owain and Maslin, 2018). Higher concentrations of crop production can increase the likelihood of conflict onset by exacerbating inequalities and livelihood disparities across regions (Vesco et al., 2021). When climate shocks lead to crop failure, rural laborers may migrate to adapt, consequently driving up resource competition in the host areas and promoting socio-political tensions. Another transmission channel between drought and civil conflict in countries such as Somalia is through livestock prices, as livestock rearing is a major source of income for rural populations in the country (Maystadt and Ecker, 2014). Drought can lead to a sequence of cascading events. Reduced water availability and fodder for livestock can drive herders to sell more of their livestock, increasing the supply in the market, decreasing the price, and diminishing herder income. In this case, migration may not be a viable strategy due to high transportation costs and limited rangeland resources at the destination during widespread, severe drought. Instead, drought intensity and length have been shown to substantially raise the likelihood of conflict in Somalia, as herders may resort to violent means to supplement their lost income (Maystadt and Ecker, 2014).

In a commentary by Mach et al. (2020) discussing future research directions on climate and conflict, the authors stress that while it is important to study climate-induced conflict that can drive displacement and outmigration, it is also essential to consider the possibility of reverse causation, where climate change drives outmigration, contributing to conflict.

The connection between migration and conflict is highly context-specific (Abel et al., 2019), yielding the need for more in-depth case-study research to test theoretical assumptions. Cantor (2023) differentiates between macro and micro dynamics of internal displacement, where the macro describes large-scale patterns and trends (e.g., the scale and distribution of disaster and climate-driven internal displacement) compared to the micro, which refers to more granular patterns of displacement, such as the livelihoods, social vulnerability, and resilience of affected populations as well as the decision-making process (e.g., anticipatory or reactive). My analysis in this chapter will be situated along the macro-micro continuum. I analyze the patterns of internal displacement in Somalia at the sub-seasonal level and consider the dominant livelihoods across different regions. However, I cannot fully address individual socio-demographic dynamics due to the coarser scale at which I examine mobility dynamics.

Patterns in African Drylands

Environmental change is having a significant impact on human migration across African drylands. In these regions, populations have been experiencing a range of environmental stressors, including droughts, soil erosion, and deforestation, which have prompted forced displacement and overall changes to migration patterns (Morrissey, 2014). African drylands have historically been impacted by environmental stressors that affect mobility decisions. These areas are highly vulnerable to the impacts of warming trends that cause worsened aridity and increase the frequency, intensity, and duration of temperature-related extremes (Hoffmann, 2022). Although migration as a response to environmental stress is often temporary, and its effects have typically been short-lived, mobility patterns are becoming more diverse in scope, direction, and duration (Morrissey, 2014). Livelihood adaptability, demographics, variations in migration response, type and duration of environmental stressors, social networks and familial bonds, abundance of natural resources, and contextual dependence of migration-environment dynamics greatly influence migration (Borderon et al., 2019).

East Africa is projected to experience increases in heatwaves, dry days, heavy precipitation, particularly over Somalia, and river flooding. These changes are expected to significantly alter human mobility patterns across the region. Furthermore, cascading risks and multi-hazard events wield dangerous threats and deepen population vulnerability (Thalheimer et al., 2021b).

Evidence from Somalia

Environmental and conflict-related shocks in Somalia have had profound negative impacts on displacement, poverty, and livelihoods. Here, climate change is leading to water scarcity due to droughts, coastal erosion, flooding, and changes in ocean dynamics. As a result, pastoralists and farmers sometimes resort to water rationing because of the reduction in arable and grazing land. This, in turn, led to increased costs of agriculture and livestock products and intensified conflict over water resources. Combined with the fragile political and economic system, extreme events contribute to widespread displacement and poor adaptive capacity (Ali et al., 2023). Forced displacement due to conflict and drought disrupts traditional livelihood strategies and negatively affects household income, food security, and access to basic services (Osman and Abebe, 2023).

Over the past few decades, protracted drought has substantially reduced household income and consumption, especially in rural areas (Pape and Wollburg, 2019). Yet, drought is not the only culprit. In 2011, for instance, a widespread crisis leading to famine was caused by the compounding factors of conflict, drought, governance failure, political instability, and constrained humanitarian assistance (Lindley, 2014; Maxwell and Fitzpatrick, 2012).

Compounding vulnerabilities worsen systemic risks in Somalia (Thalheimer et al., 2021a). Climate change will likely deepen water scarcity and food security (Ajuang Ogallo et al., 2018). In one study, Warsame et al. (2023) quantified mortality rates and the excess death toll related to Somalia's 2017-2018 drought-triggered crisis. Analyzing household surveys, the authors identified predictors of mortality, reconstructed population denominators for each district and month, and found excess mortality to be moderately correlated with the severity of the crisis predicted by the Integrated Phase Classification food insecurity scale. Addressing the root causes of displacement, health, and poverty in Somalia requires a comprehensive and integrated analysis considering the country's context and multiple drivers of vulnerability.

Several researchers recently conducted quantitative assessments of mobility in Somalia to better understand situational mechanisms. Predictive modeling techniques can aid in monitoring the movements of refugees and internally displaced people Pham and Luengo-Oroz (2022). One such machine learning method that has been explored in the Somalia context is known as long short-term memory (LSTM) modeling, which is a type of recurrent neural network (RNN) that was used to predict monthly arrivals of Internally Displaced Persons (IDPs) across Somalia's 18 regions. Project Jetson, an applied experiment by UNCHR, used this method along with nontraditional data such as market prices and climate anomalies to estimate the numbers of IDPs within Somalia and refugees that moved to southern Ethiopia (Earney and Moreno Jimenez, 2019). However, machine learning approaches have several shortcomings, including the potential for overfitting, computational costs, and limitations towards capturing the magnitude of unexpected events or sudden spikes in displacement trends (Pham and Luengo-Oroz, 2022).

In an ecological analysis of longitudinal panel data on displacement in Somalia, negative binomial regression models reveal strong associations between Internally Displaced Person (IDP) out-migration rates and failed rains at a three-month lag, food insecurity at a one-month lag, and the presence of therapeutic food services with no lag (Yuen et al., 2022). Conversely, the IDP out-migration rate is not associated with armed conflict intensity and cash- and rations-based food security services. In parallel, another study implemented statistical and econometric models with the same disaggregated dataset tracking internal displacement across Somalia. Thalheimer et al. (2023b) find that both weather and conflict play substantial roles in perpetuating displacement in Somalia, though there is little evidence of feedback from displacement to conflict. Oh et al. (2024) used network analysis to study the emergent movement patterns of IDPs due to disasters and conflict. Disaster-induced networks were denser and more modular than conflict-induced IDP networks, suggesting that those affected by disasters tend to move within regional boundaries compared to those affected by conflicts who relocate to relatively remote areas outside the regional boundaries.

3.2 Methods

3.2.1 Study Area

Somalia faces numerous environmental and social risks within the Horn of Africa, including consecutive drought events, intense floods, and ongoing armed conflict (Thalheimer et al., 2021a). These challenges greatly affect population health, food supply, and general well-being. The country frequently experiences below-average rainfall, leading to severe droughts, displacement, and epidemics (Warsame et al., 2023). Worsening consequences of climate change, including floods, droughts, river depletion, sea-level rise, and poor water quality, have significantly stressed water resources in Somalia (Ali et al., 2023). The environment is characterized by a semi-arid climate that is prone to sporadic floods during the rainy season along the two major rivers, the Juba and Shabelle (Mohamed and Adam, 2022; Osman and Das, 2023; Billi and Sebhat, 2022), as well as prolonged droughts that have lead to famine (Maxwell and Fitzpatrick, 2012; Warsame et al., 2023).

The protracted regional conflict has intensified these issues, transforming drought-induced food shortages into famines and causing extensive mortality, disease, and displacement (Seal and Bailey, 2013). Moreover, the country has a history of colonial rule and a struggle for independence, followed by civil war and political unrest. As a result, these events have culminated in a fragile central government, regional power struggles, and the presence of militant groups (Menkhaus, 2014). Somalia is economically vulnerable, largely due to its high dependence on volatile agriculture and livestock prices, with some supplementary support from remittances (Warsame et al., 2021, 2022; Lindley, 2010). Widespread poverty and unemployment, minimal industrialization, and poor basic services, including education and healthcare, exacerbate the socio-economic situation (Lwanga-Ntale and Owino, 2020; Ahmed et al., 2020). The amalgamation of these issues considerably impacts population health, livelihoods, and displacement (Achour and Lacan, 2011; Wakabi, 2009; Raleigh and Kniveton, 2012).

The trifecta of environmental stressors, armed conflicts, and socio-economic instability in Somalia amounts to high levels of internal displacement. Over recent decades, millions of people have been displaced annually within Somalia as a result of tribal territorial disputes, clan clashes, local conflicts, and resource scarcity (Maystadt and Ecker, 2014). Protracted violence and lack of security continue the cycle of displacement, famine, and disrupted humanitarian assistance efforts (Lindley, 2011; Seal and Bailey, 2013). Land degradation strains farming and pastoralist communities, further driving population displacement (Warner et al., 2010; Hermans and McLeman, 2021). The struggle for water and grazing land, among other resources, has also intensified conflict (Ali et al., 2023).

Livelihoods of Somalia

The geography and climatic conditions play a significant role in determining the dominant regional livelihoods across Somalia. These include pastoralism, agropastoralism, riverine irrigation, pastoralism/fishing, and urban livelihoods (FEWSNET, 2015; Nelson et al., 2020). The spatial variation of each livelihood zone indicates how the people of Somalia adapt to and confront challenges within their surroundings. Pastoralists rely on herding livestock, including cattle, goats, camels, and sheep. Largely practiced in the arid and semi-arid regions of the country, pastoralism is a way of life highly attuned to harsh, dry environments (Ahmed et al., 2023; Nelson et al., 2020). As mobile communities, pastoralists follow seasonal migration patterns depending on water accessibility and rangeland conditions. Agropastoralism is a more diversified livelihood approach whereby communities engage in agriculture and pastoralism in areas where conditions are conducive to farming and raising livestock. As a dual strategy, agropastoralism is a way of fortifying income and food security, though it is still susceptible to environmental disasters such as droughts and floods, which can devastate both crop production and livestock health. In fertile riverine areas, especially along the Juba and Shabelle rivers, communities practice irrigated agriculture by pumping or gravity systems. While these areas can provide a stable source of income, communities are still vulnerable to flooding and water resource conflict (Osman and Abebe, 2023). Along the coastline, particularly along the eastern shore meeting the Indian Ocean, communities engage in a mix of pastoralism and fishing. The combination of livelihood strategies affords local consumption and some larger-scale commercial fishing. Lastly, urban areas, notably the larger cities of Mogadishu and Hargeysa, provide trade, services, and manufacturing opportunities. City dwellers often send remittances to their rural family members (Lindley, 2010). In these cities, however, overpopulation, rent-seeking and dispossession, and security concerns are additional stressors that have hindered livelihoods and deepened poverty Bakonyi (2021).

3.2.2 Data

Internal Displacement

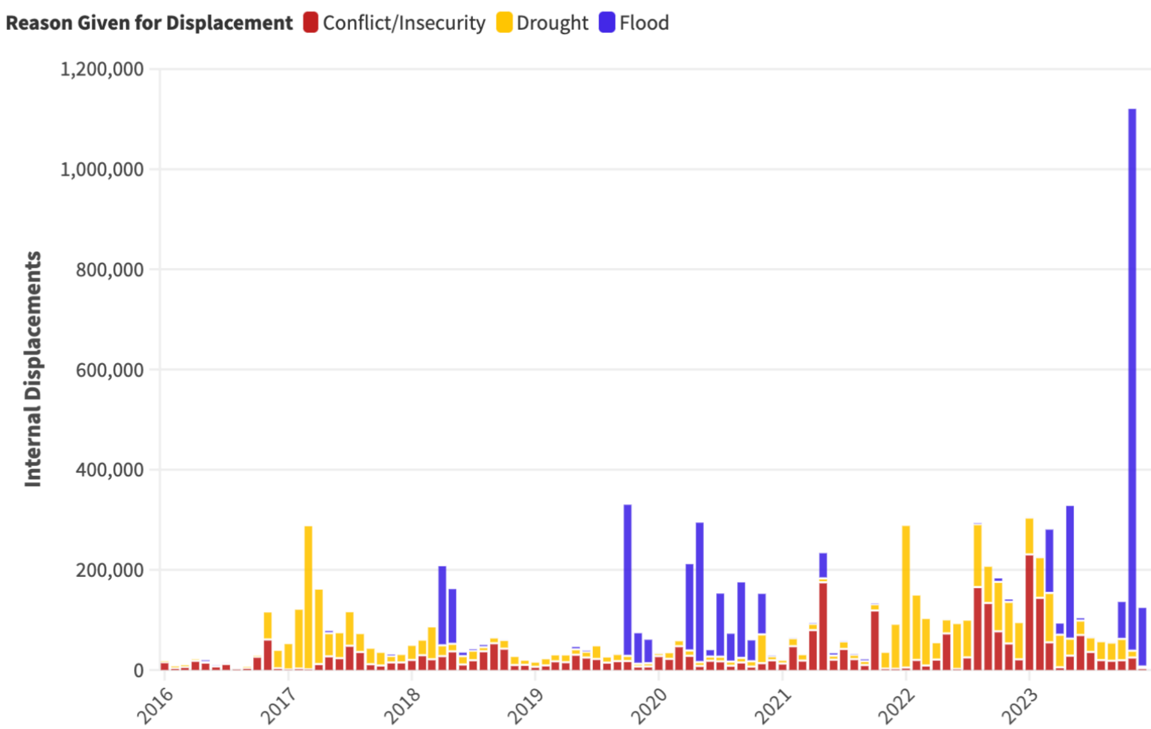

Figure 3.1: Time series of internally displaced people recorded by the United Nations High Commissioner for Refugees (UNHCR) Protection and Return Monitoring Network (PRMN) dataset from 2016 to 2023. Colors distinguish the reason individuals give for why they were displaced, whether by flood, drought, or conflict.

The United Nations High Commissioner for Refugees (UNHCR) leads a multi-stakeholder initiative known as the Protection and Return Monitoring Network (PRMN), which is tasked with identifying and reporting on internal displacement in Somalia via key-informant surveys (UNHCR, 2017; Earney and Moreno Jimenez, 2019). The PRMN publicly releases a dataset that disaggregates by location (district and region) and time

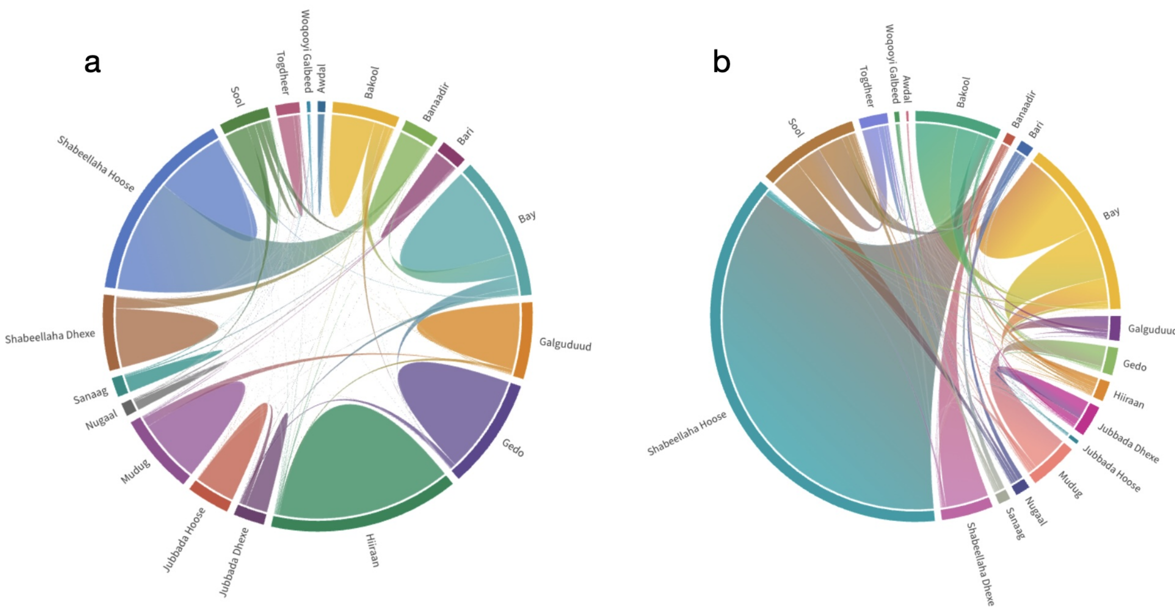

Figure 3.2: Circos diagram of total internal displacements between regions in Somalia from 2016 to 2023 where (a) represents all migration flows and (b) leaves out the flows that occurred within the same region.

scale (week and month), supplying a high granularity unique among country-wide migration datasets. The dataset provides a continuous record from January 2016 to the present. The records also include details on populations' reasons (3.1) or triggers for displacement as well as their humanitarian needs (UNHCR, 2017; Thalheimer and Oh, 2023; Pham and Luengo-Oroz, 2022). While the PRMN dataset is exceptional among public displacement data in its breadth of coverage and opportunity for near real-time displacement identification, it is not exhaustive, as data collection relies on field observers' presence. The figures, rather, should be taken as representative of potentially larger movement trends and their underlying causes. Issues in reliability can arise, for instance, during periods of conflict, where there may be areas that enumerators can not safely access (Pham and Luengo-Oroz, 2022; UNHCR, 2017).

In this study, I analyze the number of people who have been displaced between regions of Somalia from 2016 to 2023. I resampled the population movement counts from weekly

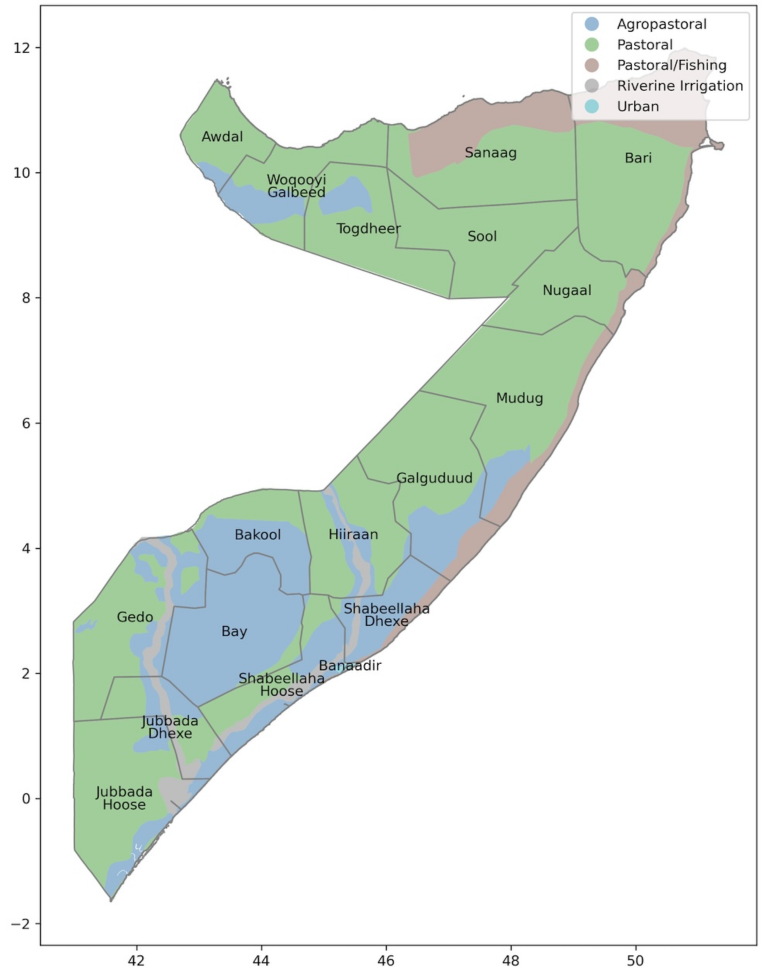

Figure 3.3: Major livelihood zones of Somalia with administrative zone 1 (region) boundaries.

to monthly. Relative displacements from origin to destination regions can be seen in Figure 3.2, where (a) represents the total displacements recorded as being between and within regions over the study period and (b) represents only movements between two regions.

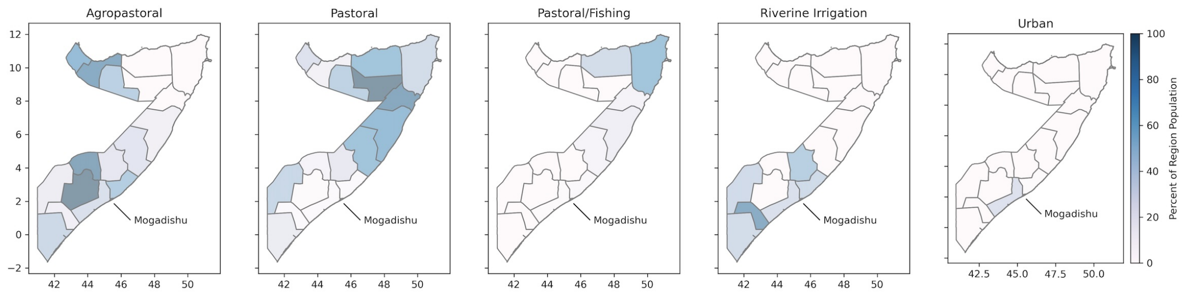

Figure 3.4: Percent of the population per region in Somalia that practices a certain major type of livelihood.

Livelihood Zones

The Livelihood Zone Map, produced by the Famine Early Warning Systems Network (FEWS NET) and the Food Security Nutrition and Analysis Unit (FSNAU), delineates geographic areas of the country that pertain to where people have similar opportunities for obtaining food and income as well as engaging in trade (FEWSNET, 2015). The most recent map was last updated in October 2015. I reclassified the 19 officially demarcated zones into five major zones: Urban, Pastoral, Agropastoral, Pastoral/Fishing, and Riverine Irrigation. Figure 3.3 displays these livelihood zones and regional administrative boundaries. Then, for each region, I calculated the percentage of the population that follows each livelihood type (Figure 3.4).

Region administrative zones and population

The administrative zones for regions were derived from the Global ADMinistrative Area (GADM) admin 1 boundaries (GADM, 2015). I computed the total populations of each region for 2020 based on data from the Global Human Settlement Layer Population (GHS-POP) dataset produced by the European Commission's Joint Research Centre (Schiavina et al., 2023).

Precipitation

The precipitation observations are derived from the Climate Hazards Center InfraRed Precipitation with Station (CHIRPS) Precipitation dataset (Funk et al., 2015). I calculated the average population-weighted z-score of each region's precipitation for every month of the study period based on historical records from 1981 to 2023.

Air Temperature

I used a blend of two global air temperature datasets to acquire high-resolution (0.05°) data from 1980 to 2023 – The Climate Hazards Center Infrared Temperature with Stations ($CHIRTS_{\max}$) product (Funk et al., 2019) and the fifth generation of European ReAnalysis (ERA5), produced by the European Centre for Medium-Range Weather Forecasts (ECMWF) (Hersbach et al., 2020). The Climate Hazards Center produces a harmonized product, which has not yet been published. The following are the methods used to create it – First, hourly ERA5 2-meter temperature data is extracted to compute daily maximum and minimum temperatures. These values are then downscaled to match the daily resolution of the $CHIRTS_{\max}$. Monthly climatological mean and standard deviation are then calculated from 1983 to 2016 for ERA5 $T_{\max}$, ERA5 $T_{\min}$, and CHIRTS $T_{\max}$. A correction factor is determined by subtracting the mean ERA5 $T_{\max}$ from the actual value and dividing the result by the standard deviation of ERA5 $T_{\max}$. This factor is multiplied by the CHIRTS $T_{\max}$ standard deviation to obtain an offset. CHIRTS-ERA5 $T_{\max}$ is computed by adding the CHIRTS monthly mean and the offset. Monthly CHIRTS-ERA5 $T_{\max}$ is calculated by averaging daily CHIRTS-ERA5 values. Finally, I calculated regional population-weighted z-scores for CHIRTS-ERA5 $T_{\max}$ using the full historical record from 1980 to 2023.

Conflict

The Armed Conflict Location and Event Dataset (ACLED) provides detailed, disaggregated information on the type, agents, location, date, and other various attributes of political violence events, demonstration events, and other non-violent, politically relevant activities in every country and territory globally (Raleigh et al., 2010). ACLED focuses on tracking violent and non-violent actions perpetrated by or affecting political agents, including governments, rebels, militias, identity groups, political parties, external forces, rioters, protesters, and civilians. Event types include battles, protests, explosions/remote violence, and violence against civilians.

My analysis considers the total number of events and fatalities per 1,000 people recorded monthly in each region as a proxy for conflict severity. I used monthly average regional z-scores of each measure based on the historical ACLED record from 1997 to 2023.

3.2.3 Theoretical Model

The gravity model is a statistical method that predicts the flow of goods, services, people, or capital between two locations. The traditional model is based on the economic size (or population stock in the case of human migration) and the distance between locations (Anderson, 2011). The model is derived from the analogy of Newton's law of universal gravitation, which states that the force of attraction between two objects is directly proportional to the mass of goods, labor, or other elements of production between the origin, Y_i, and destination, E_j, while the potential flow is minimized by, or inversely proportional to, the square of the distance between them, d_{ij}^2. The equation is as follows,

$$X_{ij} = \frac{Y_i E_j}{d_{ij}^2} \tag{3.1}$$

where X_{ij} is the predicted flow of goods or labor between i and j. According to spatial interaction theory, individuals aim to maximize migration benefits while minimizing costs regarding the reason for and distance of migration (Garcia et al., 2015). Additional specifications can be incorporated into the model to improve its fit and accuracy in predicting migration flows. While some factors may add friction that impedes migration flow, such as transportation costs, others encourage movement between locations through added benefits such as economic opportunities or better living conditions. The extended equation is represented as follows,

$$X_{ij} = \alpha + \beta_1 Y_i + \beta_2 Y_j + \beta_3 D_{ij} + \beta_4 [Z_{ij}] + \gamma_1 (P_i) + \gamma_2 (P_j) + \epsilon_{ij} \tag{3.2}$$

where X_{ij} is the bilateral flow between location i and country j, Y_i and Y_j represent the mass (e.g., population) of the two locations, D_{ij} is the distance between them, and $[Z_{ij}]$ is a vector of other variables that can supplement the model to capture additional factors that affect migration flows. The β coefficient terms measure quantitative changes in the observable factors.

The equation also includes fixed effects for each location, defined by P_i and P_j, which capture unobserved time and location-specific characteristics that affect migration flows, and γ_1 and γ_2 are the associated coefficients. The error term, ϵ_{ij}, represents the random variation in population displacement flows that the model's variables do not explain.

Finally, the Poisson pseudo-maximum likelihood (PPML) method is a reliable way to estimate the gravity model. This method effectively handles zero values and heteroskedasticity in migration data. PPML works by maximizing the likelihood that observed migration flows come from a Poisson distribution. Thus, the approach ensures robustness when incorporating additional complexities such as zero migration flows and fixed effects.

3.2.4 Empirical Model

I constructed a suite of gravity models with different specifications, beginning with a standard gravity model with only region population and distance between regions, and then iteratively added subsequent models with additional explanatory variables. The distance between regional centroids is calculated in kilometers. Movements within regions were given a distance of 10 kilometers to avoid zero measurements. Population and distance were expressed in logarithmic form for all models as the Akaike Information Criterion (AIC) value was lower than a z-score estimation. Successive models included weather variables – monthly regional average precipitation and temperature z-scores – and monthly conflict variables – the z-score of the total number of events and fatalities per 1,000 people in a region. To evaluate temporal lags and compounding effects driving migration patterns, I evaluated the influence of present weather and conflict conditions followed by successive models with the addition of lagged observations of one to two months. Figure 3.5 is a conceptual diagram of how lagged variables are added to each observation, representing how compounding pressures such as two to three months of anomalously low rainfall or prolonged conflict can further exacerbate a situation and incite populations to move. The decision and ability to migrate may also take individuals longer than a month after a stressful event occurs.

I also tested how the interaction between the present climate conditions for each month and the percentage of the population that follows a certain livelihood type in each region affects migration flows. Month dummy variables, as well as region and year fixed effects, were included in each model. The dependent variable is the total population that moved between regional administrative zone boundaries in a given month. To avoid multicollinearity, I excluded one year (2023) and one month (January) from the model estimations. Region fixed effects with high multicollinearity were also automatically omitted from the model estimation. The percentage of the population with urban livelihoods interacting with the climate variables was excluded and designated as the reference category, allowing for a comparison of the effects of various non-urban livelihoods on migration relative to urban settings. All fitting procedures were computed using the Gravity Modeling Environment (GME) Python package.

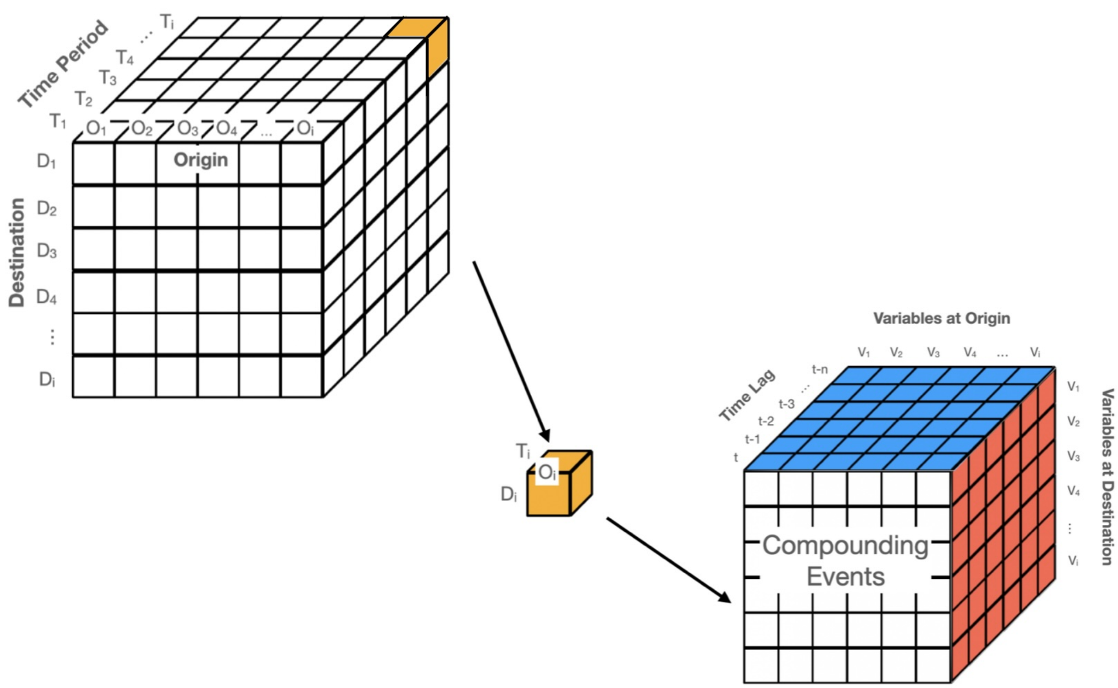

Figure 3.5: A conceptual diagram of the gravity model estimation between origin and destination regions with the addition of explanatory variables and their lags to account for compounding effects.

3.3 Results

3.3.1 Baseline model findings

In the base PPML model (model 1 of B.1), the coefficient for the logarithm of distance (-1.521) provides insights into the impact of geographical separation on migration. Specifically, for every 1% increase in the distance measured in kilometers between origins and destinations, the number of migrants moving between the locations decreases by approximately 0.015. The coefficient's high statistical significance ($p < 0.001$) and its consistency across different model specifications reflect the strong negative relationship between distance and migration. This finding confirms the hypothesis that increased distances significantly deter migration due to considerable challenges and costs associated with longer migration routes.

Contrary to distance, the coefficients for the logarithm of the population at both the origin and destination displayed no significant influence on migration patterns in any of the model specifications. In the base model, the coefficient for the logarithm of the departure (origin) population (0.062) indicated a marginal and statistically insignificant decrease in the number of migrants by 0.0062 for every 1% increase in the origin population. Similarly, the coefficient for the logarithm of the destination population (0.765) suggested a modest and equally non-significant increase of approximately 0.0076 migrants for every 1% increase in the destination's population. Although intuitive, these subtle effects lacked statistical significance and thus do not support strong conclusions about the role of population size in driving migration flows in this case study.

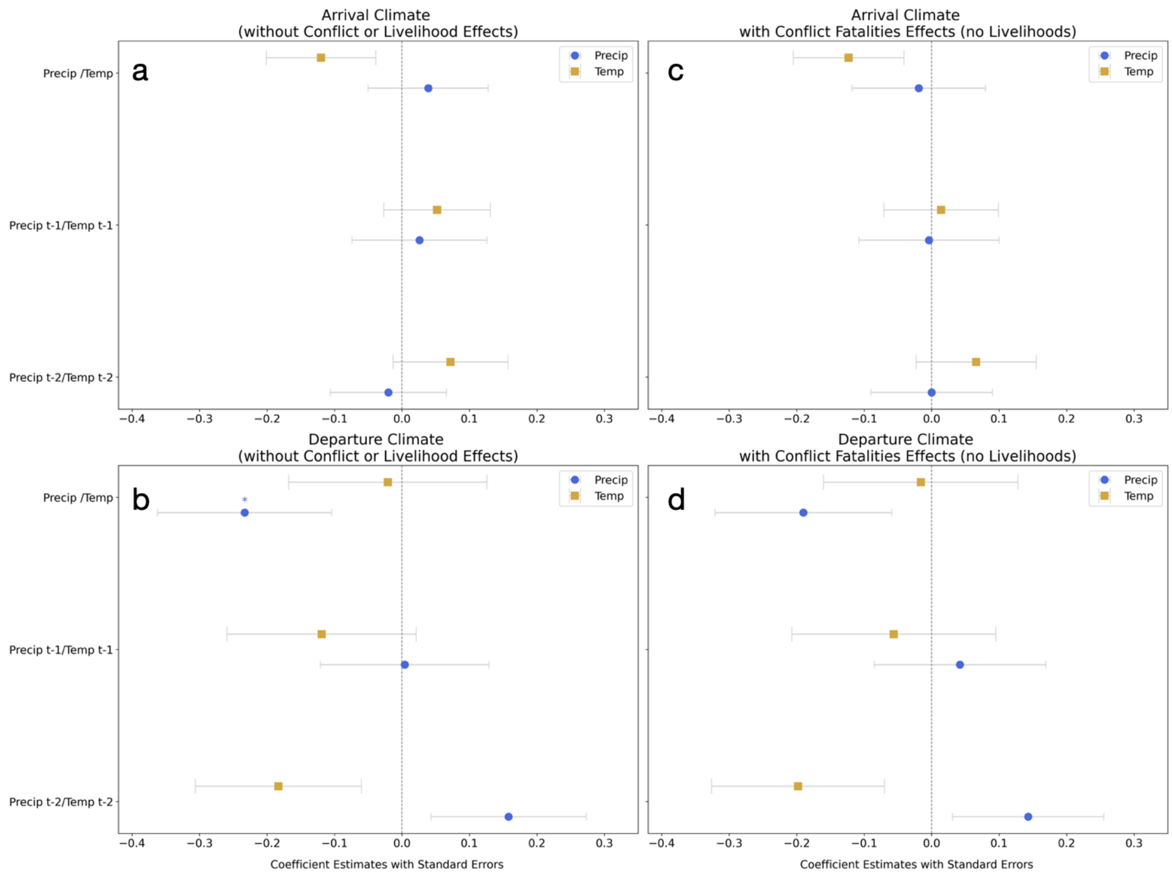

Figure 3.6: Coefficient estimates with standard errors for arrival (a) and departure (b) climate effects without conflict or livelihood effects (model 4 from B.1) and with conflict fatalities added for arrival (c) and departure (d) estimates (model 10 from B.1). The lagged inputs are labeled with "t-" and the number of months. Significant coefficients are marked with an asterisk, indicating a p-value of 0.001, 0.05, or 0.1.

3.3.2 Anomalous rainfall, particularly in pastoralist zones, is a significant driver of migration

Next, we turn to the analysis of environmental and livelihood factors. When considering the effects of weather alone with lags of up to 2 months (model 4 from B.1), the coefficient for the z-score of current departure (origin) precipitation is -0.233 (see Figure 3.6b), indicating a moderately statistical relationship with migration outcomes ($p < 0.1$). This coefficient signifies that for every one standard deviation increase in

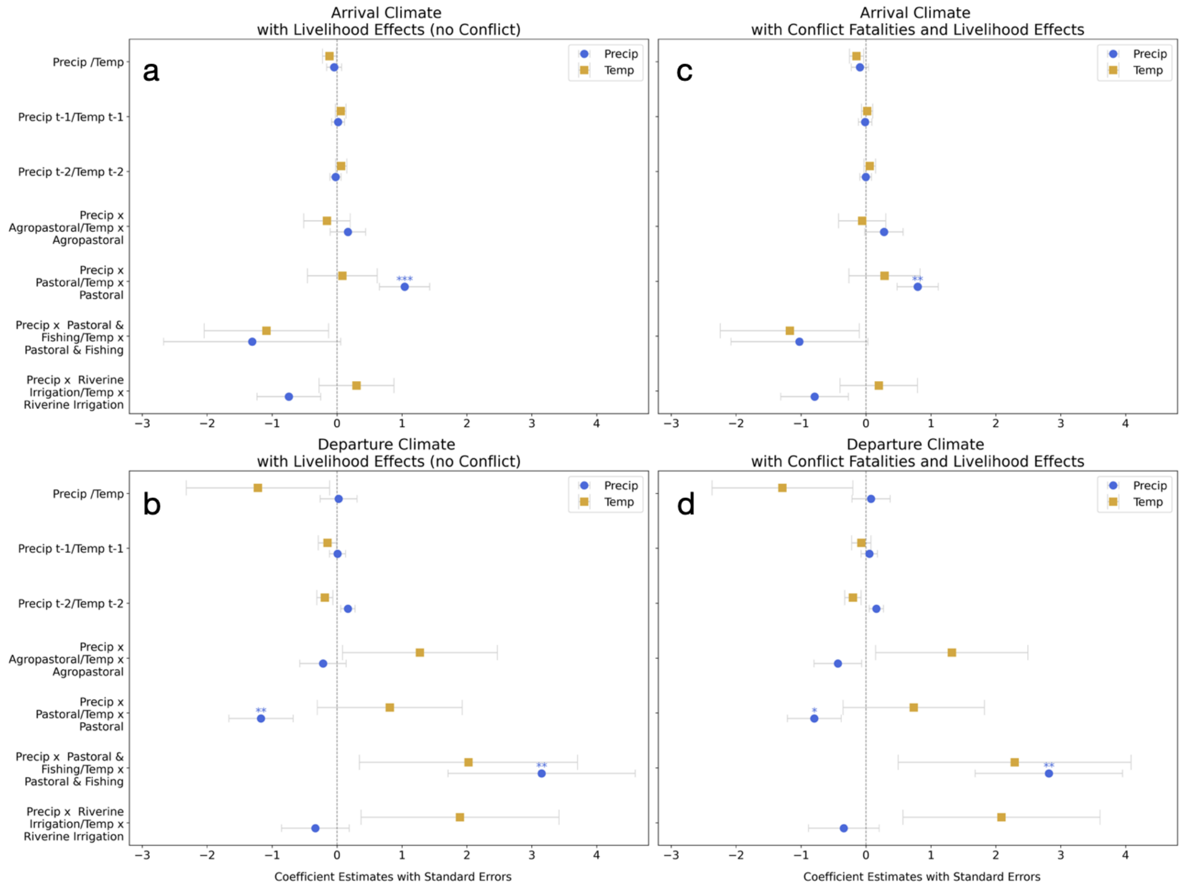

Figure 3.7: Coefficient estimates with standard errors for arrival (a) and departure (b) climate effects and livelihood interaction terms without conflict effects (model 13 from B.2) and with conflict fatalities added for arrival (c) and departure (d) estimates (model 19 from B.2. The lagged inputs are labeled with "t-" and the number of months. Significant coefficients are marked with an asterisk, indicating a p-value of 0.001, 0.05, or 0.1.

precipitation above the mean at the origin, migration counts are expected to decrease by 0.233. This result suggests that adverse weather conditions deter individuals from initiating migration, potentially due to the enhanced risks associated with travel under such circumstances. The moderate level of statistical significance, however, points to a noticeable but not overwhelmingly strong relationship between precipitation and the decision to migrate when the weather drivers are considered alone. Air temperatures alone were not significant across the various models. This may be because high air temperatures, while physically uncomfortable, do not directly or as strongly influence the decision to migrate in the short term (0 to 2 months) as they may take a longer time to affect livelihoods.

I will now explain how multiplicative effects between weather and livelihood zones impact migration patterns. When the percent of the region's population that follows a certain livelihood is added (model 13 from B.2 and Figure 3.7), the coefficient for the z-score of current origin precipitation drops out as no longer significant, while three of the variables for weather interacting with livelihood types stand out.

The z-score of current arrival (destination) precipitation interacting with the percent of the population that is pastoral is highly significant ($p < 0.001$) with a coefficient of 1.042, and the coefficient of arrival precipitation is -0.043. With an average regional percent population that is pastoral of 34.13%, the effect of a 1% change in the standard deviation of precipitation is about 0.31 migrants, or in other words, an approximately 31% increase in migration for a one standard deviation increase in precipitation, holding the pastoralist livelihoods constant. This is calculated by $-0.043 + (1.042 \times 0.3413)$. With a 10% increase in pastoralists at the arrival, this effect increases to nearly 35%.

On the other hand, at the departure locations, two distinct patterns emerged. The interaction between departure precipitation and the percentage of the pastoral population showed a notable inhibitive effect on migration with a coefficient of -1.170. As the coefficient of departure precipitation is 0.024, this interaction term can be interpreted as an approximately 37.5% decrease in migration for every one standard deviation increase in precipitation at the departure region, holding the pastoralist livelihoods constant, as calculated by $0.024 + (-1.170 \times 0.3413)$. This substantial effect stresses the strong relationship between environmental conditions and socio-economic characteristics of the destination region, highlighting how climatic factors particularly amplify migration responses in areas with significant pastoral communities. Enhanced precipitation might make local conditions more favorable for pastoral activities, thereby reducing the push factors for migration from these areas.

Similarly, for the interaction of precipitation with pastoral/fishing populations, a coefficient of 3.159 indicates that a dramatic increase in migration occurs under the combined influence of increased precipitation and a significant presence of these livelihoods. Holding the percentage of regional populations with pastoral/fishing livelihoods constant at the mean (7.3%), the effect of a one standard deviation change in precipitation in the origin location results in a 25.5% increase in migrants and a 10% increase in pastoralist/fishing livelihoods would lead to an approximately 28% increase in migrants leaving. The results reflect how adverse conditions, possibly flooding (especially in late 2023) or loss of fishing and/or grazing lands, prompt a significant migration response.

3.3.3 Conflict has a strong effect on migration over and above that of weather

In analyzing conflict's impacts on migration patterns, the coefficients associated with the z-scores of conflict fatalities per 1,000 people reveal important influences at both departure and arrival locations (Figure 3.8). According to the model specifications with both weather and conflict fatalities effects but no livelihood effects (model 10 from B.1, the z-score of the number of fatalities per 1,000 people is very significant for the arrival region at the current period ($p < 0.05$) as well as at a lag of one month ($p < 0.05$). Similarly, the current departure fatalities effect is also highly significant ($p < 0.001$). At the departure locations, the positive coefficient for current fatalities suggests that an increase in fatalities by one standard deviation is associated with 0.174 more migrants. This indicates that higher levels of violence push more individuals to flee from these areas. On the other hand, at arrival locations, both the current and lagged one-month fatality

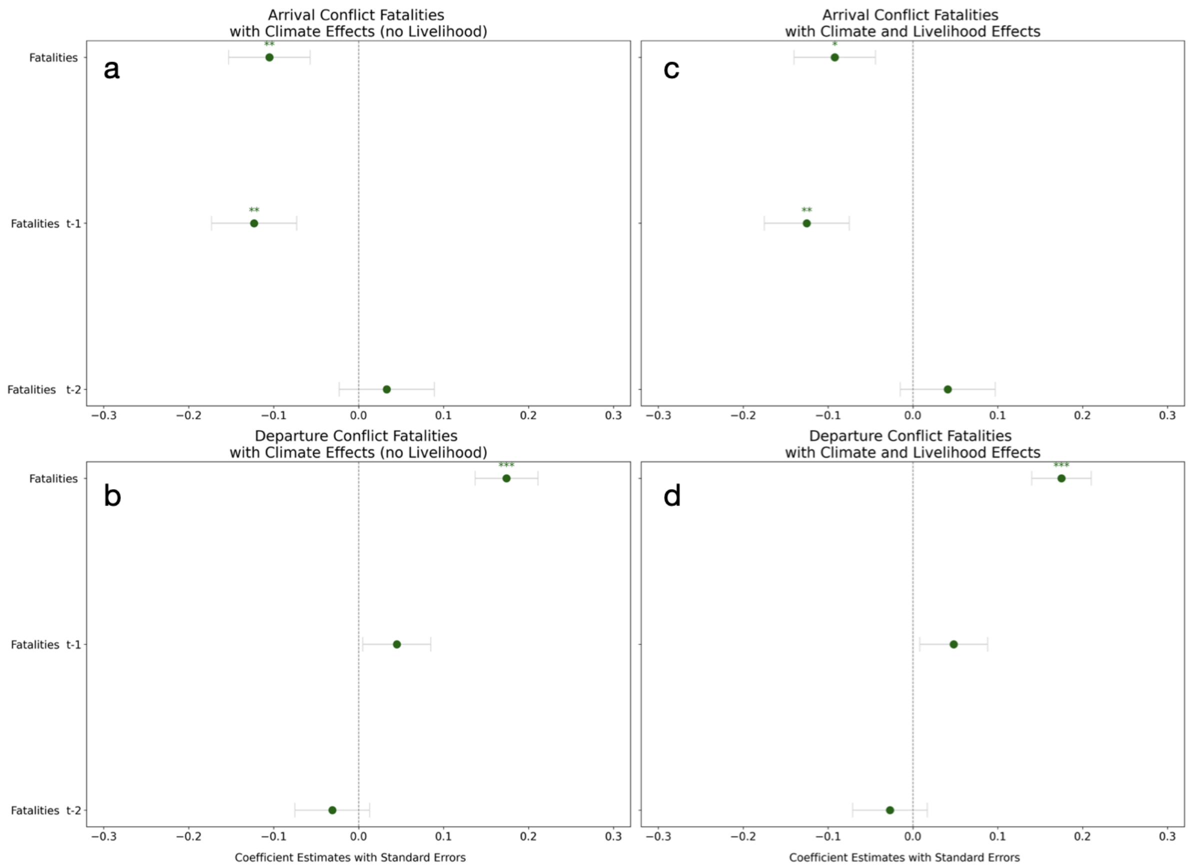

Figure 3.8: Coefficient estimates with standard errors for arrival (a) and departure (b) conflict fatalities effects with climate effects and no livelihood inputs (model 10 from B.1) and with livelihood interaction terms added for arrival (c) and departure (d) estimates (model 19 from B.2). The lagged inputs are labeled with “t-” and the number of months. Significant coefficients are marked with an asterisk, indicating a p-value of 0.001, 0.05, or 0.1.

rates exhibit negative coefficients (-0.105 and -0.123, respectively) for each standard deviation increase in fatalities. These findings suggest that higher immediate and recent past violence at potential destinations deters migrants from moving to these regions. Note that I show the effects of the number of conflict events per 1,000 people per month and region as a robustness check in the appendix (Figure B.3), where the results indicate similar levels of significance.

3.3.4 Overall interpretation

The models reveal nuanced and significant influences in examining the effects of climate, conflict, and their interactions with specific livelihood demographics on migration patterns (model 19 from B.2 and Figure 3.7). First, the standalone climate variables, including both current and lagged precipitation and temperature, did not yield statistically significant effects. This suggests that climate variables alone may not directly predict migration decisions without considering the context of local economic livelihoods or conflict scenarios. The coefficient of -0.092 with a marginal significance level ($p < 0.1$) for current arrival fatalities suggests that an increase in conflict fatalities tends to slightly reduce migration into those areas. More pronounced is the effect of fatalities from the previous month (-0.125, $p < 0.05$), suggesting that the recent history of conflict remains a significant factor deterring migration, possibly due to lingering safety concerns and destabilized conditions. An increase in fatalities at the departure location (coefficient of 0.175 with $p < 0.001$) significantly increases migration, suggesting that violence pushes residents to flee from these areas in search of safety or stability.

The interaction term for arrival precipitation with the percentage of the pastoral population in a region shows a significant positive effect (coefficient of 0.976, $p < 0.05$). This suggests that increased precipitation, when combined with a higher proportion of pastoralists at the destination, enhances migration inflows, possibly due to improved grazing conditions or other favorable factors for pastoral activities. The negative coefficient of -0.763 ($p < 0.1$) for the interaction at the departure location suggests that increased precipitation coupled with a high percentage of pastoralists reduces migration. This could reflect that better water availability might temporarily improve local conditions for pastoralism, decreasing the necessity to migrate. The coefficient for departure precipitation and combined pastoral/fishing populations is high with a coefficient of 2.818 ($p < 0.05$), indicating a strong push factor, where increased precipitation exacerbates conditions negatively for combined pastoral and fishing communities, likely worsening local economic conditions and driving migration.

The full regression results tables with 19 different model specifications are displayed in the appendix. Among the models without livelihood effects (models 1 to 10: B.1), the version that includes weather with lags of up to two months and conflict fatalities with lags of up to two months has the lowest AIC and, therefore, the best fit. With the addition of livelihood interaction terms (models 11 to 19: B.2), the AIC value decreases overall for all models, and similarly, the version that includes weather lags up to two months, and conflict fatalities lags up to two months has the lowest AIC and therefore is the best fit across all model versions.

3.4 Discussion

3.4.1 Migration as a livelihood adaptation strategy

While I find that weather as a whole is not a primary driver of migration, it does play an important role in places where people are experiencing certain circumstances. Livelihood zones differentially affect how precipitation impacts migration. Most notably, pastoral and pastoral/fishing regions are significant drivers of migration. I find that precipitation has a larger effect on pastoralists, whereby individuals are likely to leave due to drought or reduced rainfall and move towards places that are experiencing more rain. Yet, while precipitation acts as a push and pull factor, specifically in places that are pastoral (and pastoral/fishing), in areas with agropastoralists, precipitation was not a significant marker of in- or out-migration. Therefore, the places where we would expect the climate to matter the most in terms of immediate push and pull factors are largely based on where individuals can move with their productive assets.

My findings align with the broader literature on how migration is often framed as a livelihood strategy for smallholder households in rural areas. Economic, social, and cultural factors shape migration decisions and their impact on household livelihoods (Greiner and Sakdapolrak, 2013). As environmentally driven migration can fall along a spectrum from forced to more voluntary forms of mobility (Hoffmann et al., 2022), access to productive land and economic opportunities strongly influence movement patterns in East African countries (Willett and Sears, 2018). During slow-onset climate hazards such as drought, migration patterns may resemble traditional practices as individuals seek to diversify their livelihood options. Circular migration between rural and urban areas is common in East Africa, especially when economic activities are tied to the local environment (Willett and Sears, 2018). This strategy may become more prevalent with climate change as natural resources decline in these regions.

Drought has been shown to significantly impact rural households dependent on agriculture in neighboring Ethiopia, leading to crop damage and drinking water shortages for humans and livestock (Hermans and Garbe, 2019). These stressors can increase mobility among affected households, triggering short-term migration to nearby locations to address immediate needs such as food insecurity. However, understanding the impacts of drought on livelihoods and migration requires considering a broader context rather than focusing solely on drought as a single driver. The decision to migrate may not be directly caused by drought but is heavily moderated by it. Other factors, such as how to cover food shortages, employment opportunities, or government support through food aid, also play an important role (Hermans and Garbe, 2019). In Tanzania, environmental shocks, such as extreme weather events, have a significant impact on migration and increase the probability of having a household member absent (Blocher et al., 2024). These shocks have an immediate impact on household livelihoods as they lead to livestock losses and crop damage. Conversely, non-environmental shocks, which include economic, social, political, or health-related disruptions, also play a role in influencing migration patterns, though these shocks can be idiosyncratic and therefore make migration less consistent (Blocher et al., 2024). Apart from migration, farmers in arid and semiarid regions may adopt other coping and adaptive strategies, including crop diversification, input adjustment, water management, asset depletion, or forms of income diversification that do not require moving, to sustain their livelihoods during periods of stress caused by extreme weather conditions (Ashraf et al., 2021). Households may also seek support from social networks or make changes in food provision and consumption before or in addition to migrating (Hoffmann et al., 2022).

Rangeland and pastoral livelihood zones in the East African Horn have been experiencing increased environmental degradation due to factors such as land fragmentation, overexploitation, extreme weather conditions, and climate variability (Pricope et al., 2013). Due to these stressors, there has been an increasing susceptibility to environmentally driven pastoral conflicts in the region as communities compete for dwindling resources. With shrinking grazing land, pastoralists and agropastoralists respond by traveling further distances.

Griffith et al. (2023) discuss the value of a "livelihood constellation" perspective in understanding the patterns of migration and livelihood in Somalia, referring to how households engage in multiple activities, which each influence one another to sustain their livelihoods. These economic activities can include traditional, seasonal, and environmental migration, as well as other forms of economic activity, such as pastoralism or small-scale trading. Finally, Sakdapolrak et al. (2024) emphasize the importance of considering livelihoods in the context of migration and climate change adaptation. They confirm my findings that there are differentiated impacts on households based on place and social scale. Livelihood decisions to migrate are shaped by socioeconomic conditions, seeking better livelihood security through adaptive actions that aim to enhance coping capacity, reduce vulnerability, and improve asset bases over time.

3.4.2 Displacement pathways may be shaped differently by short-run shocks compared to prolonged events

While I did find that there were immediate effects of migration due to precipitation, air temperatures were not a significant driver in the context of my study region and time period. This could be because it may take a longer period of time for temperatures to result in a bad harvest or negatively affect livestock health. The literature on heat stress as a driver of migration is thin. While Mueller et al. (2014) find that over the long-term, heat stress can increase the migration of men from rural areas due to negative effects on farm and non-farm income, there is scant evidence that short-term heat waves would result in migration. Additionally, in a review of the heat-migration research nexus, Issa et al. (2023a) conclude that heat may not be a driver of migration in all circumstances, and moderating elements include other climatic factors, agricultural productivity, economic opportunities, and demographics. They also find that none of the analyzed literature reported a "temperature threshold" above which migration is inevitable. Using land surface temperatures, instead, could reflect when crop or grazing seasons fail and, therefore, indicate when pressures are higher for people to move elsewhere.

I would also expect that droughts and floods would impact migration decisions differently depending on the time scale analyzed. Mobility as a response to slow-onset environmental hazards such as droughts is challenging to quantify due to the indirect effects between livelihood stability and environmental change (Oakes et al., 2023). While flash droughts or flash floods can lead to immediate population displacement, the effects of prolonged stressors from multi-year drought or frequent flooding may not have shown up in my analysis as affecting migration, particularly when farmers or pastoralists have developed long-term coping mechanisms in their place of residence.

Assessing patterns on a rolling three-month average rather than a per-month basis could be a way to test how ongoing stressors from environmental drivers affect displacement. In a study by Backhaus et al. (2015), the authors suggest that future research analyzes the relative contributions of abrupt versus gradual changes in climate.

Similar patterns may be associated with conflict as well. As discussed in Section 3.1.1 on "Climate, Conflict, and Migration," extreme weather can provoke conflict. Regardless of the origin, however, conflict is a more salient situation overall and has a universal effect on all of the country's population rather than only impacting specific livelihood groups. It is possible, however, that ongoing conflict would have a different effect on migration compared to immediate shocks as populations must learn to cope with their surroundings. Future analyses could explore how conflict-migration trends relate to the temporal unit of analysis.

3.4.3 Limitations and Future Research Opportunities

Several limitations of this study suggest prospects for further inquiry. First, it is important to acknowledge issues with the Somalia internal displacement dataset itself. The accuracy of population redistribution of different locations based on internal displacement movements depends on the precision of PRMN reports. These reports are based on ground informants instead of statistically representative estimation methods. Although the PRMN project captures both departures and returns, it is possible that the returning flows are reported less systematically (Warsame et al., 2023).

Next, it was not possible to characterize migrant individuals without the availability of demographic information on, for example, age, gender, or wealth. Fanning (2018) argues for the importance of gender-sensitive research on displacement in Somalia, capturing the specific needs of different populations, particularly with respect to safety, services, and livelihood opportunities. Researchers in the field of human mobility in the context of climate change call for producing differentiated knowledge that accounts for groups that are particularly vulnerable, including young or elderly populations, as well as in terms of access to resources, work, services, and impacts on health, both physical and mental for those that are mobile and trapped (Oakes et al., 2023). In my model estimation, I was unable to account for immobile populations. Benveniste et al. (2022) find that lower-income and resource-constrained populations globally may be less likely to be able to migrate in the future due to climate change. These populations will face additional vulnerabilities and exacerbated poverty from staying in place. Research agendas that also prioritize the concerns of trapped populations are needed.

There may also be confounding factors that I did not consider, which could have a larger role in driving migration behaviors. For instance, in a study by Owain and Maslin (2018), the authors determined that climate variations, measured by the Palmer Drought Severity Index and the global temperature record, played little or no part in the causation of conflict and displacement of people in East Africa over the last 50 years. Rather, they attribute such trends largely to rapid population growth, low or falling economic growth, and political instability.

Another opportunity for further analysis is to incorporate food security as another branch of migration drivers. Compounding events raise systemic risks to food systems and affect displaced populations already vulnerable to climate variability (Thalheimer et al., 2023a). (Tuholske et al., 2024) present a conceptual framework for linking the climate-food-migration nexus in low- and middle-income countries. While the authors examine the "agricultural pathway" hypothesis as a possible mechanism to explain the food security and migration relationship, particularly in explaining rural out-migration as an adaptation strategy, they also emphasize the need for more empirical evidence and fine-grained data to determine the direct connections. Additional parameters in the gravity model estimation of migration in Somalia, such as food prices or access to food markets, may yield new insights into how agricultural livelihoods relate to mobility.

Finally, the 2023 torrential deyr rain season (October to December) in Somalia led to severe flooding, which caused extraordinary levels of internal displacement as seen by the large spike towards the end of the time series of Figure 3.1. According to a situation report by OCHA (2023), roughly 2.48 million people were affected by the floods, including 1.2 million displaced people. Incorporating flood extent and impact data into the model estimation, alongside drought severity indices to capture strong drought years like in 2017 and 2022, could provide more direct evidence of how and when disasters lead to mass displacement.

3.5 Conclusion

In this chapter, I offer a nuanced, quantitative view of climate, conflict, and socio-economic-driven migration. With access to a uniquely high spatiotemporal resolution dataset of internal displacement in Somalia over a seven-year period, I derive novel insights into how environmental characteristics and socio-economic status influence internal displacement. While my research contributes to a thread of researchers that have used the PRMN dataset in their work (Oh et al., 2024; Yuen et al., 2022; Pham and Luengo-Oroz, 2022; Thalheimer et al., 2021a, 2023b) (see "Evidence from Somalia," Section 3.1.1 for details on each study), none thus far have implemented a gravity modeling approach. Using this method, I distinguish whether singular and combined elements may explain the challenges displaced populations face and differentiate between push/pull factors. Precipitation can be an important driver of both in- and out-migration, though the influence varies widely by livelihood zone. Regions with a greater prevalence of pastoral or pastoral/fishing populations and anomalous rainfall have an outsized effect on migration compared to other livelihood types interacting with precipitation. While it is unsurprising that conflict is a strong driver of migration, I quantify the magnitude to which violence triggers migration above that of anomalous weather conditions.

The PRMN dataset exemplifies the type of rich, consistently collected information that other countries need to better monitor the risks and vulnerabilities of specific populations. We must also continue refining quantitative approaches that enhance our awareness of how certain stressors impact migration and feedback to one another. An improved understanding of historical and current drivers of internal displacement can guide efforts to project future trends, inform policy, and aid interventions under a changing climate.

Chapter 4

The Application of Large Language Models for Multi-hazard Disaster Event Classification

Abstract Disasters pose a significant threat to lives, livelihoods, and development worldwide. The consequences can be even more damaging when disasters happen in succession or overlap. Rapid and accurate categorization of disaster events is critical for effective disaster response and risk-reduction efforts. However, the growing volume of disaster-related news and reports presents challenges for timely analysis and insight generation. This study utilizes recent advancements in artificial intelligence, specifically large language models (LLMs), to automatically classify news articles and reports by disaster type and assign relevant topical tags. Applying OpenAI's GPT-3 language model to a large dataset of articles from ReliefWeb, a leading humanitarian information portal, I demonstrate the suitability and value of AI-assisted multi-label classification for disaster news streams. I test the model with zero- and few-shot prompting and then fine-tune it using historical ReliefWeb articles and their disaster labels. I analyze per-

formance across different disaster types using three evaluation metrics: subset accuracy, Hamming loss, and Jaccard similarity. The fine-tuned model responds more appropriately according to the prompt compared to the base model, though it sometimes leans towards over-classifying multiple tags or confuses similar types of events. This chapter presents important implications for improving the specificity and timeliness of disaster monitoring systems.

This is the first study to apply LLMs to perform multi-label classification of disaster-related news at scale. The approach suggests promising avenues to accelerate the synthesis of unstructured text into structured, actionable data to inform disaster risk management. I introduce an AI-driven solution that enables more efficient tracking of disaster events, impacts, and trends to support rapid needs assessments, resource allocation decisions, and strategic planning for long-term risk reduction by humanitarian organizations, governments, and other stakeholders. The study illustrates how AI can be used for good to improve global disaster resilience and social welfare.

4.1 Introduction

The world has witnessed a substantial increase in the frequency and severity of climate-related disasters in recent years. This alarming trend is closely linked to shifts in our climate, marked by increasingly erratic and extreme global temperatures and rainfall patterns (Thomas and López, 2015). The consequences of disasters are intensifying, fueled by the simultaneous factors of population growth, expanding development, and an escalating vulnerability attributed to aging infrastructure AghaKouchak et al. (2020). As a result, communities worldwide are facing unprecedented challenges in terms of human casualties and displacement, economic losses, and long-term social and environmental repercussions.

Moreover, there has been a growing number of multi-hazard and compound events, which are characterized by the co-occurrence of hazards that may interact or cascade upon one another (Claassen et al., 2023). Figure 4.1 highlights subregional vulnerabilities and differences in disaster occurrence, highlighting where certain compounding events have occurred over time. Multiple events transpiring in the same period and location can intensify the overall impact and place additional challenges on response efforts (Raymond et al., 2020; Zscheischler et al., 2020). Connected events often manifest in unpredictable and intense ways that outpace singular disasters and call into question traditional disaster management practices that may not be sufficient to meet new or additional demands (Cutter, 2018; van den Hurk et al., 2023). For instance, multivariate hydrological extremes such as sequential flood-to-drought events (Rezvani et al., 2023; Brunner, 2023), or heightened health risks from joint exposure to heatwaves and drought (Tripathy et al., 2023; Wang et al., 2023; Hao et al., 2022; Mukherjee and Mishra, 2021; Hao et al., 2018), generate complex humanitarian crises that require novel systems of risk reduction and mitigation.

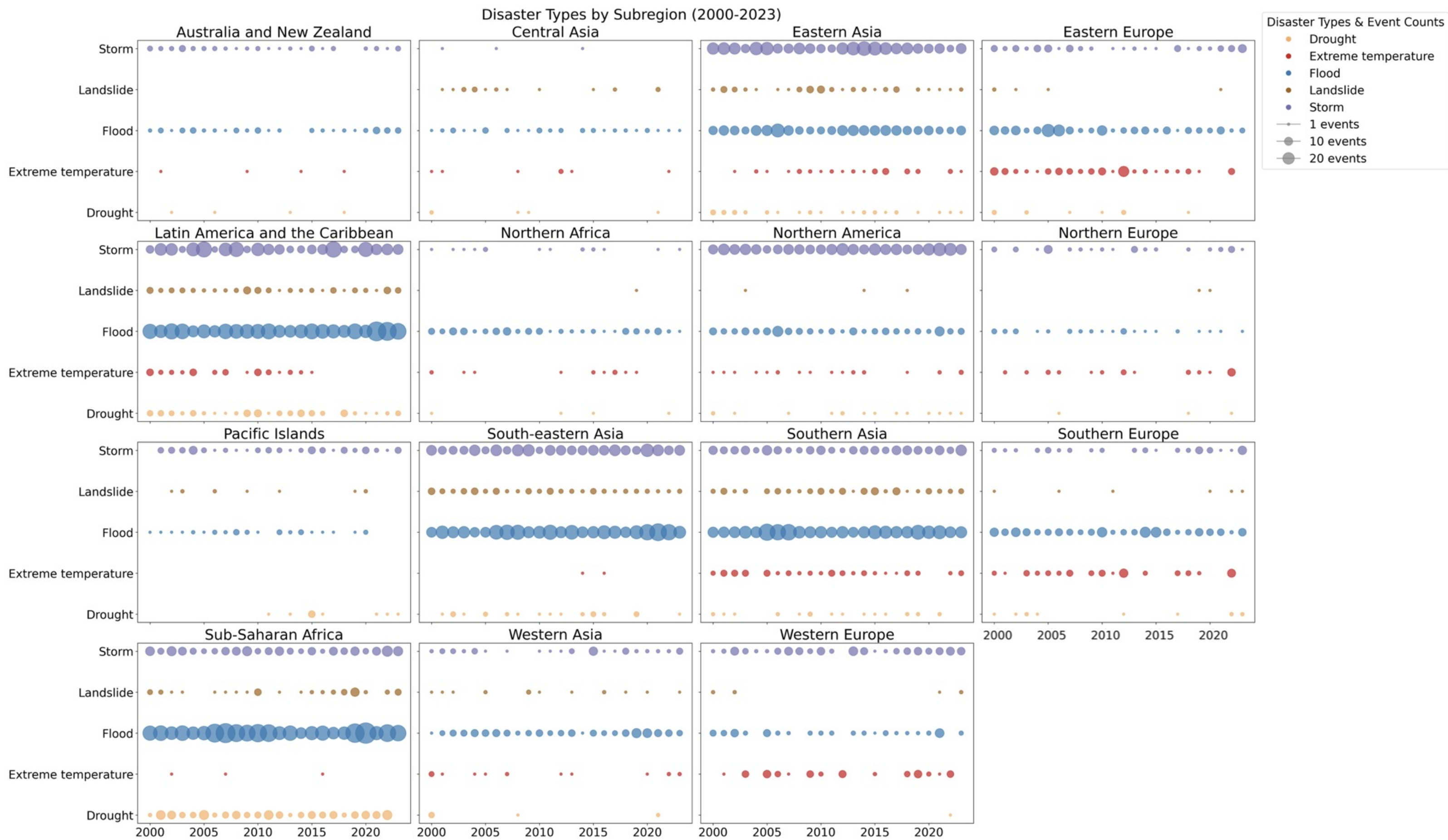

Figure 4.1: Overview of climate-related disaster frequency by type across global subregions from 2000 to 2023 according to the Emergency Events Database (EM-DAT). Each panel represents a different subregion, such as Latin America and the Caribbean, Northern Africa, and Eastern Europe. Within each panel, disasters are categorized by type: drought, extreme temperature, flood, landslide, and storm. Dot size indicates the number of events, with larger dots representing more events in a given year.

The compounding effects of these multi-hazard events can greatly strain emergency response resources and expose the vulnerabilities of our current disaster risk reduction strategies. Traditional approaches focusing on single hazards may prove inadequate for complex, interrelated risks. To effectively address the challenges posed by multi-hazard events, it is essential to have access to timely, accurate, and comprehensive information about these disasters. Humanitarian and media organizations produce news highlights, situational reports, maps, and infographics surrounding a disaster that inform timely and effective intervention. How information is transmitted from the epicenter of a disaster zone to the international community influences how events are perceived in their severity and prioritized for response.

It is crucial to produce rapid and accurately distilled updates to adeptly address and mitigate the added pressure of multi-hazard events. The information should facilitate a comprehensive understanding of the mechanisms and impacts of these events, guiding the formulation of effective preparedness and response strategies. Improving how we gather, analyze, and disseminate disaster-related information is paramount for building a more resilient world in the face of more complex emergencies.

Considerable obstacles persist in detecting and identifying the severity of multi-hazard events. Existing systems are limited in their capability to address the multi-dimensional aspects of such events, which can lead to delayed and inaccurate communication. Most information retrieval systems struggle to handle diverse formats of unstructured text data from various monitoring sources. This limitation is particularly significant for multi-hazard events, where the complexity of situations makes effective data analysis and information utilization more challenging.

A promising solution to the challenges in disaster management is the advancement of artificial intelligence (AI) tools, which offer innovative contributions to the field. Large language models (LLMs), advanced AI systems that are trained on vast amounts of text to perform various language-related tasks, can quickly process and analyze large volumes of text data, pushing the boundaries of disaster information collection and synthesis to a new level. While traditional methods of disaster management rely on human intervention and manual analysis, AI offers powerful automation, efficiency, and insights (Alam et al., 2020; Goecks and Waytowich, 2023).

Natural Language Processing (NLP), a field of computer science that combines computational linguistics and machine learning to enable computers to understand, interpret, and generate human language, is not yet widely used for detecting and evaluating extreme events (Tounsi and Temimi, 2023). In this chapter, I demonstrate a use case for AI-based NLP in disaster management. Specifically, I present a multi-label classification approach to identify multi-hazard disaster events from unstructured text derived from humanitarian news and reports.

As individuals, humanitarian organizations, and authorities collect, seek out, and disseminate information about a crisis, the process of sifting through the surge of news articles or social media posts can be laborious, slow, and inefficient Imran et al. (2020); Tamagnone et al. (2023); Pereira et al. (2023). With the rise of new technologies such as remote sensing and social media, the humanitarian sector is receiving abundant information. However, not all data and analytical tools are useful. Currently, the humanitarian community is struggling to meet early action needs due to the overwhelming amount of sources that need to be collected and analyzed to make informed decisions (Lentz and Maxwell, 2022).

Rocca et al. (2023) argue that humanitarian organizations, which work with large amounts of unstructured text from many different sources and formats, could dramatically benefit from tools that automatically analyze these data and derive actionable insights. However, the systematic adoption of NLP is presently limited in the humanitarian sector. NLP methods for large-scale digestion of unstructured text are still in their infancy and changing rapidly. Data scarcity and standardization remain an issue when NLP is used, and models can produce biases that pose ethical risks (Rocca et al., 2023).

AI innovations present new opportunities and challenges in processing incoming data and extracting key insights. In the context of disaster response and management, deep learning techniques for NLP can be used to detect crisis events, understand public reaction and sentiment, identify eyewitnesses, build situational awareness, communicate warnings and risks, assess damage, gather actionable insights, and verify information (Imran et al., 2020). Automated text summarization and event classification could better equip specialists to address all stages of disaster risk management: mitigation, preparedness, response, and recovery (Yela-Bello et al., 2021).

In this study, I investigate the potential role of LLMs in revolutionizing the synthesis of crisis information from diverse sources. I demonstrate how LLMs can offer disaster and humanitarian relief information management solutions. By showcasing the practical application of advanced AI models, I explore avenues to enhance the efficiency and effectiveness of information retrieval. The need for swift and accurate access to information during disasters underscores the significance of LLMs, as they can filter through data and identify essential details.

This chapter introduces an application of LLMs for performing multi-label categorization of disaster-related information. I discuss the steps to prepare these models and compare their performance with human-led classification. My comparative analysis sheds light on the value that LLMs provide as well as opportunities for improvement. Looking ahead, I propose paths for future research and applications. The versatility of LLMs and other emerging technologies in disaster information management opens up numerous possibilities. I contribute to the discourse by highlighting opportunities for innovation and cross-disciplinary collaboration among researchers and practitioners to use these tools for improved disaster response. In the following section, I will discuss the literature on various forms of disaster events and the state of AI applications for disaster risk management.

4.1.1 Literature Review

Disaster event terminology

Extreme impacts often result from converging multiple variables or events, even if none are individually extreme. This amalgamation of factors can significantly increase the severity of the impact (Leonard et al., 2014). Several terms can be used to differentiate complex hazard events in disaster risk reduction. Among these, a *compound event* is defined as a scenario where two or more drivers happen simultaneously or sequentially. The concurrence or succession of multiple drivers often results in situations that lead to increased difficulty in response and recovery than those caused by a singular driver. In turn, compound events often exhibit increased uncertainty and greater impacts (Raymond et al., 2020; Cutter, 2018).

Another term, *multi-hazard event*, can be distinguished as the presence of multiple natural or human-caused hazards within a defined area or time frame. While there is no prerequisite of interaction between these hazards, there may be interrelated effects (UNDRR, 2016; Claassen et al., 2023).

Other related terminologies include *consecutive disasters*, which represents when a series of natural hazard events occur in sequence, with each disaster potentially influencing the vulnerability and impacts of subsequent events. Dependencies between natural hazards can trigger these disasters or can occur independently but may overlap spatially and/or temporally. The word “consecutive” is used to describe disasters that happen one after the other, regardless of their size and impact. Consecutive disasters can have a range of effects, both tangible and intangible, such as damage to buildings and infrastructure, loss of life, reduced institutional capabilities, and decreased welfare (de Ruiter et al., 2020).

Similarly, *cascading hazards* describe when one primary hazard triggers a secondary hazard. Cascading hazards create a chain reaction of events that progressively gain complexity (Sakahira and Hiroi, 2021). The progression from a hazard to a disaster to a catastrophe is characterized by the interconnectedness of systems (e.g., the hazard, critical infrastructure, and preexisting vulnerabilities) and the escalation of consequences (Cutter, 2018). *Complex emergencies* describe disaster situations alongside political instability, conflict, and societal disruptions, which give rise to multi-dimensional crisis scenarios. *Connected extreme events* transpire when there is an inherent linkage between extreme weather or climate hazard events and their impacts due to shared societal mechanisms or physical drivers (Raymond et al., 2020).

Lastly, the term *paired events* has been used to represent two events of the same hazard type (e.g., floods or droughts) that occurred in the same geographical area several years apart. Studying paired events can reveal how exposure, vulnerability, and management strategies may have changed between the two events to identify patterns, trends, and lessons learned (Kreibich et al., 2022).

In this study, I use *multi-hazard event* when articles or reports discuss more than one hazard affecting a given region or population. I recognize, however, that the context of each event may differ. For instance, an article may include information about a flood and landslide that both happened in relatively the same time frame and location, while another article may compare two flood events from different time frames and locations. I use the term *multi-hazard event* as the main term throughout the rest of the chapter because I do not instruct the AI system to determine how the discussed disasters interact. Instead, I only instructed the system to identify the hazards discussed in a document.

Information retrieval for disaster management and humanitarian response

Crisis informatics is an emerging area of research focused on devising techniques and frameworks to process and classify extensive data related to crises, as disseminated across both mainstream and social media platforms (Alam et al., 2021). In response to the challenges of extracting and deciphering vast amounts of crisis-related data, Alam et al. (2021) introduced *CrisisBench*. This dataset merged eight different human-annotated social media datasets to allow for more effective, standardized, and context-sensitive training of machine learning models for tasks aimed at humanitarian situational understanding. Further, *CrisisBench* offers benchmarks for binary and multiclass classification tasks with various deep learning models.

Mishra and Saini (2014) exemplified how sentiment analysis and text mining methods can automatically identify interlinked events within disaster management. Utilizing AI algorithms, their research showed that improving the identification and evaluation of disaster-related occurrences, recovery initiatives, and public responses could lead to more efficient disaster response strategies. This could be achieved by facilitating prompt assessments and enhancing decision-making processes.

CrisisFACTS, introduced by McCreadie and Buntain (2023), was a data challenge motivated by the need to address limitations in evaluating crisis information and enhance situational awareness during emergencies. The findings from the 2022 pilot edition of *CrisisFACTS* showed promising advancements in automated technologies for extracting and summarizing online content during crises.

In another study, Padhee et al. (2020) demonstrate how deep learning methods using language models, including Bidirectional Encoder Representations from Transformers (BERT) and Robustly Optimised BERT Approach (RoBERTa), can effectively classify social media messages during crises. The authors categorized messages into three main categories: informativeness, intent type (whether a message refers to an individual, group, or organization "need" or "supply"), and the type of humanitarian aid ("Food", "Shelter", "Health" and "WASH" – Water, Sanitation, and Hygiene). The use of advanced deep learning and NLP technologies can automate the classification tasks that are traditionally time-consuming and impractical when done manually, thus facilitating more efficient humanitarian aid responses (Padhee et al., 2020).

Similar techniques can also be used to identify sub-events during disasters (i.e., noun-verb pairs that represent specific actions or incidents related to a particular event, such as infrastructure damage or missing persons) from social media messages. Driven by humanitarian organizations increasingly relying on social media for disaster response efforts, Rudra et al. (2018) use clustering methods and dependency parsing to detect and summarize sub-events from tweets. The authors assert that real-time processing over large datasets can deliver actionable insights. Arachie et al. (2020) develop an unsupervised learning framework to detect sub-events from tweets for retrospective crisis analyses on Hurricane Harvey in 2017 and the Nepal earthquake in 2015. A key advancement of their study is the introduction of a crisis-specific ontology for ranking sub-events based on their relevance to a disaster. They cluster these sub-events to organize, categorize, and evaluate how each component impacted different scenarios.

One initiative that implements AI techniques for humanitarian use is The Data Entry and Exploration Platform (DEEP). The organization, Data Friendly Space, developed this service, which aims to help organizations streamline the process of inter-agency response by gathering and maintaining documentation and structured qualitative information from data and reports (Belliardo et al., 2023).

Other research efforts have compiled multilingual humanitarian text datasets to test extractive summarization. Yela-Bello et al. (2021) presented "MultiHumES," the first collection of 50,000 multilingual documents, of which approximately 35,000 have been tagged with annotated informative excerpts provided by humanitarian analysts that can be used for training and evaluating extractive summarization models.

Fekih et al. (2022) later developed "HumSet," a novel multilingual, expert-annotated dataset designed for information retrieval and classification for humanitarian crisis response. It is one of the first datasets for the humanitarian context that offers the ability to test complex tasks in entry extraction and multi-label entry classification. With approximately 17,000 annotated documents covering multiple humanitarian emergencies from 2018 to 2021, "HumSet" can be used to train and benchmark predictive models for humanitarian text data (Rocca et al., 2023). The "HumSet" dataset is now used in the DEEP platform for NLP-assisted article tagging and summarization.

More recently, Tamagnone et al. (2023) built upon "HumSet," creating "HumBERT," which is a further customized multilingual dataset attuned to the complexity of the humanitarian domain (e.g., knowledge of specific vocabulary, topics, and concepts). The data corpus was collected from ReliefWeb, The United Nations High Commissioner for Refugees (UNHCR), Refworld, and the Europe Media Monitor News Brief.

Applications of natural language processing with AI for disaster management

Natural Language Processing (NLP) is a domain that combines linguistics, computer science, and artificial intelligence to process and analyze text and speech data. Common NLP tasks include extracting main topics from texts (*topic modeling*), identifying named entities such as locations and people (*named entity recognition*), extracting sentiment (*sentiment classification*), *automated text summarization*, language translation (*machine translation*), and automated *question answering*. In recent years, NLP techniques in disaster management have started to gain attention for use in trend analysis, event detection, and impact assessment (Tounsi and Temimi, 2023).

Predating the rise of and expanded access to LLMs, traditional NLP methods have been used to extract relevant text from mainstream and social media to facilitate building situational awareness during mass emergency events. Word embeddings, linguistic processing, geographical taxonomies, and supervised classification can be employed to retrieve information such as semantics, syntax, key details (e.g., locations and dates), and event impacts from articles or tweets (Petroni et al., 2018). Machine learning methods, including Naïve Bayes and Maximum Entropy, have also been used to classify features such as subjectivity, sentiment, register, and tone from tweets related to crisis events (Verma et al., 2021). Other classification approaches such as Support Vector Machines (SVM), Random Forests, Convolution Neural Networks, and Hierarchical Attention Networks have been tested to classify articles based on event types (Nugent et al., 2017). For instance, Sakahira and Hiroi (2021) used an SVM to learn and detect causal sentences within Japanese newspaper articles detailing cascading disasters. They constructed a network that visually represents the interconnected events by extracting these casual relationships. This approach can enhance the objectivity and comprehensiveness of analyses compared to traditional methods that rely on manual extraction of causal relations.

As LLMs have become more powerful in recent years, several studies have emerged to test their capabilities for disaster situation synthesis and knowledge building.Pereira et al. (2023) use a search engine (NeuralSearchX) and the General Pre-training Transformer 3 Language Model (GPT-3) to create summaries of crisis event situations by querying multiple documents, ranking their relevancy and then merging results from various sources. With few-shot learning and chain-of-thought prompting, the authors could generate comprehensive summaries without collecting training data, which can be particularly beneficial when working with inconsistent data structures.

Graph neural networks can also augment transformer-based language models, bolster understanding, and generate structured, synthesized information from disaster-related text. Ghosh et al. (2022) introduced a framework called GNoM (Graph Neural Network

Enhanced Language Model) to improve disaster-related multilingual text classification under limited supervision. GNoM addresses the challenges of data inadequacy and non-representativity found in disaster-related text data. Likewise, Goecks and Waytowich (2023) built DisasterResponseGPT, which leverages graph neural networks and LLMs to quickly generate action plans to user input disaster response scenarios. The algorithm offers an interactive means to explore options during the planning phase of a response.

While not a focus of this study, multiple data modes, such as text and imagery, can also be processed to categorize crisis events. NLP and computer vision can extract valuable insights from social media during disaster events that may outperform image-only or text-only approaches (Abavisani et al., 2020; Alam et al., 2020).

Beduschi (2022) acknowledge the potential benefits of AI for disaster management, including enhancing preparedness, response, and recovery efforts and shifting towards an anticipatory approach. However, they also recognize the significant risks associated with AI. These include algorithmic bias, challenges in ensuring the accuracy and reliability of training data, and concerns regarding data privacy. Finally, Nguyen and Rudra (2022) present another framework for classifying and summarizing disaster-related tweets from microblogs such as Twitter. In their study, the authors focus on interpretability in their model design. According to Nguyen and Rudra (2022), although classification explanations and rationales may reduce accuracy, interpretable models are essential for transparency, accountability, and fairness.

4.2 Methods

4.2.1 Data

Disaster Articles

ReliefWeb (https://reliefweb.int/) is a widely recognized humanitarian information service provided by the United Nations Office for the Coordination of Humanitarian Affairs (UNOCHA). Information posted on the site is monitored and collected from over 4,000 key sources, including humanitarian agencies, research institutions, and the media. Reports, maps, new press releases, and infographics are delivered on the website and accessible by an API at https://reliefweb.int/help/api. Launched in 1996, the service provides global content on a 24/7 basis.

Using the ReliefWeb API, I extracted all updates on the service that had been tagged with at least one disaster event. I excluded posts that only focused on conflict, health, or other non-disaster-related crises and general global updates such as climate change reports unrelated to specific events. In total, I extracted 301,306 articles. The time frame of the data set spans from March 1, 1981, to June 28, 2023. The initial data set included 3143 unique disasters labeled by ReliefWeb (e.g., Peru: Floods and Landslides - March 2023) and 2658 disasters labeled with a GLobal IDEntified (GLIDE) number, which is a globally common unique ID code for disasters. The GLIDE number "DR-2015-000137-MWI," for example, represents a drought in Malawi that was the 137th global recorded event in 2015. Figure 4.2 depicts the distribution of different disaster types recorded globally by GLIDE from 2000 to 2023. Meanwhile, Figure 4.3 presents the number of countries that have experienced a certain number of major disasters (climate and non-climate-related) in relation to El Niño and La Niña events during this time period.

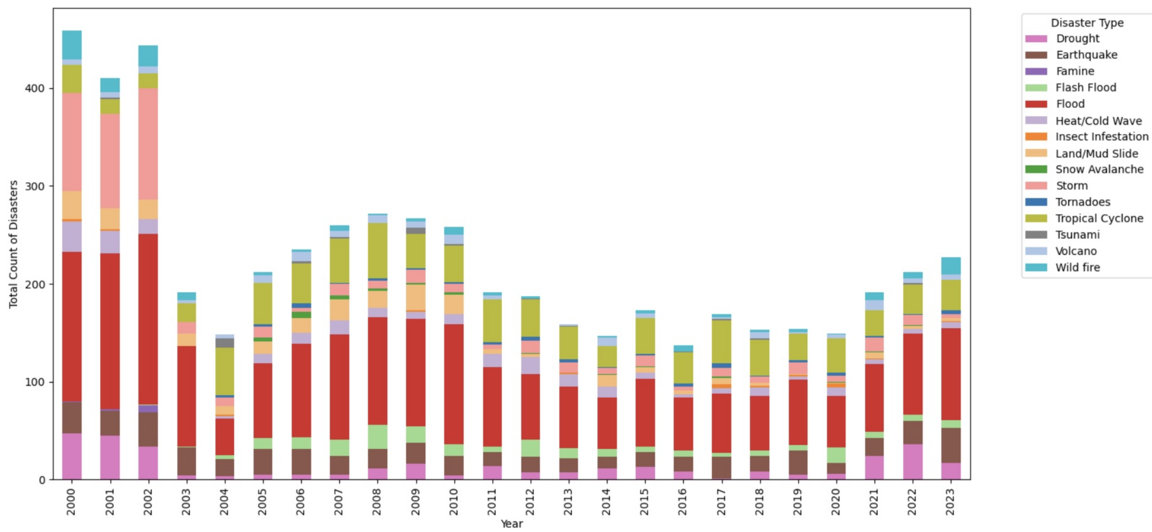

Figure 4.2: Annual global distribution disasters given a GLobal IDEntified (GLIDE) number from 2000 to 2023, segmented by disaster type. Each bar represents the total count of disasters for a given year, with individual segments colored to denote different disaster types, ranging from droughts and earthquakes to storms and wildfires. The graph highlights variations and trends in the frequency of specific disasters, illustrating the persistent prevalence of floods and storms alongside the episodic occurrences of other disasters like droughts and heat/cold waves.

For each article, I retrieved the following annotated information: the date posted, the primary country mentioned, a list of all countries mentioned, disaster types, disaster names, themes, source, format, language, title, and the full text. For my analysis, I only used the body articles posted as plain text on ReliefWeb and did not scrape any attached PDF reports accompanying some posts. I then selected articles for the study based on specific criteria: those written in English and tagged with up to five countries and/or disaster types. Figure 4.4 represents the distribution of this subset of articles by the top 30 combinations of disaster type tags. Most articles were tagged with one disaster type, the most common being Flood, Earthquake, Tropical Cyclone, Epidemic, and Drought. There were, however, numerous articles tagged with multiple disaster types. To contextualize why some articles were tagged with several disaster types, I present a

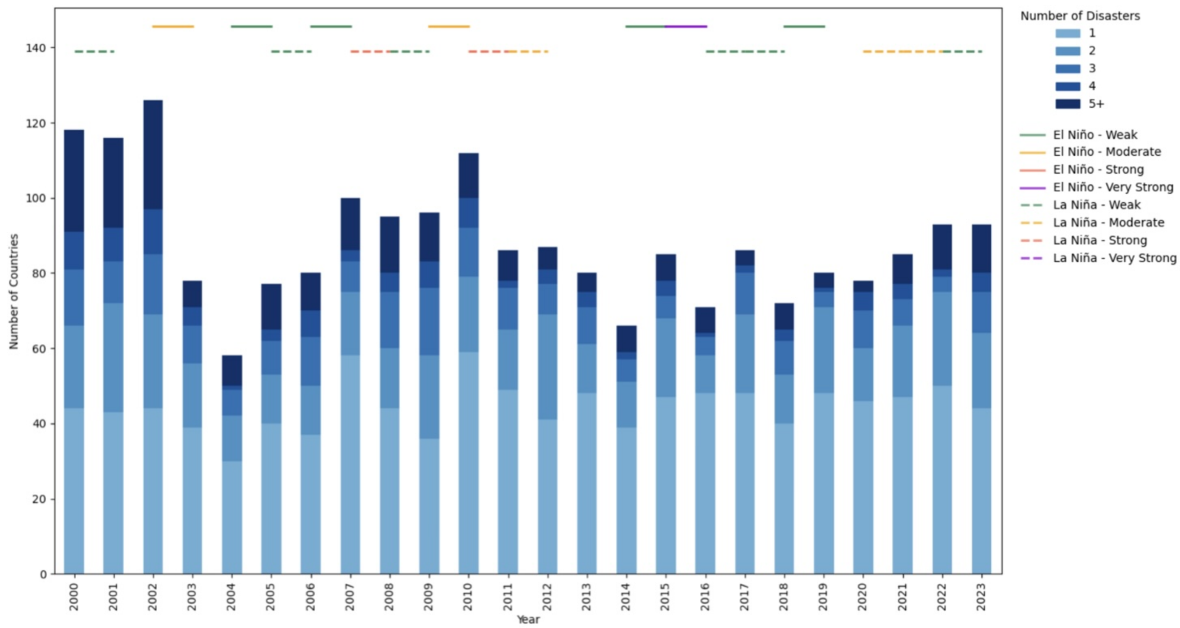

Figure 4.3: Annual distribution of disasters given a GLobal IDEntified (GLIDE) number across countries from 2000 to 2023, differentiated by the number of disasters experienced per country. Each bar represents the number of countries experiencing 1 to 5 or more disasters in a given year, with color intensities increasing with the number of disasters. Overlaying dashed lines indicate the occurrence and intensity of El Niño and La Niña events according to the Oceanic Niño Index, categorized from weak to very strong. Note that the disasters in the figure include climate-related and non-climate-related types.

few examples in Table 4.1 of the type of information summarized from certain articles alongside their disaster type tags and overall classification according to the previously discussed terminology.

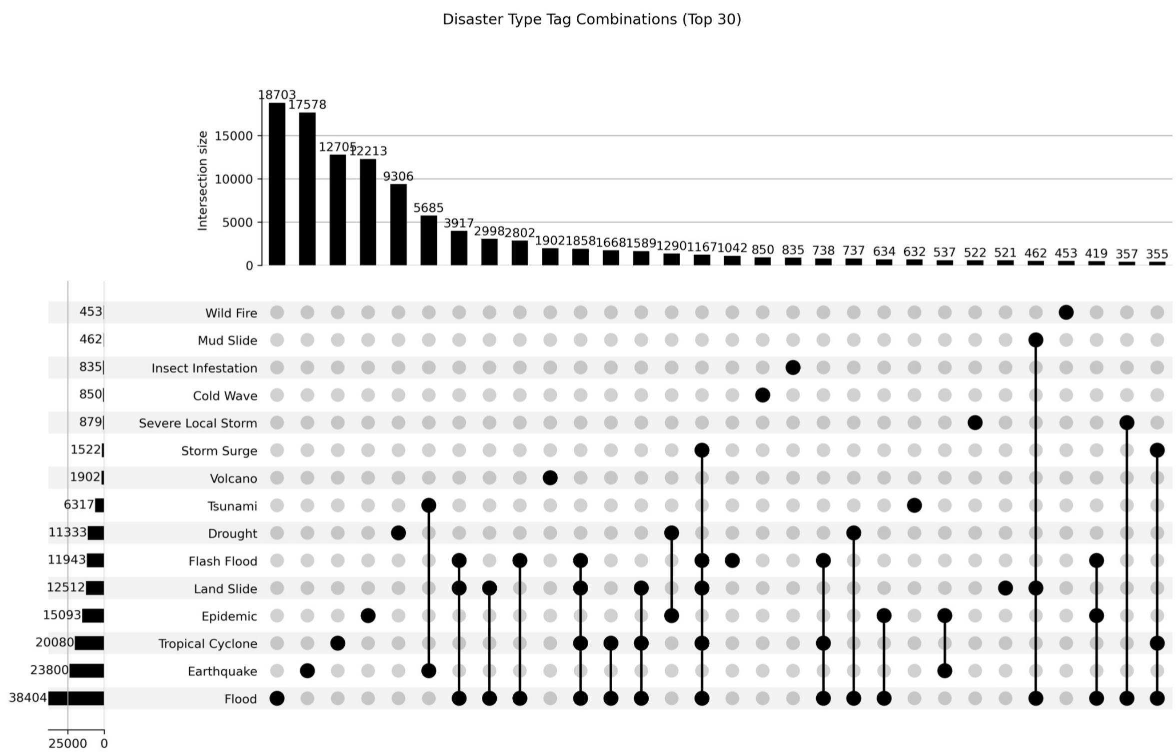

Figure 4.4: An UpSet plot of the distribution and overlap of articles tagged with various disaster types on ReliefWeb. Each verticle bar represents a set of articles tagged with a specific disaster type, with the height of the bar indicating the number of articles. The horizontal bars at the bottom of the plot show the intersection between different disaster types. These intersections reveal the number of articles that are tagged with multiple disasters, providing insights into how often certain disasters are reported together. Only the top 30 combinations are displayed.

Table 4.1: Multi-hazard event classification examples summarized from select ReliefWeb articles.

Classification	Disaster Types	Description
Cascading Hazard	Earthquake, Tsunami	An earthquake off the coast of Sri Lanka and India caused a major tsunami.
Cascading Hazard	Flash Flood, Flood, Landslide	Water levels of a river are becoming dangerously high, prompting scientists to monitor the river bank and warn citizens about the possibility of a landslide.
Complex Emergency, Connected Extreme Events	Drought, Epidemic, Flash Flood	Humanitarian efforts following a drought in Afghanistan are halted, female humanitarians are limited in their ability to participate, and monetary value and surrounding wars have created a multidimensional conflict in the state.
Complex Emergency	Drought, Flood, Heat Wave	The "Zero Hunger Program" has failed to reduce childhood hunger. Aid is not reaching those in the most vulnerable states because of a government possibly withholding funds.
Multi-Hazard Event	Tropical Cyclone, Earthquake	Disasters occurred at relatively the same time in the Philippines (floods/landslides), Samoa (tsunami), and Indonesia (earthquakes).
Cascading Hazard	Epidemic, Flood, Landslide	A tropical cyclone hit Mozambique, leading to floods and outbreaks of cholera in displacement camps.
Compound Event	Epidemic, Flood, Tropical Cyclone	People in Libya are in need because of conflict, displacement, and lack of humanitarian services. Healthcare is becoming less accessible, and the COVID pandemic is spreading in migrant camps.
Connected Extreme Events	Drought, Epidemic, Insect Infestation	A severe drought across Somalia has caused human and livestock deaths. The livestock carrying mosquitos and diseases have not been vaccinated because veterinarians refuse to leave their towns. Goats coming from nearby Ethiopia have destroyed the local market. The cash card system has also not been working for months.
Complex Emergency	Heat Wave, Wild Fire	In Greece, the combined effects of a heatwave, hot winds, drought, and arson crimes have created unprecedented forest fires.
Cascading Hazard	Drought, Epidemic	People are facing food insecurities because humanitarian aid is not reaching those most in need. The drought has caused a lack of healthy living conditions, leading to epidemics across the country.

4.2.2 Large Language Models (LLMs) and Prompt Engineering

Large Language Models (LLMs) are a class of artificial intelligence systems designed to understand and generate human-like text by learning from a vast dataset of diverse internet text. One of the most prominent advances in natural language processing is GPT-3. Developed by OpenAI, it comprises 175 billion parameters, enabling the model to process and produce contextually relevant and highly coherent text, even over long passages (Floridi and Chiriatti, 2020). This makes it suitable for complex language tasks, including text classification, summarization, and question-answering.

Prompt engineering is a strategic process that involves creating inputs (prompts) that guide language models such as GPT-3 to perform specific tasks. The design of these prompts significantly influences the accuracy and relevance of the model's outputs. When prompt engineering is done effectively, it ensures that the model understands the task at hand, improving its performance without requiring extensive retraining. Creating effective prompts involves crafting clear and concise instructions, utilizing specific keywords that the language model can recognize, and iteratively testing and refining prompts based on initial outputs.

4.2.3 Operational modes of LLMs

Zero-Shot Learning

In zero-shot learning, GPT-3 applies its pre-trained knowledge to new tasks without specific examples or prior exposure. This mode is particularly useful for tasks where collecting a large annotated dataset is impractical. In this case, the task is described directly in the prompt and the model must rely on its general understanding of language and context.

Few-Shot Learning

Few-shot learning refers to the process of training GPT-3 with a limited number of examples to prepare it for a specific task. This method enhances the model's capacity to produce responses that align with the desired output. The model's predictions can often be refined with a few annotated examples, improving accuracy and consistency.

Fine-Tuning

Fine-tuning is a technique for adjusting a model's parameters on a dataset to achieve higher precision for a specific task. When a higher level of accuracy is required, fine-tuning narrows the model's focus and provides additional context. This involves training GPT-3 on a corpus of relevant texts so that the model can adapt its responses by reflecting the specific linguistic patterns and terminology associated with different text structures.

4.2.4 Multi-label classification

Multi-label classification refers to the task of assigning multiple associated labels or categories to a single document or data point (Song et al., 2022; Wu and Zhu, 2020). In this study, I aimed to accurately predict and assign all relevant disaster-type labels to a given ReliefWeb article. I test the ability of a human annotator and an LLM to perform this task in parallel.

The human annotator was tasked with reading through the titles and texts of a sample set of articles and assigning between one to five relevant disaster types according to the context of the article. The annotator completed tagging 220 articles, which became the test set for the AI. Figure C.3 displays the UpSet plot showing the distribution and overlap of how the test set articles were originally tagged by disaster type. Only the top 30 most common tag names and combinations of names are shown.

4.2.5 AI model implementation

To operationalize GPT-3 for disaster-type detection from ReliefWeb article text, I interacted with OpenAI's API to run a prompt against the test set of articles using zero- and few-shot learning. Regarding the few-shot learning, I provided three examples of different titles, texts, and disaster-type labels per OpenAI's recommendations. I designed the prompt in a direct and specific manner while maximizing a limited number of tokens. Common best practices for prompt engineering are assigning the AI a role to narrow its focus and then providing details on how the user would like the model to output the results. Therefore, after rigorous testing, I used the following prompt:

> "You are an AI specialized in reading comprehension and disaster identification. Your task is to categorize articles by analyzing their text and title. Assign each article the relevant disaster type(s) from the following list: Cold Wave, Drought, Earthquake, Epidemic, Extratropical Cyclone, Flash Flood, Flood, Heat Wave, Insect Infestation, Land Slide, Mud Slide, Severe Local Storm, Snow Avalanche, Storm Surge, Tropical Cyclone, Tsunami, Volcano, Wild Fire. Output categorizations as a comma-separated list, using your best judgment for articles fitting multiple or unclear categories."

For the fine-tuning training and validation sets, I randomly selected articles until there were at least 100 samples of every disaster type, per the recommendations by OpenAI. This led to certain disasters with far more than 100 samples, such as Floods and Cyclones, when they were commonly tagged with other disasters. However, I wanted to ensure that there were sufficient examples of each disaster type being tagged in the articles. In total, this amounted to 1241 training articles and 290 validation articles. The fine-tuning model was trained on three epochs, and the step-wise training and validation loss can be seen in C.4. The final training loss was 0.979, and the final validation loss was 0.5565. Figures C.1 and C.2 show the UpSet plots of the most common disaster-type labels for the training and validation datasets, respectively.

Finally, I used gpt-3.5-turbo-1106 as the base model. I also set the temperature for each model to zero and the maximum number of output tokens to 100 to minimize randomness and ensure the models' responses were brief.

4.2.6 Evaluation metrics

I used three types of multi-label classification evaluation metrics: subset accuracy, Hamming loss, and Jaccard similarity, to assess the human annotator's skill against the performance of zero-shot, few-shot, and fine-tuned LLM testing in detecting the correct names and numbers of disasters. Next, I will briefly describe each metric, including how it is used and calculated.

Subset Accuracy

Subset accuracy, also known as "exact match" or "zero-one loss", is a performance metric used in multi-label classification that evaluates if the predicted set of labels exactly matches the true set of labels. It is a strict metric requiring that every label in the predicted set matches the corresponding label in the true set, with no additional or missing labels, for a sample to be considered correctly classified.

$$\text{Subset Accuracy} = \frac{1}{N}\sum_{i=1}^{N}\mathbf{1}(\hat{y}_i = y_i) \tag{4.1}$$

where N is the total number of instances in the dataset, $\hat{y}_i$ is the predicted label set for the i-th instance, and y_i is the true label set for the i-th instance. $\mathbf{1}(\hat{y}_i = y_i)$ is an indicator function that returns 1 if the predicted label set for the instance is exactly the same as the true label set and 0 otherwise. When calculating subset accuracy, each value is summed for all instances and then divided by the total number of instances N. This calculation gives a value between 0 and 1, where 0 indicates no instances were correctly predicted and 1 indicates all instances were perfectly predicted. Values between 0 and 1 indicate the proportion of instances that have a perfect match between the predicted and true label sets.

Subset accuracy is a simple and intuitive metric but can be too harsh for some applications, particularly in cases where partial correctness is still meaningful. Therefore, I also consider the following two metrics.

Hamming Loss

Hamming loss is a metric that measures the fraction of incorrect predictions compared to the total number of predictions. It is used in situations where each instance can be classified into multiple categories and is particularly useful when the classification error on each label is equally important. The equation for measuring Hamming loss is as follows:

$$\text{Hamming Loss} = \frac{1}{N}\sum_{i=1}^{N}\frac{\text{xor}(y_i, \hat{y}_i)}{L} \tag{4.2}$$

where N is the number of instances in the dataset, L is the number of labels, y_i is the true label set for the i-th instance, and $\hat{y}_i$ is the predicted label set for the i-th instance. $\text{xor}(y_i,\hat{y}_i)$ is the symmetric difference between the true and predicted labels, essentially counting the number of labels where the predicted label differs from the true label.

The Hamming loss values range from 0 to 1, where 0 means perfect classification (no error), and 1 means all predictions are incorrect.

Jaccard Similarity

Jaccard similarity – also known as the Jaccard index or the Intersection over Union – is a statistic used for gauging the similarity and diversity of sample sets. In the context of classification, particularly multi-label classification, it measures the size of the intersection divided by the size of the union of the predicted and true label sets. This metric is useful for assessing the similarity between sets as it computes the average similarity between the predicted and true label sets across all instances. It evaluates how many labels are common between the true and predicted labels relative to the number of labels present in either the true or predicted labels (or both). The Jaccard Similarity equation is as follows:

$$\text{Jaccard Similarity} = \frac{1}{N}\sum_{i=1}^{N}\frac{|y_i \cap \hat{y}_i|}{|y_i \cup \hat{y}_i|} \tag{4.3}$$

where is N the total number of instances in the dataset, y_i is the true label set for the i-th instance, $\hat{y}_i$ is the predicted label set for the i-th instance. $|y_i \cap \hat{y}_i|$ is the size of the intersection of the true and predicted label sets, representing the number of labels correctly predicted. $|y_i \cup \hat{y}_i|$ is the size of the union of the true and predicted label sets, representing the total number of unique labels in both the true and predicted sets.

Jaccard similarity ranges from 0 (no overlap) to 1 (perfect overlap), where higher values indicate higher similarity between the predicted and true labels. This metric is particularly effective in scenarios where it is beneficial to consider the proportion of correct predictions to the potential errors made in the form of false positives and false negatives.

4.3 Results

4.3.1 Evaluation of human versus AI effectiveness in classifying multi-hazard disaster events

Figure 4.5 depicts the performance of the annotator and AI models in correctly identifying the originally tagged disaster types from the 220 article test set. For the subset accuracy (panel a), the annotator (maroon) exhibits a significant decline in performance as the number of tags increases, starting from a relatively high accuracy with one to two disaster-type tags. This decrease alludes to the difficulty in understanding complex emergencies. The zero-shot (orange) model is consistently low across all tag complexities, indicating a lack of adaptability to the task without prior specific training, particularly in multi-tag cases. The few-shot (yellow) model also shows a sharp decrease in performance with an increase in the number of original tags. However, there does not appear to be a distinct advantage between the few-shot with additional training examples compared to the zero-shot, and both reach a subset accuracy score of zero once the articles reach three or more disaster-type tags. The fine-tuned model (purple) starts off lower than the other tests and decreases to zero when there are three disaster types but then rebounds with four to five tags.

According to the Hamming loss (panel b), the annotator makes more incorrect label predictions in more complex situations, as seen by the gradual line increase. The zero-shot and few-shot models similarly display an increasing trend with only a minimal differentiation between the two and generally lower outcomes compared to the annotator. The fine-tuned model remains relatively stagnant as the complexity in the number of tags decreases, demonstrating consistency in predicting labels and perhaps a superior ability to minimize incorrect labels and adapt better to the task.

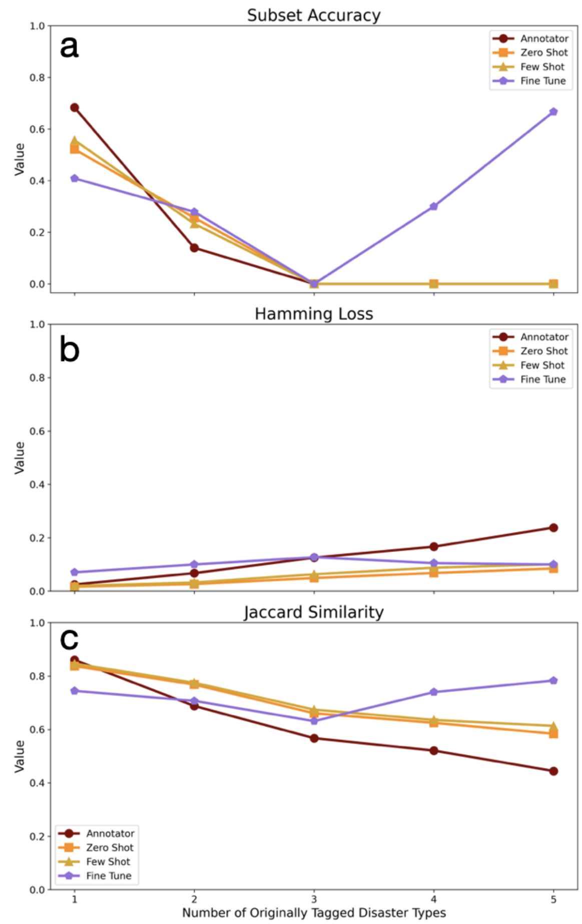

Figure 4.5: Performance comparison of human annotator and AI models across multi-label classification metrics: subset accuracy (a), Hamming loss (b), and Jaccard similarity (c) as a function of the number of originally tagged disaster types.

With the Jaccard similarity (panel c), the annotator's performance gradually declines with increasing tag numbers, reflecting difficulties in attaining overlap between the predicted and actual labels as complexity increases. The zero-shot model and few-shot model's skills are nearly identical, with both showing a more modest decrease compared to the annotator as the number of original tags increases. The fine-tuned model starts with slightly worse skill than the others but finishes with the highest Jaccard similarity, highlighting its effectiveness in predicting correct label sets even under more challenging conditions.

The fine-tuned model outperforms the other approaches overall, revealing stronger robustness and accuracy in handling multi-label classifications, especially as the task complexity increases. While the human annotator proves effective in simpler scenarios, their performance does not scale well with increased complexity. This contrasts with the few-shot and zero-shot models, which show similar limitations in handling complex label sets. Few-shot marginally outperforms zero-shot, indicating some potential benefits from minimal targeted learning.

I then compared the skill of the three AI models – zero-shot, few-shot, and fine-tuned – relative to the number of tags assigned by the annotator. According to Figure 4.6, the zero-shot model's subset accuracy remains relatively flat across different numbers of tags, indicating that the model's ability to completely match the annotator's tagged set does not significantly change with the complexity of the tag count. Similarly, the few-shot model subtly decreases from one to two tags but generally remains consistent as the number of tags increases. However, it begins with slightly higher accuracy than the zero-shot model, possibly benefiting from limited examples during training. Contrary to expectations, the fine-tuned model shows the lowest subset accuracy across all levels of tags. This trend could indicate that the model may have been excessively tuned to specific types of data, which reduces its generalizability to broader or more varied tag combinations seen during testing. On the other hand, in certain cases, the annotator was considered "incorrect" compared to the original human tagging system, which is reflective of differences in context interpretation.

The zero- and few-shot models exhibit near-zero and relatively constant Hamming loss against the annotator's tags across all levels of tag complexity. This indicates that both models consistently make few label prediction errors, irrespective of the number of tags. The models' low error rate indicates good alignment with annotator perception in identifying primary disaster types. The fine-tuned model shows a slightly higher

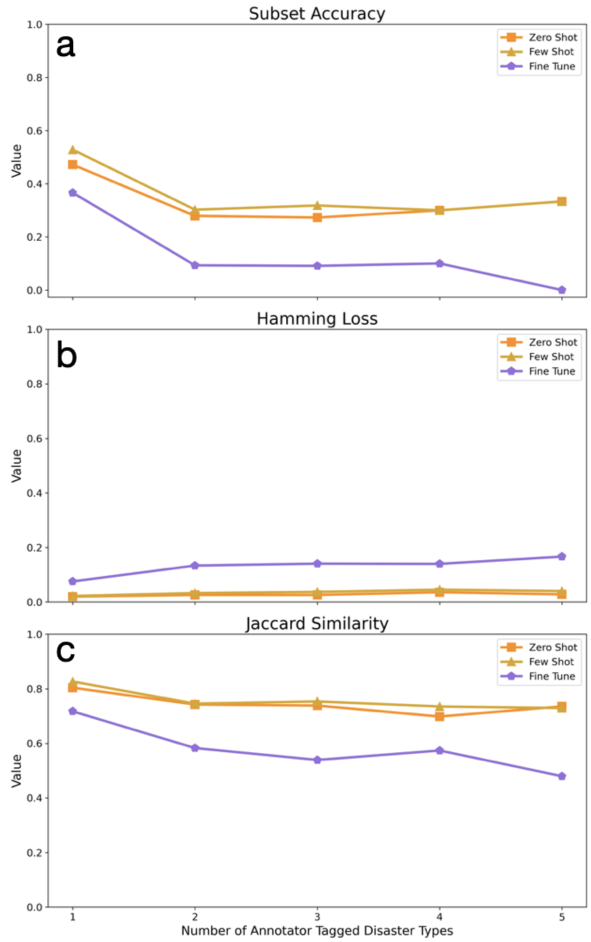

Figure 4.6: Performance comparison of AI models across multi-label classification metrics: subset accuracy (a), Hamming loss (b), and Jaccard similarity (c) as a function of the number of the annotator tagged disaster types.

Hamming loss in comparison, which slightly increases as the number of tags increases. Based on the pattern observed, it appears that the fine-tuned model, which underwent more intensive training, faces more challenges with labeling as the complexity of the task increases. In some instances, the model either misses correct labels or predicts incorrect ones, indicative of some overfitting to certain disaster types over others.

Finally, the zero- and few-shot models maintain high and relatively stable Jaccard similarity across different tag numbers. This pattern implies that the models are effective at predicting a large proportion of the correct labels relative to the union of predicted and actual labels, demonstrating good overall precision and recall. On the other hand, the fine-tuned model starts with a lower Jaccard similarity compared to the zero- and few-shot models and shows a slight decreasing trend as the number of tags increases. The decrease in performance suggests that the model is having a harder time accurately identifying the correct labels, as reported by the annotator. This is particularly the case in more complex scenarios, possibly due to the model's over-reliance on the training data, resulting in poor generalization of new label combinations.

In most cases, articles were originally tagged with three or fewer disaster types, and the annotator primarily assigned up to two disaster-type labels to the articles. This suggests that overall, the AI models predicting three or more tags either identified additional labels that the annotator missed or inaccurately over-predicted labels. This discrepancy highlights the challenge of evaluating model accuracy without corresponding ground truth for these tag counts, raising questions about the models' ability to generalize from their training data. While the models are often good at identifying types of disasters that humans missed, the model is also biased to selecting certain disaster types over others due to an imbalance in training examples. Further validation is needed after the AI assessment with expert review or additional data sources to confirm the accuracy of each model's predictions.

4.3.2 Classification skill by disaster type

When evaluating the classification performance by disaster type in relation to the original number of tags for each type, I find that the three language model strategies, zero-shot, few-shot, and fine-tuned, perform similarly overall (Figure 4.7). Each test identified common disasters such as floods, earthquakes, tropical cyclones, and epidemics with relatively high accuracy, but their prevalence in the training and validation datasets also caused some incorrect responses. In other words, disaster types that I had supplied ample examples for when fine-tuning the model were more likely to have been correctly identified when testing in some cases but, at the same time, overly misclassified articles with that type as well. Hence, strong negative bars (incorrect classification) of the top more common disaster types exist. Certain types of disasters, including floods, flash floods, and landslides, as well as storm surges and severe local storms, are also highly similar events that are more difficult for the LLMs to distinguish between. Disasters that were less common in the training, validation, and test datasets, such as wildfires, heat waves, and extratropical cyclones, were also more often misidentified.

Similar trends are revealed when making the same comparison in relation to the annotator's tags. However, for the fine-tuned classifications by disaster type, responses were almost equally likely to be correct and incorrect for certain disasters, such as earthquakes. The gaps between the annotator's classifications and those of the LLMs call into question the context awareness of the AI systems. It appears that the AI was more likely to hallucinate responses when, in the prompt, I specified that it was required to choose at least one disaster type from a list.

I also find that, overall, the fine-tuned model is largely successful at adhering to the list of disaster types and avoiding creating new labels or responding in phrases rather than stating the type(s). However, this did not necessarily lead to more accurate responses regarding the original and annotator tags. The fine-tuned model only generated the names "Fire" and "Hurricane" in two instances each, which were out of the scope of the pre-defined list of disaster types yet are reasonably similar to "Wildfire" and "Extratropical Cyclone." There were far more invalid responses by the zero- and few-shot models. For instance, these two model versions were significantly more likely to add additional responses outside the list I supplied, such as "Famine," "Conflict," and "Population Displacement," or in some cases, responded with a full sentence that was unrelated to the

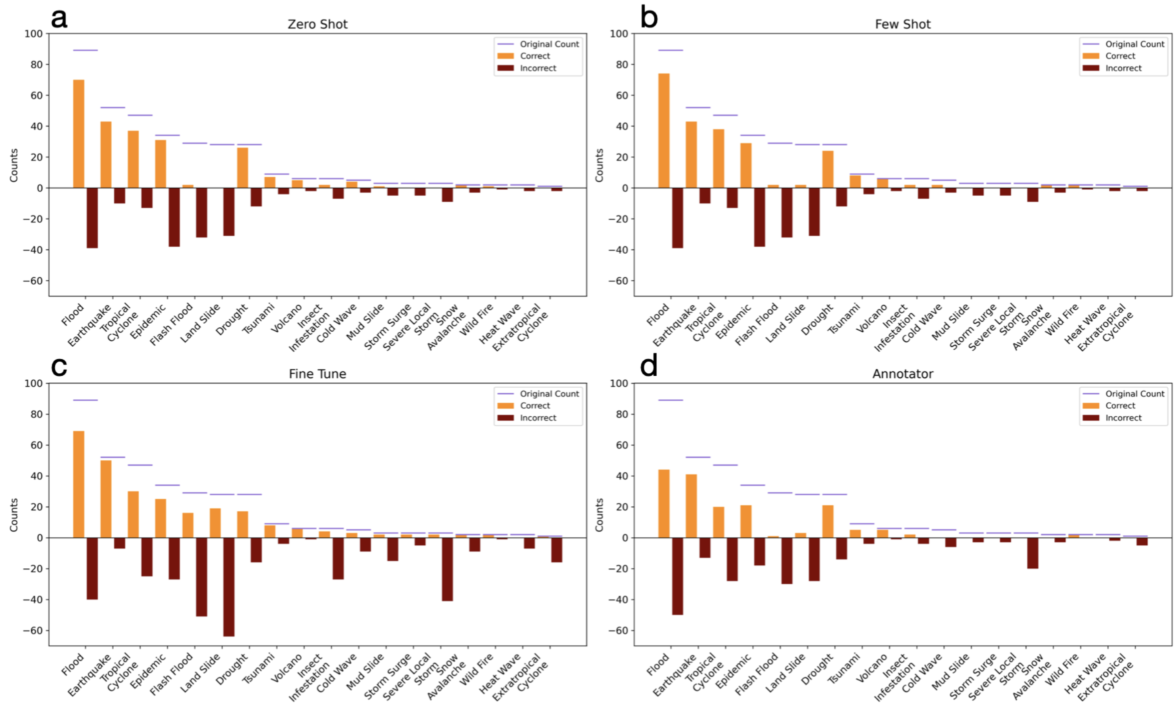

Figure 4.7: Comparison of disaster type identification in articles by different LLM strategies – zero-shot (a), few-shot (b), and fine-tuned (c) – alongside human annotation. Positive bars (orange) indicate the number of correct classifications for each disaster type, while negative bars (maroon) reflect the number of incorrect responses. The light purple line indicates the total count of each disaster type originally tagged across all articles.

prompt but showed that the model was trying to explain why it could not select one of the items from the list.

4.3.3 Annotator labeling experience

The annotator initially found the experience of tagging articles challenging, but as they grew more familiar with the structures and themes of the articles, their ability to classify the articles systematically improved over time. They observed needing to make both subjective and objective interpretations of the texts. In some instances, the articles were straightforward, with opening lines identifying the disaster type, such as "Today's powerful 7.3 magnitude earthquake..." For these cases, the annotator could immediately

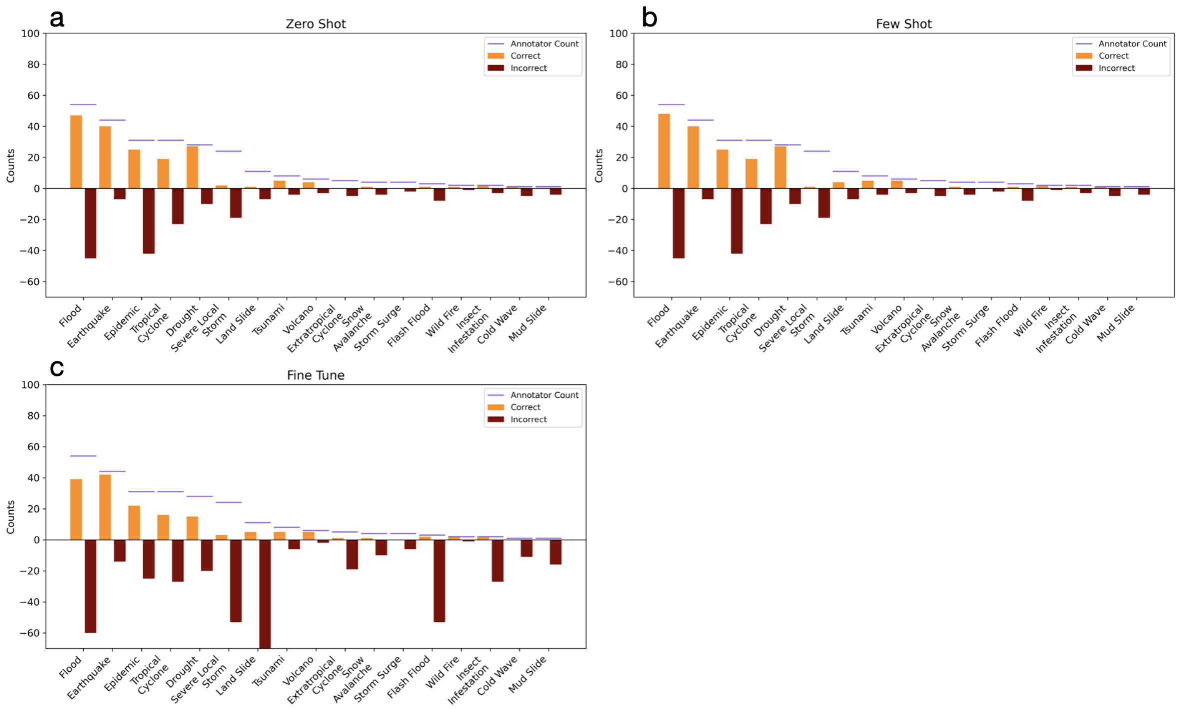

Figure 4.8: Comparison of disaster type identification in articles by different LLM strategies – zero-shot (a), few-shot (b), and fine-tuned (c) – relative to the human annotation. Positive bars (orange) indicate the number of correct classifications for each disaster type, while negative bars (maroon) reflect the number of incorrect responses. The light purple line indicates the total count of each disaster type the human annotator tagged across all articles.

tag the article accordingly. Most articles were formatted this way, making identifying the associated tag within the first few sentences a simple process. Articles involving fewer disasters were the easiest to tag, especially when a brief, concise history was given before the disaster report, as this made it easier to identify the context. Articles that opened by explicitly stating the disasters upfront, followed by a report of their effects, comprised most of the annotator's correctly tagged articles.

When articles included a variety of forced migration causes, the annotator found it difficult to interpret the most pressing cause of displacement. Cascading hazards, characterized by sequential events, were challenging to identify accurately due to their nature. For instance, according to one article, there was initially a tropical cyclone in a location, which later led to floods and landslides. While reading, the annotator mistakenly tagged the disaster type as only "Tropical Cyclone" because it was the first event mentioned, failing to account for the subsequent floods and landslides.

The annotator spent many hours reading through the lengthy texts. They found the experience tedious and unreasonable to scale up to a larger production. However, the annotator reported that the overall tagging process was straightforward and clear. Most articles had the disaster type in the title, while the text provided additional details describing the impacts of the aftermath. As the annotator had minimal prior knowledge of the subject matter, they found that more concise and explicit reports were easier and faster to understand, interpret, and identify the associated tags. Conversely, ambiguity and lack of crucial details posed challenges, requiring subjective interpretations from the annotator's perspective.

4.4 Discussion

4.4.1 The role of AI in disaster information retrieval

Artificial intelligence offers great potential to progress our ability to synthesize and retrieve key information in a flood of data. In this study, I demonstrate the viability of using an LLM to perform a relatively simple task of labeling text. Complexity emerges when requesting the system to conduct multi-label classification and make tagging decisions when the context and structure of the articles are highly variable. Fine-tuning a language model is one way of improving the consistency of the output, but it does not always guarantee accuracy. These fine-tuned models are only as good as the quality of their training data, and avoiding overfitting is a balancing act that requires supplying just enough diverse examples. Similarly, prompt engineering is a dance between being brief versus verbose, narrow versus broad, and rigid versus flexible to guide the model toward a desired output.

While LLMs are still in their infancy, I envision a space for this technology to grow into a force for good in crisis informatics. Emergency responders face the considerable challenge of sifting through extensive media to identify critical and actionable information in the face of disasters. The sheer volume of incoming social media posts alone can hamper the ability of responders to quickly grasp the situation and make informed decisions regarding the distribution of resources. Media content's informal and unstructured nature adds complexity to extracting pertinent information. Furthermore, the diverse needs of various stakeholders complicate the situation further. While first responders typically seek precise situational awareness to act effectively, policymakers often look for higher-level information to guide their decision-making processes (Arachie et al., 2020). This chapter introduces the concepts and techniques needed to begin utilizing LLMs for rapid disaster information retrieval that can benefit various stakeholders.

I focus on the concept of multi-hazard disaster events as an application of multi-label classification. Disasters are often addressed in silos as single independent events rather than part of a larger system of instability and damage tied to other disasters. In the process of identifying multiple disaster types from the ReliefWeb articles, I highlight the complications of either human- or AI-led decision-making, furthering the case for additional research on these situations.

Multi-hazard events are more common than perceived. In a study by Lee et al. (2024), the authors reclassified historically recorded disasters from the Emergency Events Database, EM-DAT, which revealed that approximately one in five reported hazards are multi-hazard events. Floods and storms are the most common primary hazards in the database. Additionally, the study underscored that multi-hazard events incurred significantly higher economic losses than single-hazard events, with storms, earthquakes, and floods causing substantially greater losses compared to others, stressing the critical need for a deeper understanding of multi-hazard interactions and their severity. Yet, de Ruiter et al. (2020) and (Raymond et al., 2020) highlight how disaster-risk management and humanitarian aid logistics typically focus on the short-term impacts of a single disaster while falling short on long-term planning and accounting for connected and/or consecutive disaster events.

"Compound thinking," a concept in disaster risk reduction discussed by van den Hurk et al. (2023), involves understanding how multiple factors interact to create more complex outcomes. By recognizing the combined impacts of various hazards and drivers and adopting a holistic approach that considers the interaction between different elements like hydrometeorological forces, societal vulnerabilities, and ecological systems, practitioners can improve their disaster preparedness and response strategies by gaining a deeper insight into interconnected risks, leading to more effective risk reduction measures and increased resilience against complex challenges. In my view, practicing "compound thinking" includes being receptive to innovative and advancing techniques that may uncover new connections between accounts of disasters in unforeseen ways.

4.4.2 Challenges of multi-label AI classification

During the course of this study, a number of issues emerged that I will address. First, sometimes ReliefWeb tags articles according to the content in an attached PDF report. This made it difficult or, at times, impossible for the annotator and LLM to identify the correct disaster types if the information was absent from the website's text. In these cases, the disaster type tags could only be detected if the AI could make "inferences" based on the context, which should have been minimized as I set the temperature (randomness parameter) to zero, meaning the model should have been more prone to choosing predictable and conservative responses. Yet, at other times, the AI made up completely new categories despite being restricted to choosing from a list of disaster types. These new categories could be helpful, however, in identifying other important aspects of the article that may describe the overall themes, such as conflict or food insecurity. Perhaps giving detailed definitions of each type of disaster in the prompt could have strengthened the AI's understanding and improved response accuracy.

Another approach to improve outcomes could be to ask the model to perform binary classification tasks first, such as asking iteratively "Is this article about a drought hazard?" or "Is this article a fire hazard?" Prompting LLMs to "think step-by-step" is a common way to ensure more appropriate responses. One could also ask the AI to first summarize an article and then classify it by disaster types, as LLMs are not as skilled at multi-task jobs.

A further opportunity lies in AI agents, which use LLMs to assist users in complex cognitive tasks and are often referred to as "copilots." They work alongside human prompting, providing tailored assistance for specific contexts or applications (White, 2023). For instance, one could run an agent that is tasked with only summarizing text and another that is explicitly designed for classification based on keywords. A different strategy could be to use different agents that are equipped to handle certain domains, such as various geographies or disaster types, which may also reduce hallucinations because the tasks are partitioned and specialized.

High costs and rate limits can pose challenges when using LLMs to process large volumes of text data. Creating and using a fine-tuned model is expensive, and testing it on the entire original dataset with hundreds of thousands of articles was not feasible. Fine-tuning a generic LLM also raises issues when data is sparse, involves complex subdomains, and has inherent biases (Tamagnone et al., 2023). It is important to have sufficient training data for effective fine-tuning, though, at the same time, larger training datasets incur more computational resources and time compared to zero-shot or few-shot learning (Chae and Davidson, 2023).

The ReliefWeb articles are highly variable in structure and lean heavily on certain geographical regions and types of disaster situations over others, which may have led to overfitting in some areas. It is not possible to grasp all forms of scenarios as training examples. For example, sometimes, an article may discuss multiple disasters by summarizing a country's situation over a year and how much aid they have received. In this case, the article is not necessarily talking about related events. It is currently unclear how truly "context aware" AI systems are, and requesting the models to distinguish between how disasters are (un)related is a much more complicated task.

While ReliefWeb publishes articles in a few major languages, I only tested the models with English articles. Training datasets for underrepresented languages need to be developed to acquire more localized information. One example of this effort is by Ghosh et al. (2022), who introduce a multilingual disaster-related classification system known as the Graph Neural network based Multilingual text classification framework (GNoM).

Several other key challenges emerge through using AI in disaster risk management. First, as mentioned, high costs can be incurred, and low-income countries facing disasters may not possess the resources and infrastructure to support such heavy computation needs. Developing and deploying AI-based solutions necessitates a high level of expertise, which may also be lacking in disaster-affected areas (Velev and Zlateva, 2023). Data quality and quantity are also a concern. Data can be scarce, unreliable, or inconsistent in many disaster scenarios, making it difficult to train AI models and make accurate predictions. AI poses questionable ethical and social implications as sensitive information is collected and analyzed. Minimizing bias and ensuring data privacy and security are critical. Existing disaster management systems may not be equipped to integrate advanced models, requiring significant investments to secure compatibility. Together, these challenges with the nature of AI may inadvertently result in the denial of protection to the most vulnerable populations in disaster situations (Moitra et al., 2022).

Moreover, Tamagnone et al. (2023) emphasize the limitations of using generic LLMs for humanitarian data analysis, highlighting issues such as ineffective performance on data-sparse subdomains and the encoding of societal biases. The authors advocate for developing domain-specific models to address these challenges. Doing so would ensure more ethical and effective humanitarian document analysis and "response entry" (i.e., text excerpt) classification. Ongoing research and development are required to address the evolving changes to disaster patterns and impacts and the AI technologies themselves (Velev and Zlateva, 2023).

In a perspective piece by Gevaert et al. (2021), the authors outline several aspects that need to be fulfilled to uphold the responsible usage of AI for disaster risk management. Tools and methods to detect and mitigate biases must be developed to achieve better accuracy and fairness in risk assessment. AI systems must be designed transparently and explainable to allow users to understand and trust how decisions are made (Ghaffarian et al., 2023). Involving local communities, experts, and other stakeholders in creating and deploying AI technologies can help ensure local values, priorities, and needs are considered. Safeguarding sensitive information and establishing governance structures for accountability and ethical conduct are crucial. Still, with fairness, transparency, and accountability in mind, Gevaert et al. (2021) echo the opportunities AI offers to the disaster management community as discussed throughout this chapter, namely rapid and accurate data processing, enhanced risk modeling and predictive capabilities, optimized resource allocation, automation of routine tasks, and improved decision support.

4.4.3 Future prospects for using new technologies in disaster informatics

Finally, I will discuss a few opportunities for future work. The power of LLMs extends beyond classification problems to summarization and question/answer tasks. Nguyen and Rudra (2022) introduce an interpretable classification-summarization framework that classifies tweets by disaster-related categories and summarizes them. The strength of their work lies in their model's ability to explain its decisions or rationales. Effective PDF summarization is another active area of development. Multi-document summarization adds a layer of complexity and potential for developing synthesized and informative summaries from several topic-related texts (Pereira et al., 2023).

Multimodal approaches that combine textual and visual information in event detection during emergency response situations can provide an even more comprehensive understanding of crises (Abavisani et al., 2020). This approach enhances the context by offering visual details from images and specific text information, improving the accuracy and reliability of crisis event detection. By integrating multiple modalities, such as images and texts, the sensitivity of event detection systems is increased, enabling the identification of subtle signals that might be missed using a single modality. Additionally, combining images and texts helps evaluate the severity of crises, understand the impact, and facilitate more effective response planning and resource allocation. Another approach, automatic sentiment analysis from social media posts, can help understand individuals' emotions, opinions, and attitudes in response to disasters, recovery efforts, and related events. By gauging public perception towards disaster management, government agencies and organizations may improve their decision-making and response strategies, particularly regarding interlinked events (Mishra and Saini, 2014).

AI is considered a disruptive technology in disaster risk management, potentially revolutionizing how disasters are predicted and addressed (Munawar et al., 2022). Other disruptive and potentially transformative technologies for disaster management include Internet of Things Devices, smart sensors, cloud computing, satellite imagery and image processing algorithms, and advanced communication networks. Integration across these technologies will enable more comprehensive data analysis for better risk assessment, early warning systems and decision-making, improved communication and coordination, and increased resilience of cities (Munawar et al., 2022).

Although not discussed in this chapter, machine learning and text-mining techniques can measure extreme events' size and geographical scope (Pita Costa et al., 2024). For instance, media has been shown to serve as a relatively good proxy for capturing the dynamics and impact of floods, though there is often a lag between the event occurrence and news coverage. On the other hand, droughts may not receive as much explicit attention in the news, making monitoring their severity and spatial extent difficult unless their coverage is combined with extreme heat events with broader societal implications (Pita Costa et al., 2024).

Another important use of AI for humanitarian aid is predictive modeling, which can be used, for example, to forecast food insecurity. Balashankar et al. (2023) demonstrate the use of deep learning to predict food crises from news streams up to 12 months ahead, which can aid humanitarian organizations like the World Food Program in prioritizing emergency food assistance allocation in a more efficient and timely manner. Machine learning predictive models can extract anticipatory signals of food insecurity episodes from text data derived from new streams, providing early warnings and insights for decision-making.

Lastly, explaining the reasoning behind NLP model decisions is difficult as they are considered "black box" systems (Rocca et al., 2023). Explainable AI techniques (e.g., feature importance identification, Shapely Additive Explanations (SHAP), and counterfactual explanations) have been instrumental in improving the transparency and interoperability of AI models for disaster risk management. They can also be pivotal in risk assessment for multi-hazard scenarios by revealing insights into the interactions between hazards. This can aid in prioritizing resources and improving preparedness for complex disaster situations (Ghaffarian et al., 2023). Observability, meaning the ability to measure and interpret how an AI system operates and arrives at an answer, is an ongoing challenge. Retrieval-augmented generation (RAG) is one method used to enhance the capabilities of generative models by integrating them with a retrieval component. Providing additional context to the model, often through a large document or knowledge base, can produce more accurate, relevant, and detailed outputs (Gao et al., 2024).

4.5 Conclusion

Disaster informatics is a growing field involving designing and applying technologies to solve or enhance understanding of information problems related to disaster areas (Ogie and Verstaevel, 2020). Artificial intelligence is one tool that is becoming an increasingly important component of emerging technologies in disaster management. Machine learning algorithms are utilized to gain cognitive insights, detect patterns within large datasets, and interpret their significance. As a result, AI contributes to more efficient decision-making, resource allocation, and overall performance improvement in disaster response and recovery operations (Vermiglio et al., 2021).

In this chapter, I walk through the implementation of one form of AI, multi-label classification. I challenge the ability of large language models to identify disaster events from humanitarian news updates and reports, particularly when multiple disasters are discussed in one source. By testing various AI approaches to improve responses, from crafting an effective prompt to using zero- and few-shot methods and finally fine-tuning the GPT-3 model, I evaluate the skill of LLMs to derive consistent and accurate responses. Fine-tuning produces more suitable but not always correct results compared to the zero- and few-shot tests. By refining the model with many example input-output pairs, the fine-tuned model is able to follow the prompt more closely but may struggle with biased responses based on number of different sample types used in the training process. Other concerns include computational costs and the quality of input unstructured data.

The field of AI is rapidly changing, and more advanced models and methods are being introduced regularly. With the increased use of AI in disaster management, these tools must be adopted with careful consideration and vetting. Institutions should respond proactively, flexibly, and with a focus on social justice and fairness to minimize biases and inflated expectations when embracing AI for disaster informatics (Gevaert et al., 2021). In light of the changing climate and the evolving human relationship with technology, interdisciplinary teams must engage in systems thinking, blending various methods that can address the interrelated nature of environmental, socioeconomic, and political compounding risks and complex emergencies (Kruczkiewicz et al., 2021).

Chapter 5

Conclusion

Climate change is a global phenomenon that is affecting every corner of the planet, and its impacts are becoming increasingly evident and severe. As temperatures rise and weather patterns become more erratic, communities worldwide face growing challenges threatening their safety and livelihoods. One of the most devastating consequences of climate change is the increasing frequency and intensity of extreme weather events, such as floods and droughts. These disasters can cause widespread destruction, loss of life, and long-term economic and social disruption. However, the impacts of climate change extend far beyond the immediate aftermath of catastrophic events. As populations become increasingly vulnerable to climate-related hazards, millions of people may be forced to leave their homes and communities and seek refuge elsewhere.

Even those who are not directly affected by disasters or displacement will likely feel the ripple effects of climate change in other ways, such as through more widespread food insecurity and water scarcity. In short, the repercussions of climate change are far-reaching and inescapable. This global crisis will leave no one untouched, from the direct impacts of extreme disasters to the indirect effects on food, water, and socio-economic security.

Given the scale and complexity of the climate change crisis, traditional approaches to understanding and addressing its impacts may no longer be sufficient. The nexus of shifting climate systems, ecosystems, and human system dynamics requires a new paradigm that utilizes the power of advanced technologies and data-driven methods. One promising avenue is using machine learning to analyze vast amounts of environmental and social data. These techniques can help identify patterns, measure predictability, and optimize decision-making in the face of uncertainty. Another key area is the development of advanced sensors and monitoring systems that can provide near real-time data on climate variables, ecosystem health, and human activities. By deploying these technologies at scale, we can create a more comprehensive and granular picture of how climate change affects different regions and communities, enabling more targeted and effective mitigation efforts. Integrating diverse data sources, including remote sensing, surveys, and news media, can provide a more nuanced understanding of environmental impacts and support more inclusive and participatory approaches to adaptation and resilience.

In this dissertation, I have explored the potential of these new technologies and data-driven methods to advance our understanding of climate impacts on environmental and population well-being. My three studies demonstrate that creative approaches can provide valuable insights for decision-makers and stakeholders by showcasing the complex interactions between climate, ecosystems, and human systems.

In the first study, I employed an empirical dynamic modeling approach to investigate the sensitivity and stability of vegetation in response to hydroclimatic variability across East Africa. By leveraging advanced computational techniques and high-resolution satellite data, I identified regions that exhibit higher sensitivity to changes in rainfall patterns and those that show greater stability. These findings have important implications for natural resource conservation and agricultural management, highlighting the need for spatially targeted interventions that account for vegetation's heterogeneous responses to hydroclimatic variability.

Using a gravity model approach, my second study focused on understanding the importance of various drivers to internal human displacement in Somalia. I integrated environmental, socioeconomic, and conflict data to interrogate the factors that shape migration patterns, from anomalous weather to conflict severity. This work emphasized the importance of considering how livelihoods can differentially determine the impact of weather on population movement as an adaptation strategy, while conflict remains a significant reason for out-migration.

In my third study, I presented a novel application of large language models for multi-hazard disaster event classification. I demonstrated how artificial intelligence can be used to identify and categorize different types of disasters from text-based descriptions, outperforming the speed and often accuracy of traditional human labeling approaches. I found that while fine-tuning a large language model can aid in improving the adherence to prompts, they may not always be the most suitable option for scalable implementation due to high computational costs and the risk of overfitting. This work has important implications for disaster risk management, as artificial intelligence can enable users to grasp situations more quickly and efficiently. These tools, in turn, can improve how we deploy resources to support affected areas.

In tandem, these studies bridge environmental science, human dynamics, and computational analysis. This dissertation contributes to the growing body of knowledge on complex adaptive systems and the imaginative solutions needed to understand them.

Appendix A

Chapter 2 Appendix

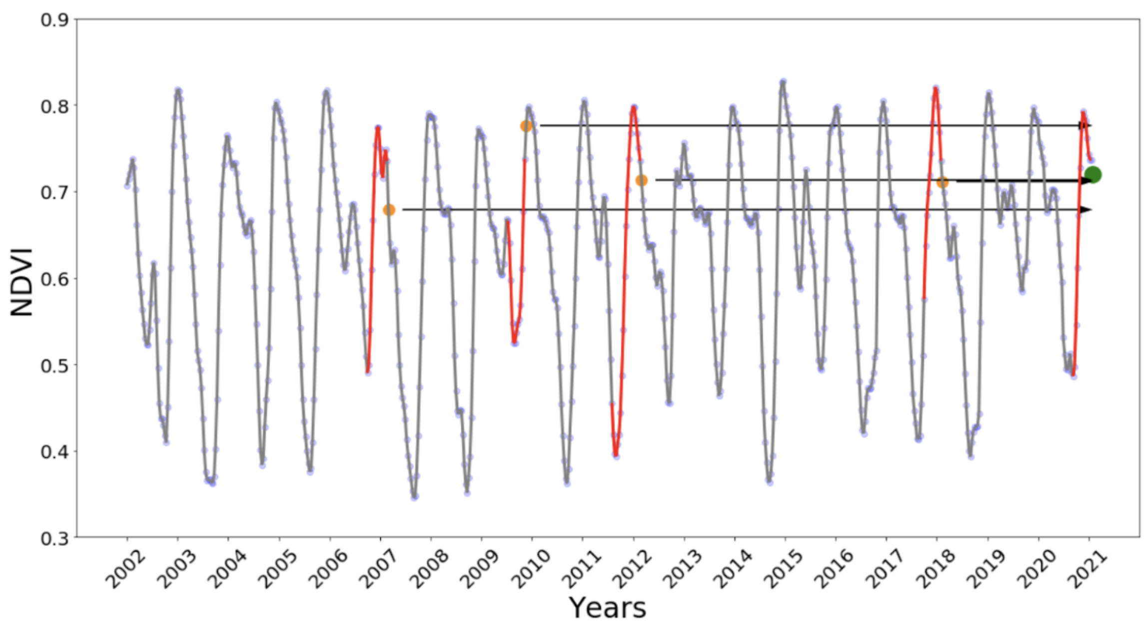

Figure A.1: Demonstration of Simplex Projection: The figure highlights time series segments that exhibit similar trajectories. Simplex projection utilizes these historical patterns to predict future outcomes. The method estimates the next state based on the dynamics observed in these historical segments by identifying and comparing similar past trajectories. The future predicted value is calculated as a weighted average of past similar outcomes. Adapted from Petchey (2016).

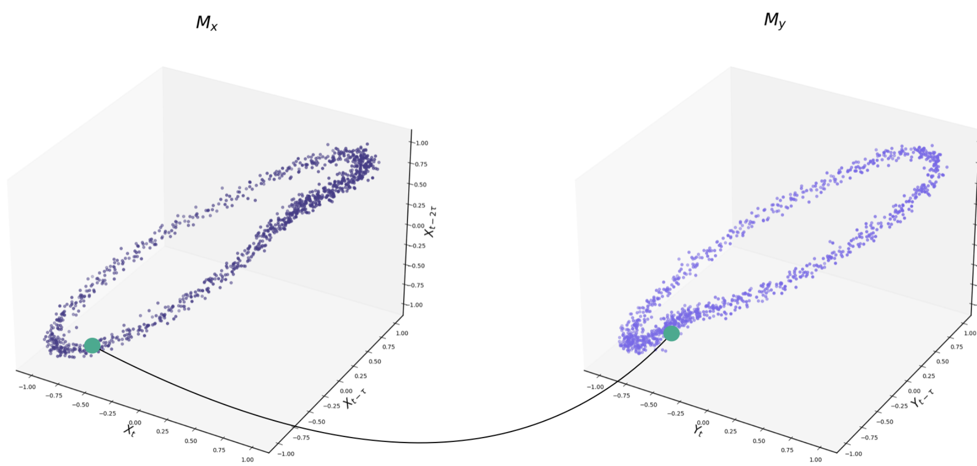

Figure A.2: If X and Y variables from a system create a one-to-one mapping, it means that for each time point t, there is a unique corresponding point between the reconstructed states $Mx(t)$ and $My(t)$. These points are referred to as mutual neighbors. The manifolds exhibit topological isomorphism, indicating that the two reconstructed state spaces (shadow manifolds) map onto each other accurately.

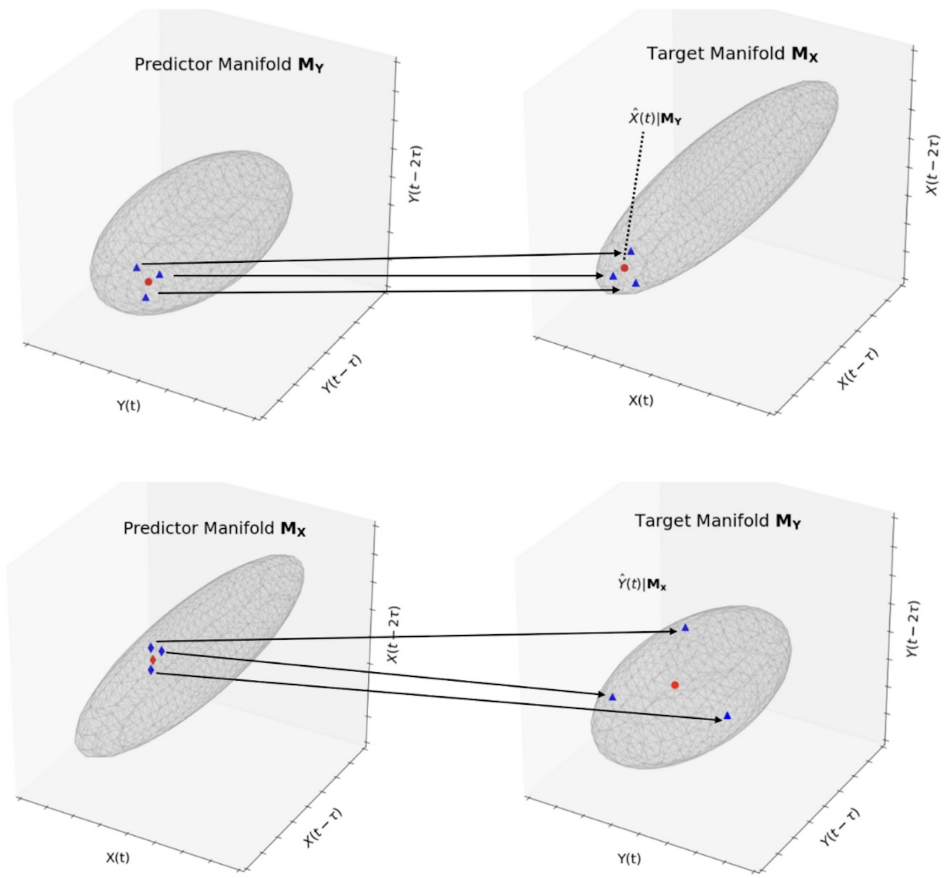

Figure A.3: Demonstration of Convergent Cross Mapping (CCM): The top panels illustrate bidirectional cross-mapping, where each variable can predict the state of the other, indicating a bidirectional causal relationship. The bottom panels show unidirectional cross-mapping, where only one variable can predict the state of the other, suggesting a unidirectional causal influence. Adapted from Sugihara et al. (2012).

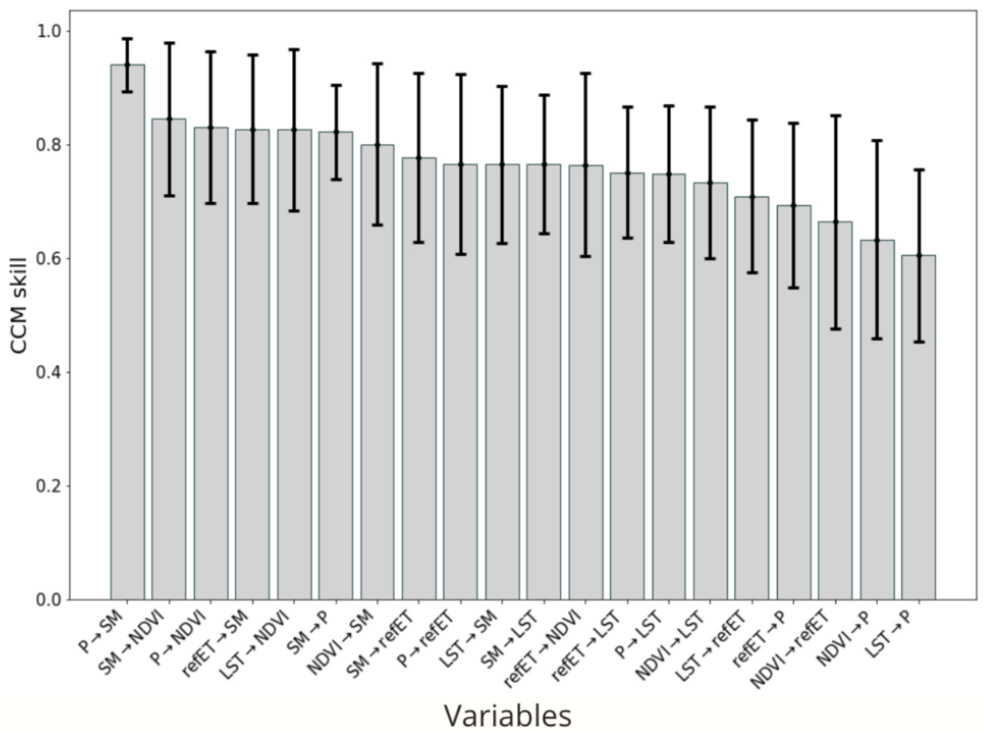

Figure A.4: Cropland convergent cross mapping skill between all combinations of the study variables: precipitation (P), soil moisture (SM), vegetation productivity (NDVI), reference evapotranspiration (refET), and land surface temperature (LST). The skill represents the average final converged value of the driving variable (whichever variable comes up "on top" as having the stronger skill when two variables are mapped onto one another). The standard error bars represent the skill spread across all pixel values.

Appendix B

Chapter 3 Appendix

Table B.1: **Internal displacement gravity model estimates for models 1 to 10**. Standard errors are reported in parentheses. Asterisks indicate significance at the 1, 5, and 10 percent level. Time lags, "t-," are in months. "Events" and "Fatalities" are conflict-related and "1k" refers to occurrence for 1 in 1,000 people. Distance and Population variables are in logarithmic form, and all other variables are z-scores. Year and region fixed effects were included in each model.

Variable	(1)	(2)	(3)	(4)	(5)	(6)	(7)	(8)	(9)	(10)
Log Distance Km	-1.521***	-1.521***	-1.522***	-1.523***	-1.525***	-1.526***	-1.527***	-1.536***	-1.543***	-1.545***
	(0.042)	(0.042)	(0.042)	(0.042)	(0.042)	(0.042)	(0.042)	(0.042)	(0.042)	(0.042)
Arrival Log Pop	0.765	0.759	0.757	0.759	0.728	0.724	0.725	0.662	0.651	0.647
	(1.658)	(1.656)	(1.657)	(1.661)	(1.650)	(1.650)	(1.656)	(1.563)	(1.571)	(1.567)
Departure Log Pop	-0.062	-0.054	-0.052	-0.057	-0.029	-0.020	-0.018	0.042	0.054	0.055
	(1.657)	(1.655)	(1.656)	(1.660)	(1.649)	(1.650)	(1.655)	(1.562)	(1.570)	(1.567)
Arrival Precip		0.043	0.043	0.039	0.038	0.043	0.045	0.012	-0.012	-0.019
		(0.089)	(0.089)	(0.089)	(0.091)	(0.093)	(0.095)	(0.096)	(0.097)	(0.099)
Arrival Precip t-1			0.035	0.026		0.049	0.039		0.001	-0.004
			(0.095)	(0.100)		(0.096)	(0.102)		(0.099)	(0.104)
Arrival Precip t-2				-0.020			-0.021			0.000
				(0.086)			(0.087)			(0.090)
Departure Precip		-0.239*	-0.234*	-0.233*	-0.211	-0.210	-0.209	-0.227*	-0.190	-0.190
		(0.131)	(0.129)	(0.129)	(0.132)	(0.132)	(0.133)	(0.129)	(0.131)	(0.131)
Departure Precip t-1			-0.017	0.004		-0.018	0.011		0.029	0.042
			(0.122)	(0.125)		(0.124)	(0.128)		(0.123)	(0.127)
Departure Precip t-2				0.158			0.154			0.143
				(0.115)			(0.114)			(0.112)
Arrival Temp		-0.124	-0.118	-0.120	-0.135*	-0.126	-0.126	-0.119	-0.127	-0.123
		(0.079)	(0.081)	(0.081)	(0.079)	(0.082)	(0.082)	(0.082)	(0.083)	(0.082)
Arrival Temp t-1			0.045	0.052		0.040	0.055		0.005	0.014
			(0.075)	(0.079)		(0.077)	(0.081)		(0.083)	(0.085)
Arrival Temp t-2				0.072			0.075			0.066
				(0.085)			(0.088)			(0.089)
Departure Temp		-0.025	-0.036	-0.021	0.017	0.006	0.012	-0.019	-0.024	-0.016
		(0.143)	(0.144)	(0.147)	(0.140)	(0.143)	(0.146)	(0.143)	(0.143)	(0.144)
Departure Temp t-1			-0.101	-0.119		-0.074	-0.091		-0.031	-0.056
			(0.145)	(0.140)		(0.145)	(0.140)		(0.152)	(0.151)
Departure Temp t-2				-0.183			-0.173			-0.198
				(0.123)			(0.122)			(0.128)

Table B.1 Continued from previous page

Variable	(1)	(2)	(3)	(4)	(5)	(6)	(7)	(8)	(9)	(10)
Arrival Events Per 1K					-0.063	-0.358**	-0.362*			
					(0.085)	(0.182)	(0.185)			
Arrival Events Per						0.301*	0.349*			
1K t-1						(0.167)	(0.208)			
Arrival Events Per							-0.037			
1K t-2							(0.127)			
Arrival Fatalities Per								-0.110**	-0.097**	-0.105**
1K								(0.045)	(0.046)	(0.048)
Arrival Fatalities Per									-0.120**	-0.123**
1K t-1									(0.057)	(0.050)
Arrival Fatalities Per										0.033
1K t-2										(0.056)
Departure Events Per					0.182**	0.170**	0.168*			
1K					(0.086)	(0.086)	(0.087)			
Departure Events Per						-0.133*	-0.137*			
1K t-1						(0.070)	(0.071)			
Departure Events Per							-0.110			
1K t-2							(0.067)			
Departure Fatalities								0.165***	0.167***	0.174***
Per 1K								(0.035)	(0.036)	(0.037)
Departure Fatalities									0.048	0.045
Per 1K t-1									(0.040)	(0.040)
Departure Fatalities										-0.031
Per 1K t-2										(0.044)
February	-0.116	-0.136	-0.147	-0.143	-0.097	-0.130	-0.150	-0.184	-0.174	-0.165
	(0.276)	(0.273)	(0.274)	(0.285)	(0.273)	(0.278)	(0.292)	(0.269)	(0.268)	(0.283)
March	0.143	0.050	0.042	0.047	0.149	0.107	0.080	0.087	0.104	0.109
	(0.291)	(0.283)	(0.284)	(0.292)	(0.285)	(0.292)	(0.301)	(0.285)	(0.281)	(0.287)
April	0.119	0.054	0.054	0.066	0.126	0.091	0.081	0.087	0.104	0.112
	(0.303)	(0.299)	(0.311)	(0.318)	(0.301)	(0.316)	(0.321)	(0.301)	(0.313)	(0.320)
May	0.488	0.462	0.458	0.521	0.503	0.474	0.506	0.470	0.467	0.525
	(0.343)	(0.345)	(0.348)	(0.347)	(0.346)	(0.350)	(0.351)	(0.348)	(0.350)	(0.350)
June	-0.583**	-0.603**	-0.610**	-0.570**	-0.567**	-0.599**	-0.588**	-0.582**	-0.588**	-0.551*
	(0.277)	(0.274)	(0.277)	(0.280)	(0.273)	(0.280)	(0.283)	(0.275)	(0.275)	(0.282)
July	-0.283	-0.243	-0.256	-0.238	-0.200	-0.235	-0.263	-0.215	-0.215	-0.196
	(0.291)	(0.290)	(0.294)	(0.299)	(0.290)	(0.297)	(0.307)	(0.292)	(0.296)	(0.301)

Table B.1 Continued from previous page

Variable	(1)	(2)	(3)	(4)	(5)	(6)	(7)	(8)	(9)	(10)
August	-0.255	-0.280	-0.283	-0.275	-0.299	-0.279	-0.273	-0.281	-0.276	-0.273
	(0.334)	(0.330)	(0.329)	(0.332)	(0.328)	(0.328)	(0.329)	(0.328)	(0.324)	(0.330)
September	-0.244	-0.260	-0.276	-0.287	-0.295	-0.280	-0.271	-0.337	-0.327	-0.341
	(0.319)	(0.313)	(0.317)	(0.324)	(0.308)	(0.313)	(0.321)	(0.311)	(0.312)	(0.322)
October	0.205	0.143	0.141	0.140	0.163	0.161	0.142	0.160	0.196	0.195
	(0.352)	(0.348)	(0.339)	(0.344)	(0.349)	(0.340)	(0.340)	(0.351)	(0.343)	(0.349)
November	0.760**	0.714**	0.714**	0.733**	0.768**	0.742**	0.749**	0.725**	0.761**	0.779**
	(0.331)	(0.325)	(0.331)	(0.333)	(0.324)	(0.328)	(0.324)	(0.333)	(0.334)	(0.330)
December	-0.467	-0.472*	-0.478*	-0.427	-0.476*	-0.476	-0.442	-0.457	-0.463	-0.417
	(0.291)	(0.284)	(0.286)	(0.291)	(0.288)	(0.291)	(0.295)	(0.287)	(0.287)	(0.294)
AIC	27524073	27368699	27356947	27282285	27156702	26985480	26794041	26961738	26818711	26723219
BIC	27185959	27030619	27018900	26944271	26818637	26647466	26456076	26623674	26480697	26385254
Likelihood	-	-	-	-	-	-	-	-	-	-
	13761982***	13684292***	13678412***	13641077***	13578291***	13492674***	13396949***	13480809***	13409290***	13361537***
N. Obs	29160	29160	29160	29160	29160	29160	29160	29160	29160	29160

Table B.2: **Internal displacement gravity model estimates for models 11 to 19**. Standard errors are reported in parentheses. Asterisks indicate significance at the 1, 5, and 10 percent level. Time lags, "t-," are in months. "Events" and "Fatalities" are conflict-related and "1k" refers to occurrence for 1 in 1,000 people. Distance and Population variables are in logarithmic form, and all other variables are z-scores. Climate and livelihood interaction terms are indicated with an "x" between the variable names. Year and region fixed effects were included in each model.

Variable	(11)	(12)	(13)	(14)	(15)	(16)	(17)	(18)	(19)
Log Distance Km	-1.525***	-1.526***	-1.527***	-1.528***	-1.529***	-1.530***	-1.536***	-1.543***	-1.546***
	(0.042)	(0.042)	(0.042)	(0.042)	(0.042)	(0.042)	(0.041)	(0.042)	(0.042)
Arrival Log Pop	0.656	0.652	0.651	0.635	0.626	0.627	0.547	0.546	0.535
	(1.627)	(1.626)	(1.633)	(1.606)	(1.604)	(1.612)	(1.512)	(1.523)	(1.519)
Departure Log Pop	0.053	0.057	0.055	0.067	0.081	0.083	0.160	0.163	0.171
	(1.626)	(1.625)	(1.632)	(1.606)	(1.603)	(1.611)	(1.510)	(1.522)	(1.518)
Arrival Precip	-0.036	-0.039	-0.043	-0.036	-0.033	-0.033	-0.068	-0.084	-0.092
	(0.114)	(0.116)	(0.116)	(0.117)	(0.122)	(0.125)	(0.131)	(0.132)	(0.133)
Arrival Precip t-1		0.027	0.017		0.038	0.027		-0.006	-0.012
		(0.095)	(0.100)		(0.096)	(0.102)		(0.098)	(0.103)
Arrival Precip t-2			-0.022			-0.022			-0.003
			(0.086)			(0.086)			(0.089)
Departure Precip	0.030	0.051	0.024	0.074	0.082	0.070	0.071	0.108	0.079
	(0.274)	(0.280)	(0.284)	(0.267)	(0.276)	(0.282)	(0.284)	(0.289)	(0.293)
Departure Precip t-1		-0.013	0.009		-0.008	0.020		0.037	0.052
		(0.121)	(0.125)		(0.122)	(0.127)		(0.120)	(0.126)
Departure Precip t-2			0.168			0.162			0.161
			(0.110)			(0.109)			(0.110)
Arrival Temp	-0.125	-0.117	-0.115	-0.140	-0.129	-0.123	-0.127	-0.153	-0.145
	(0.104)	(0.108)	(0.107)	(0.105)	(0.109)	(0.109)	(0.107)	(0.111)	(0.109)
Arrival Temp t-1		0.051	0.057		0.043	0.057		0.010	0.019
		(0.079)	(0.082)		(0.080)	(0.083)		(0.084)	(0.087)
Arrival Temp t-2			0.065			0.071			0.059
			(0.086)			(0.089)			(0.090)
Departure Temp	-1.166	-1.206	-1.217	-1.196	-1.266	-1.262	-1.298	-1.281	-1.286
	(1.090)	(1.103)	(1.104)	(1.101)	(1.091)	(1.089)	(1.095)	(1.092)	(1.084)
Departure Temp t-1		-0.126	-0.145		-0.095	-0.113		-0.049	-0.072
		(0.145)	(0.141)		(0.145)	(0.142)		(0.149)	(0.149)
Departure Temp t-2			-0.187			-0.174			-0.201
			(0.123)			(0.122)			(0.127)

Table B.2 Continued from previous page

Variable	(11)	(12)	(13)	(14)	(15)	(16)	(17)	(18)	(19)
Arrival Events Per 1K				-0.050	-0.356**	-0.362**			
				(0.082)	(0.179)	(0.183)			
Arrival Events Per					0.315*	0.364*			
1K t-1					(0.166)	(0.208)			
Arrival Events Per						-0.038			
1K t-2						(0.127)			
Arrival Fatalities Per							-0.099**	-0.084*	-0.092*
1K							(0.044)	(0.046)	(0.048)
Arrival Fatalities Per								-0.119**	-0.125**
1K t-1								(0.056)	(0.050)
Arrival Fatalities Per									0.041
1K t-2									(0.056)
Departure Events Per				0.185**	0.172**	0.169**			
1K				(0.080)	(0.079)	(0.081)			
Departure Events Per					-0.140**	-0.144**			
1K t-1					(0.071)	(0.072)			
Departure Events Per						-0.101			
1K t-2						(0.068)			
Departure Fatalities							0.168***	0.168***	0.175***
Per 1K							(0.032)	(0.034)	(0.035)
Departure Fatalities								0.052	0.048
Per 1K t-1								(0.039)	(0.040)
Departure Fatalities									-0.027
Per 1K t-2									(0.044)
Arrival Precip x Perc	0.157	0.167	0.169	0.140	0.155	0.154	0.308	0.253	0.278
Pop Agropastoral	(0.268)	(0.272)	(0.273)	(0.273)	(0.280)	(0.286)	(0.284)	(0.292)	(0.296)
Arrival Precip x Perc	1.046***	1.051***	1.042***	1.022***	1.011***	1.015***	0.770**	0.794**	0.796**
Pop Pastoral	(0.381)	(0.384)	(0.387)	(0.356)	(0.358)	(0.365)	(0.316)	(0.319)	(0.317)
Arrival Precip x Perc	-1.318	-1.314	-1.307	-1.356	-1.334	-1.345	-0.965	-1.014	-1.024
Pop Pastoral Fishing	(1.356)	(1.352)	(1.364)	(1.293)	(1.276)	(1.301)	(1.065)	(1.049)	(1.053)
Arrival Precip x Perc	-0.762	-0.763	-0.742	-0.805	-0.774	-0.747	-0.704	-0.789	-0.791
Pop Riverine	(0.489)	(0.499)	(0.491)	(0.492)	(0.500)	(0.490)	(0.507)	(0.526)	(0.520)
Irrigation									
Departure Precip x	-0.218	-0.242	-0.215	-0.236	-0.215	-0.213	-0.485	-0.449	-0.433
Perc Pop	(0.346)	(0.351)	(0.357)	(0.342)	(0.357)	(0.365)	(0.355)	(0.362)	(0.367)
Agropastoral									

Table B.2 Continued from previous page

Variable	(11)	(12)	(13)	(14)	(15)	(16)	(17)	(18)	(19)
Departure Precip x Perc Pop Pastoral	-1.194**	-1.222**	-1.170**	-1.147**	-1.158**	-1.138**	-0.795**	-0.840**	-0.795*
	(0.475)	(0.487)	(0.495)	(0.450)	(0.459)	(0.473)	(0.401)	(0.413)	(0.414)
Departure Precip x Perc Pop Pastoral Fishing	3.111**	3.109**	3.152**	3.159**	3.066**	3.084**	2.686**	2.731**	2.818**
	(1.435)	(1.429)	(1.441)	(1.367)	(1.347)	(1.371)	(1.144)	(1.134)	(1.135)
Departure Precip x Perc Pop Riverine Irrigation	-0.341	-0.342	-0.332	-0.373	-0.419	-0.376	-0.396	-0.353	-0.340
	(0.523)	(0.516)	(0.521)	(0.516)	(0.508)	(0.511)	(0.539)	(0.537)	(0.544)
Arrival Temp x Perc Pop Agropastoral	-0.139	-0.141	-0.153	-0.098	-0.095	-0.120	-0.129	-0.037	-0.057
	(0.357)	(0.358)	(0.358)	(0.355)	(0.353)	(0.359)	(0.362)	(0.364)	(0.364)
Arrival Temp x Perc Pop Pastoral	0.095	0.089	0.083	0.121	0.105	0.087	0.217	0.287	0.286
	(0.535)	(0.534)	(0.537)	(0.529)	(0.530)	(0.534)	(0.557)	(0.557)	(0.548)
Arrival Temp x Perc Pop Pastoral Fishing	-1.073	-1.058	-1.087	-1.133	-1.118	-1.193	-1.116	-1.097	-1.172
	(0.947)	(0.948)	(0.957)	(0.973)	(0.977)	(0.982)	(1.059)	(1.075)	(1.071)
Arrival Temp x Perc Pop Riverine Irrigation	0.296	0.310	0.301	0.290	0.325	0.318	0.229	0.198	0.198
	(0.578)	(0.579)	(0.577)	(0.573)	(0.572)	(0.575)	(0.588)	(0.593)	(0.596)
Departure Temp x Perc Pop Agropastoral	1.212	1.250	1.278	1.233	1.302	1.302	1.369	1.306	1.323
	(1.179)	(1.188)	(1.193)	(1.192)	(1.174)	(1.174)	(1.187)	(1.181)	(1.173)
Departure Temp x Perc Pop Pastoral	0.770	0.794	0.813	0.830	0.881	0.887	0.757	0.720	0.737
	(1.102)	(1.116)	(1.116)	(1.108)	(1.101)	(1.098)	(1.102)	(1.098)	(1.089)
Departure Temp x Perc Pop Pastoral Fishing	1.963	1.964	2.026	2.229	2.255	2.425	2.228	2.216	2.290
	(1.692)	(1.687)	(1.680)	(1.727)	(1.701)	(1.675)	(1.817)	(1.816)	(1.792)
Departure Temp x Perc Pop Riverine Irrigation	1.819	1.842	1.895	1.949	2.007	2.022	2.088	2.050	2.088
	(1.510)	(1.523)	(1.525)	(1.511)	(1.497)	(1.503)	(1.521)	(1.522)	(1.517)
February	-0.135	-0.148	-0.145	-0.109	-0.142	-0.163	-0.202	-0.204	-0.197
	(0.258)	(0.259)	(0.270)	(0.255)	(0.259)	(0.273)	(0.252)	(0.253)	(0.268)
March	0.013	0.002	0.011	0.106	0.063	0.044	0.039	0.042	0.050
	(0.277)	(0.279)	(0.286)	(0.280)	(0.287)	(0.295)	(0.277)	(0.277)	(0.282)
April	0.019	0.012	0.024	0.077	0.038	0.033	0.041	0.049	0.052
	(0.290)	(0.303)	(0.311)	(0.294)	(0.309)	(0.312)	(0.290)	(0.304)	(0.312)
May	0.467	0.458	0.530	0.502	0.473	0.517	0.474	0.459	0.530
	(0.331)	(0.337)	(0.336)	(0.335)	(0.339)	(0.339)	(0.333)	(0.339)	(0.340)

Table B.2 Continued from previous page

Variable	(11)	(12)	(13)	(14)	(15)	(16)	(17)	(18)	(19)
June	-0.623**	-0.632**	-0.588**	-0.592**	-0.625**	-0.604**	-0.606**	-0.611**	-0.565**
	(0.272)	(0.274)	(0.276)	(0.270)	(0.276)	(0.277)	(0.272)	(0.270)	(0.274)
July	-0.246	-0.265	-0.247	-0.209	-0.250	-0.272	-0.221	-0.230	-0.211
	(0.271)	(0.276)	(0.280)	(0.272)	(0.277)	(0.286)	(0.273)	(0.276)	(0.281)
August	-0.270	-0.274	-0.267	-0.301	-0.284	-0.279	-0.275	-0.272	-0.267
	(0.323)	(0.322)	(0.326)	(0.323)	(0.322)	(0.326)	(0.324)	(0.318)	(0.324)
September	-0.281	-0.301	-0.313	-0.328	-0.316	-0.310	-0.378	-0.379	-0.394
	(0.300)	(0.305)	(0.311)	(0.291)	(0.296)	(0.304)	(0.297)	(0.300)	(0.309)
October	0.115	0.110	0.111	0.122	0.119	0.105	0.120	0.145	0.146
	(0.330)	(0.323)	(0.327)	(0.332)	(0.324)	(0.325)	(0.333)	(0.329)	(0.335)
November	0.664**	0.661**	0.682**	0.710**	0.684**	0.700**	0.669**	0.692**	0.706**
	(0.301)	(0.307)	(0.310)	(0.303)	(0.306)	(0.303)	(0.306)	(0.311)	(0.306)
December	-0.534*	-0.543**	-0.490*	-0.546**	-0.555**	-0.517*	-0.533*	-0.552**	-0.504*
	(0.273)	(0.276)	(0.280)	(0.275)	(0.280)	(0.285)	(0.275)	(0.278)	(0.285)
AIC	26874787	26857085	26775861	26627621	26438551	26263776	26436157	26301685.020	26190943
BIC	26536838	26519170	26437979	26289689	26100669	25925943	26098225	25963802.950	25853110
Likelihood	-	-	-	-	-	-	-	-	-
	13437319***	13428464***	13387849***	13313735***	13219193***	13131800***	13218003***	13150761***	13095383***
N. Obs	29160	29160	29160	29160	29160	29160	29160	29160	29160

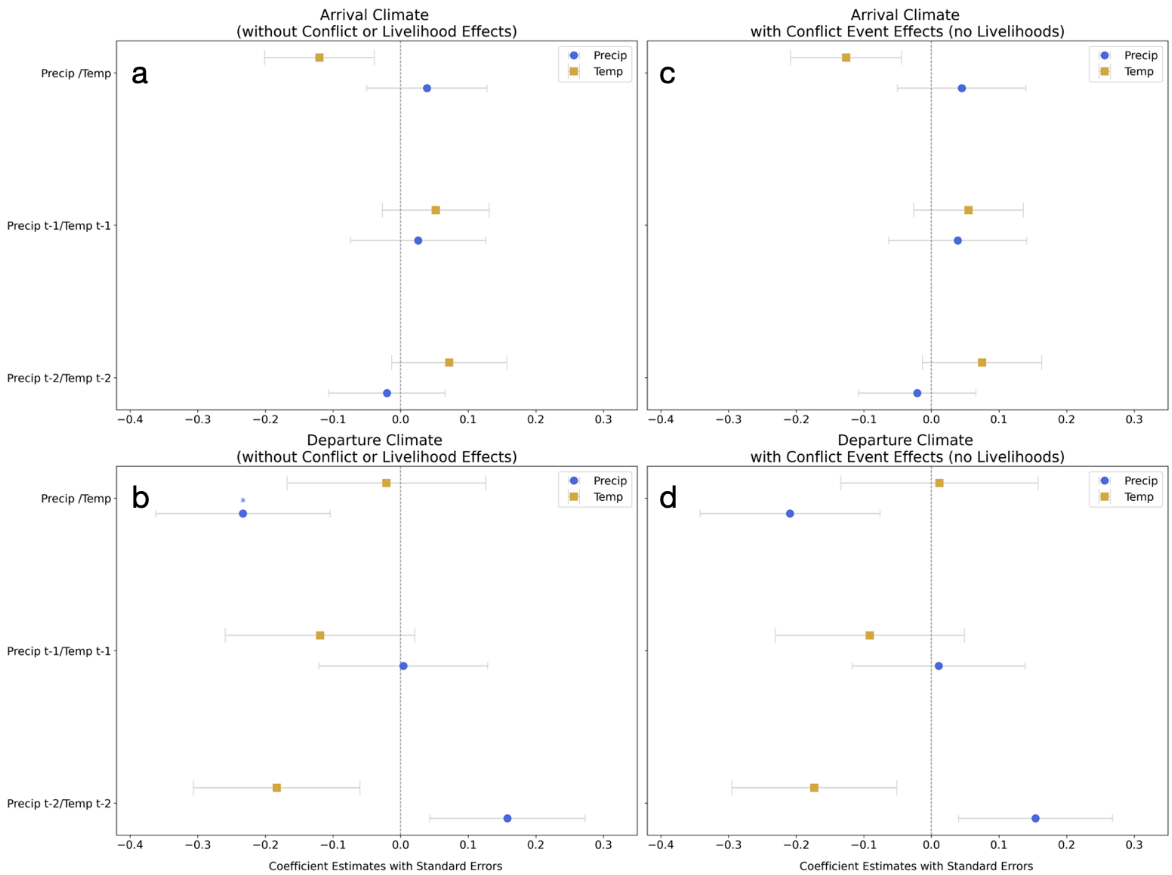

Figure B.1: Coefficient estimates with standard errors for arrival (a) and departure (b) climate effects without conflict or livelihood effects (model 4 from B.1) and with conflict events added for arrival (c) and departure (d) estimates (model 7 from B.1). The lagged inputs are labeled with "t-" and the number of months. Significant coefficients are marked with an asterisk, indicating a p-value of 0.001, 0.05, or 0.1.

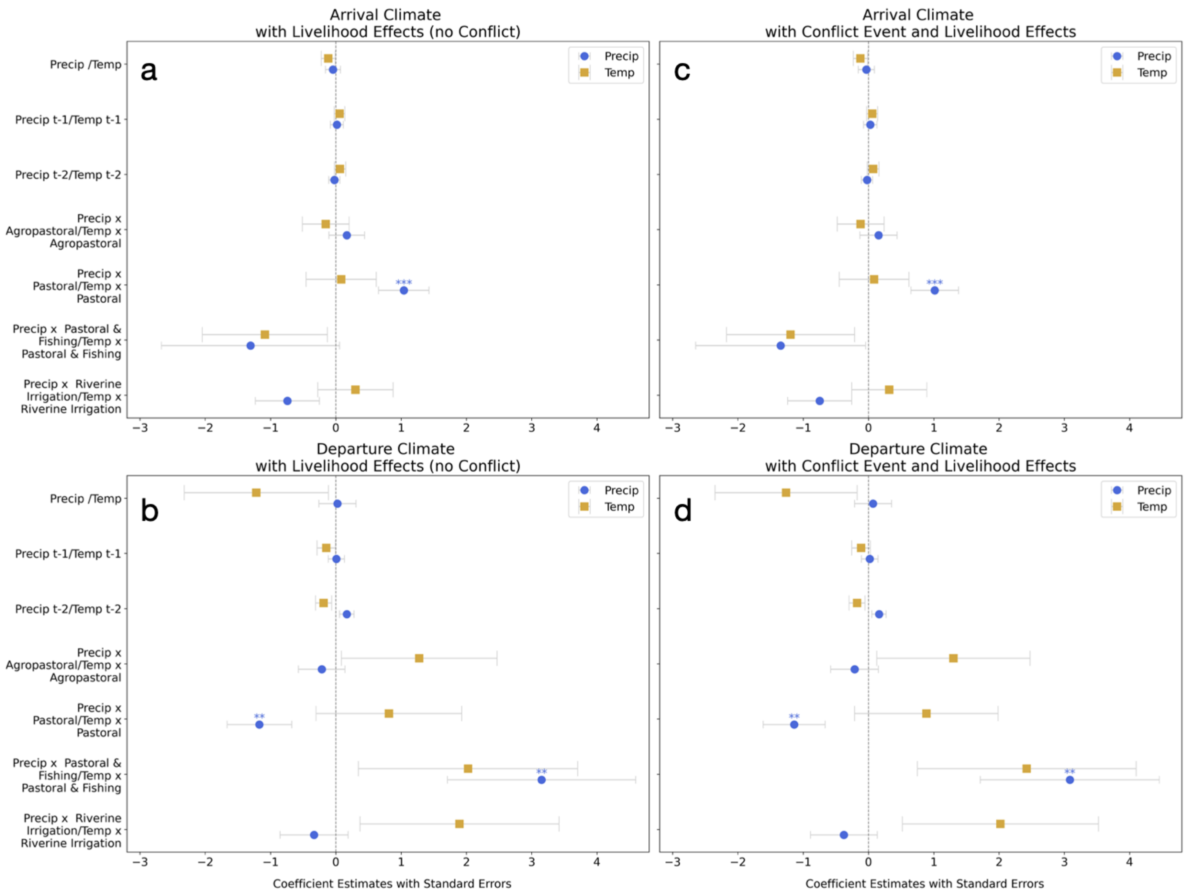

Figure B.2: Coefficient estimates with standard errors for arrival (a) and departure (b) climate effects and livelihood interaction terms without conflict effects (model 13 from B.2) and with conflict events added for arrival (c) and departure (d) estimates (model 16 from B.2. The lagged inputs are labeled with “t-” and the number of months. Significant coefficients are marked with an asterisk, indicating a p-value of 0.001, 0.05, or 0.1.

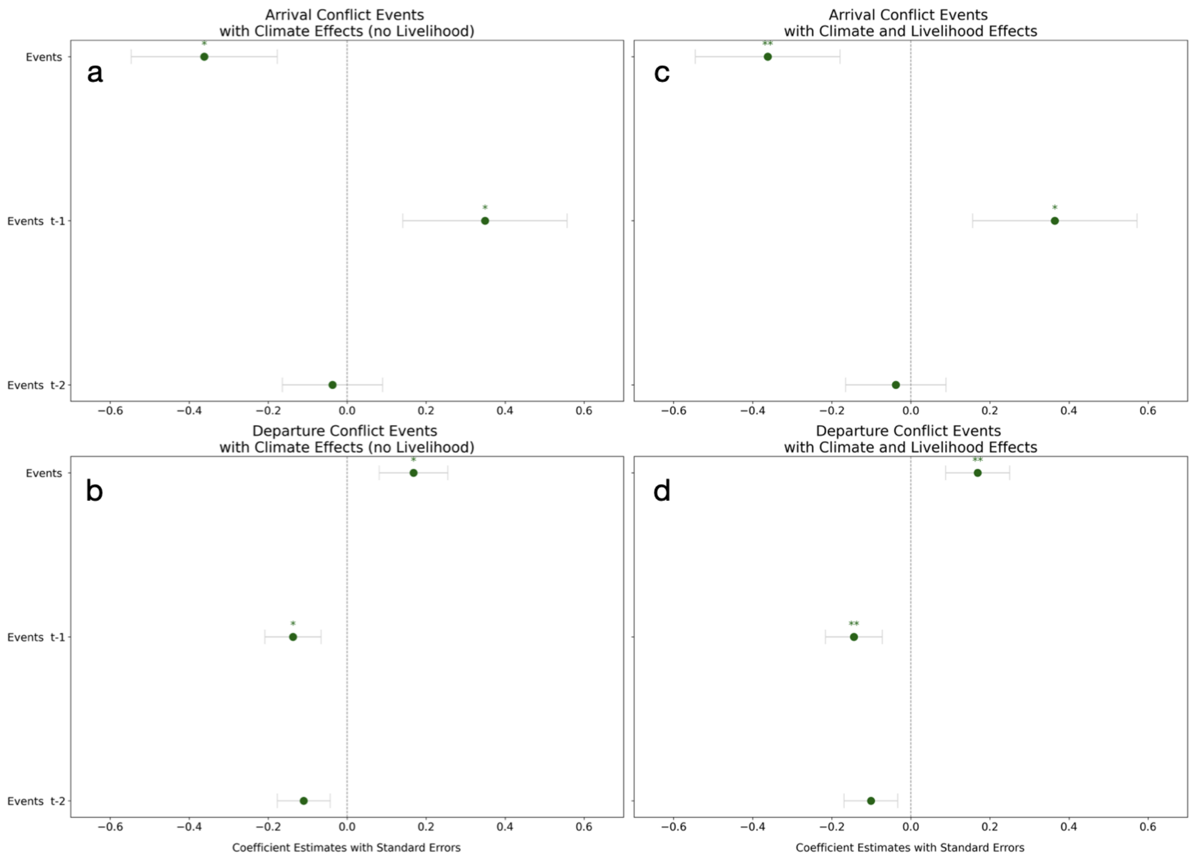

Figure B.3: Coefficient estimates with standard errors for arrival (a) and departure (b) conflict events effects with climate effects and no livelihood inputs (model 7 from B.1) and with livelihood interaction terms added for arrival (c) and departure (d) estimates (model 16 from B.2). The lagged inputs are labeled with "t-" and the number of months. Significant coefficients are marked with an asterisk, indicating a p-value of 0.001, 0.05, or 0.1.

Appendix C

Chapter 4 Appendix

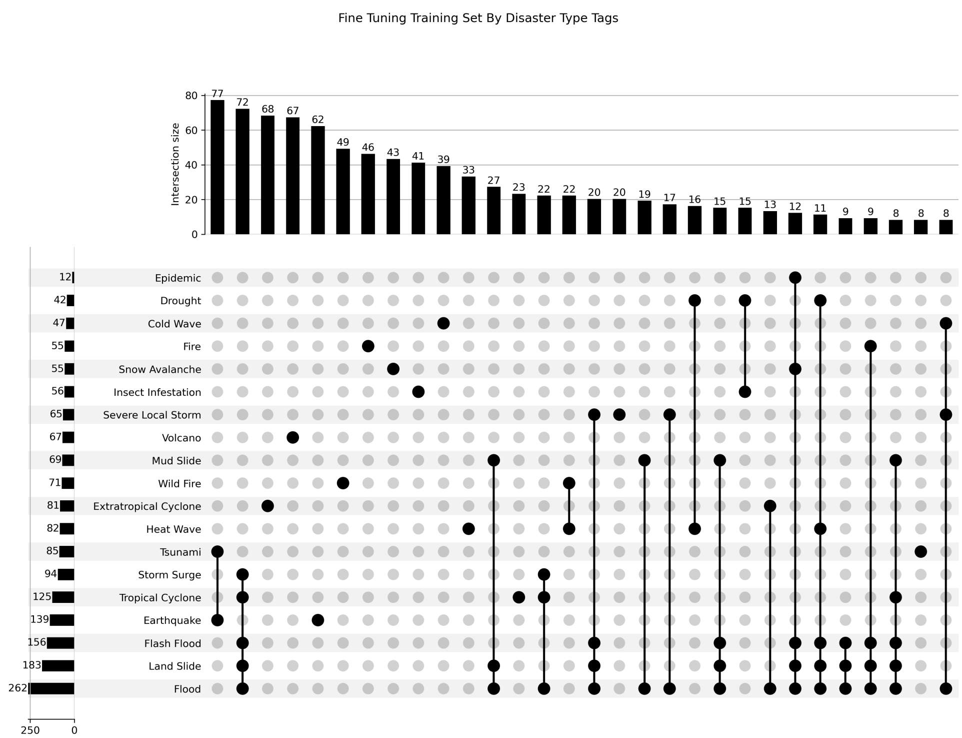

Figure C.1: An UpSet plot of the distribution and overlap of articles used in the training dataset. Each verticle bar represents a set of articles tagged with a specific disaster type, with the height of the bar indicating the number of articles. The horizontal bars at the bottom of the plot show the intersection between different disaster types. These intersections reveal the number of articles from the training dataset that are tagged with multiple disasters. Only the top 30 combinations are displayed.

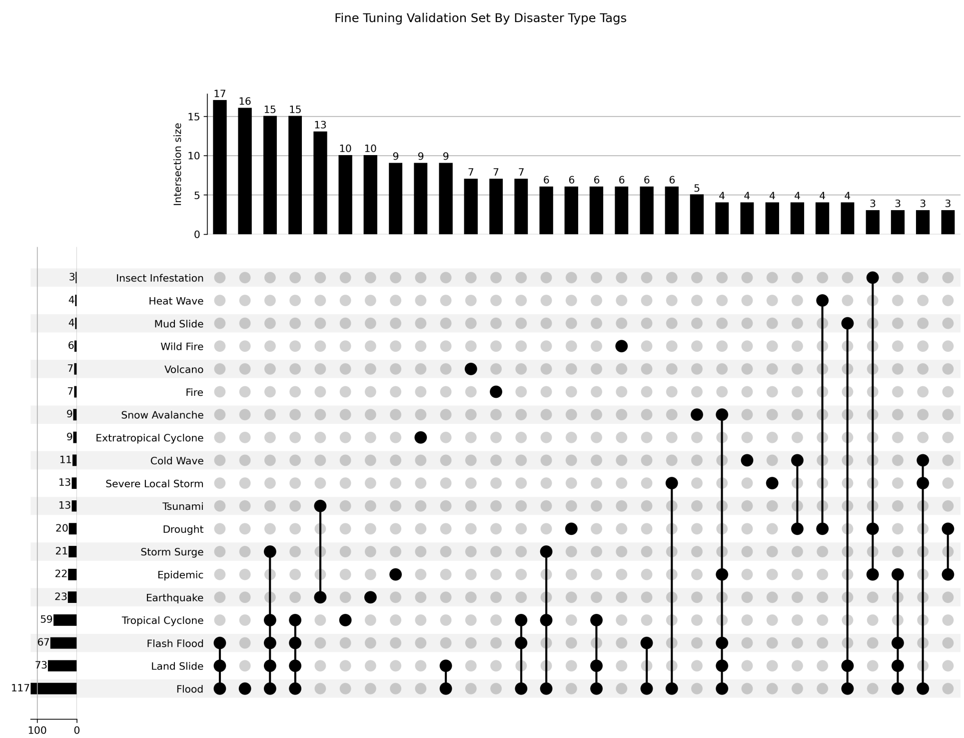

Figure C.2: An UpSet plot of the distribution and overlap of articles used in the validation dataset. Each verticle bar represents a set of articles tagged with a specific disaster type, with the height of the bar indicating the number of articles. The horizontal bars at the bottom of the plot show the intersection between different disaster types. These intersections reveal the number of articles from the validation dataset that are tagged with multiple disasters. Only the top 30 combinations are displayed.

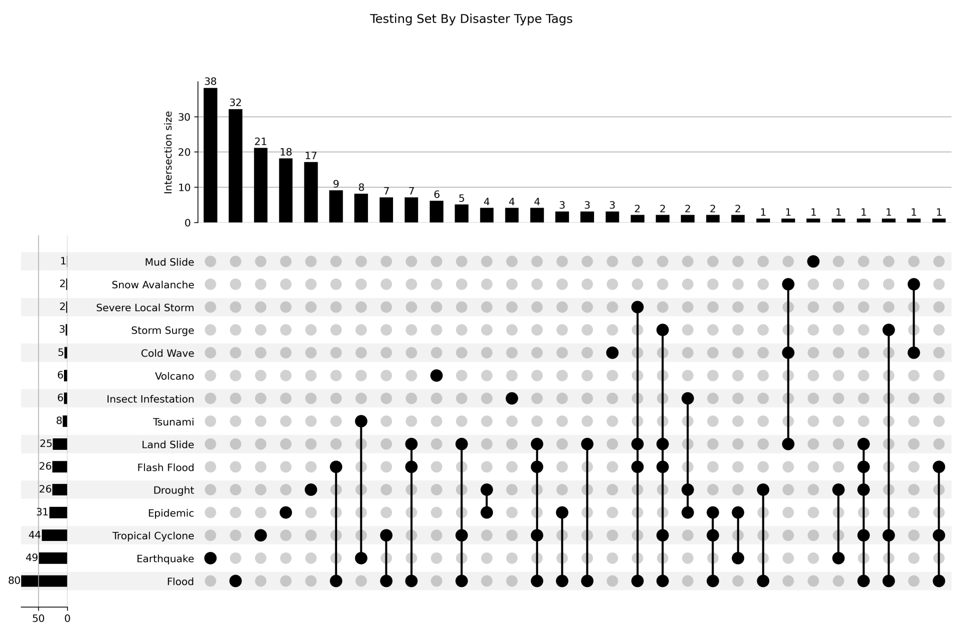

Figure C.3: An UpSet plot of the distribution and overlap of articles used in the test dataset. Each verticle bar represents a set of articles tagged with a specific disaster type, with the height of the bar indicating the number of articles. The horizontal bars at the bottom of the plot show the intersection between different disaster types. These intersections reveal the number of articles from the test dataset that are tagged with multiple disasters. Only the top 30 combinations are displayed.

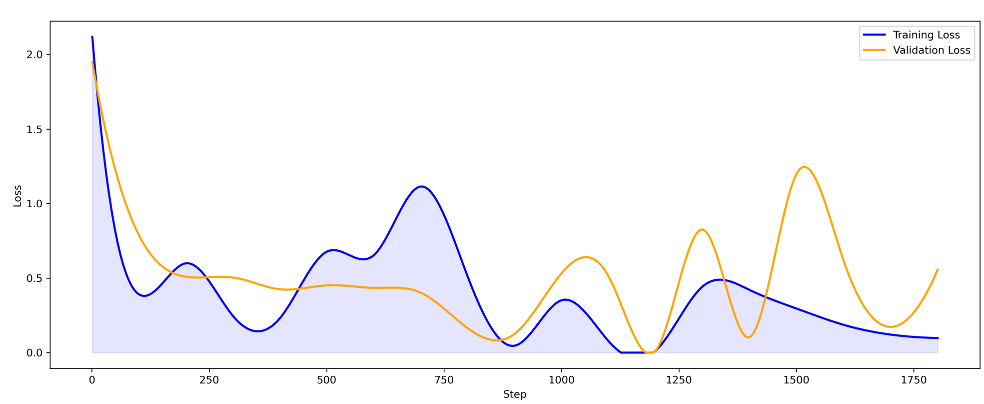

Figure C.4: Fine tuning training and validation loss metrics by step.

Bibliography

Abavisani, M., Wu, L., Hu, S., Tetreault, J., and Jaimes, A. (2020). Multimodal Categorization of Crisis Events in Social Media. In *2020 IEEE/CVF Conference on Computer Vision and Pattern Recognition (CVPR)*, pages 14667–14677. ISSN: 2575-7075.

Abel, G. J., Brottrager, M., Crespo Cuaresma, J., and Muttarak, R. (2019). Climate, conflict and forced migration. *Global Environmental Change*, 54:239–249.

Achour, M. and Lacan, N. (2011). DROUGHT IN SOMALIA: A MIGRATION CRISIS. page 16.

Adaawen, S., Rademacher-Schulz, C., Schraven, B., and Segadlo, N. (2019). Chapter 2 - Drought, migration, and conflict in sub-Saharan Africa: what are the links and policy options? In Mapedza, E., Tsegai, D., Bruntrup, M., and Mcleman, R., editors, *Current Directions in Water Scarcity Research*, volume 2 of *Drought Challenges*, pages 15–31. Elsevier.

Adhikari, U., Nejadhashemi, A. P., and Woznicki, S. A. (2015). Climate change and eastern Africa: a review of impact on major crops. *Food and Energy Security*, 4(2):110–132. _eprint: https://onlinelibrary.wiley.com/doi/pdf/10.1002/fes3.61.

AghaKouchak, A., Chiang, F., Huning, L. S., Love, C. A., Mallakpour, I., Mazdiyasni, O., Moftakhari, H., Papalexiou, S. M., Ragno, E., and Sadegh, M. (2020). Climate Extremes and Compound Hazards in a Warming World. *Annual Review of Earth and Planetary Sciences*, 48(1):519–548. _eprint: https://doi.org/10.1146/annurev-earth-071719-055228.

Ahmed, M., Mohamed, M. D., and Muhammad, F. (2023). Pastoralists Adaptation Strategies, and Resilience Capacity to Climate Change in Somalia: A Scoping Review. preprint, In Review.

Ahmed, Z., Ataullahjan, A., Gaffey, M. F., Osman, M., Umutoni, C., Bhutta, Z. A., and Dalmar, A. A. (2020). Understanding the factors affecting the humanitarian health and nutrition response for women and children in Somalia since 2000: a case study. *Conflict and Health*, 14(1):35.

Ajuang Ogallo, L., Omondi, P., Ouma, G., and Wayumba, G. (2018). Climate Change Projections and the Associated Potential Impacts for Somalia. *American Journal of Climate Change*, 07(02):153–170.

Alam, F., Ofli, F., and Imran, M. (2020). Descriptive and visual summaries of disaster events using artificial intelligence techniques: case studies of Hurricanes Harvey, Irma, and Maria. *Behaviour & Information Technology*, 39(3):288–318. Publisher: Taylor & Francis _eprint: https://doi.org/10.1080/0144929X.2019.1610908.

Alam, F., Sajjad, H., Imran, M., and Ofli, F. (2021). CrisisBench: Benchmarking Crisis-related Social Media Datasets for Humanitarian Information Processing. arXiv:2004.06774 [cs].

Ali, A. I., Kassem, Y., and Gökçekuş, H. (2023). Examining the impact of climate change on water resources in Somalia: The role of adaptation. *Future Technology*, 2(4):45–58. Number: 4.

Anderson, J. E. (2011). The Gravity Model. *Annual Review of Economics*, 3(1):133–160. _eprint: https://doi.org/10.1146/annurev-economics-111809-125114.

Arachie, C., Gaur, M., Anzaroot, S., Groves, W., Zhang, K., and Jaimes, A. (2020). Unsupervised Detection of Sub-Events in Large Scale Disasters. *Proceedings of the AAAI Conference on Artificial Intelligence*, 34(01):354–361. Number: 01.

Ashraf, M., Arshad, A., Patel, P. M., Khan, A., Qamar, H., Siti-Sundari, R., Ghani, M. U., Amin, A., and Babar, J. R. (2021). Quantifying climate-induced drought risk to livelihood and mitigation actions in Balochistan. *Natural Hazards*.

Asoka, A. and Mishra, V. (2015). Prediction of vegetation anomalies to improve food security and water management in India. *Geophysical Research Letters*, 42(13):5290–5298.

Ayugi, B., Shilenje, Z. W., Babaousmail, H., Lim Kam Sian, K. T. C., Mumo, R., Dike, V. N., Iyakaremye, V., Chehbouni, A., and Ongoma, V. (2022). Projected changes in meteorological drought over East Africa inferred from bias-adjusted CMIP6 models. *Natural Hazards (Dordrecht, Netherlands)*, pages 1–26.

Backhaus, A., Martinez-Zarzoso, I., and Muris, C. (2015). Do climate variations explain bilateral migration? A gravity model analysis. *IZA Journal of Migration*, 4(1):3.

Bakonyi, J. (2021). The Political Economy of Displacement: Rent Seeking, Dispossessions and Precarious Mobility in Somali Cities. *Global Policy*, 12(S2):10–22. _eprint: https://onlinelibrary.wiley.com/doi/pdf/10.1111/1758-5899.12849.

Balashankar, A., Subramanian, L., and Fraiberger, S. P. (2023). Predicting food crises using news streams. *Science Advances*, 9(9):eabm3449. Publisher: American Association for the Advancement of Science.

Bartsev, S., Saltykov, M., Belolipetsky, P., and Pianykh, A. (2021). Imperfection of the convergent cross-mapping method. *IOP Conference Series: Materials Science and Engineering*, 1047(1):012081. Publisher: IOP Publishing.

Beduschi, A. (2022). Harnessing the potential of artificial intelligence for humanitarian action: Opportunities and risks. *International Review of the Red Cross*, 104(919):1149–1169. Publisher: Cambridge University Press.

Belliardo, E., Kalimeri, K., and Mejova, Y. (2023). Leave no Place Behind: Improved Geolocation in Humanitarian Documents. In *Proceedings of the 2023 ACM Conference on Information Technology for Social Good*, pages 31–39, Lisbon Portugal. ACM.

Benveniste, H., Oppenheimer, M., and Fleurbaey, M. (2022). Climate change increases resource-constrained international immobility. *Nature Climate Change*, 12(7):634–641. Number: 7 Publisher: Nature Publishing Group.

Berg, A., Findell, K., Lintner, B., Giannini, A., Seneviratne, S. I., van den Hurk, B., Lorenz, R., Pitman, A., Hagemann, S., Meier, A., Cheruy, F., Ducharne, A., Malyshev, S., and Milly, P. C. D. (2016). Land–atmosphere feedbacks amplify aridity increase over land under global warming. *Nature Climate Change*, 6(9):869–874. Number: 9 Publisher: Nature Publishing Group.

Billi, P. and Sebhat, M. Y. (2022). River Hydromorphology and Flood Hazard in Somalia. In Billi, P., editor, *Landscapes and Landforms of the Horn of Africa: Eritrea, Djibouti, Somalia*, World Geomorphological Landscapes, pages 281–311. Springer International Publishing, Cham.

Black, R., Adger, W. N., Arnell, N. W., Dercon, S., Geddes, A., and Thomas, D. (2011). The effect of environmental change on human migration. *Global Environmental Change*, 21:S3–S11.

Blocher, J. M., Hoffmann, R., and Weisz, H. (2024). The effects of environmental and non-environmental shocks on livelihoods and migration in Tanzania. *Population and Environment*, 46(1):7.

Bonotto, G., Peterson, T. J., Fowler, K., and Western, A. W. (2022). Identifying Causal Interactions Between Groundwater and Streamflow Using Convergent Cross-Mapping. *Water Resources Research*, 58(8):e2021WR030231. _eprint: https://onlinelibrary.wiley.com/doi/pdf/10.1029/2021WR030231.

Borderon, M., sakdapolrak, p., muttarak, R., Kebede, E., Pagogna, R., and Sporer, E. (2019). Migration influenced by environmental change in Africa: A systematic review of empirical evidence. *Demographic Research*, 41:491–544.

Brown, J. F., Howard, D., Wylie, B., Frieze, A., Ji, L., and Gacke, C. (2015). Application-Ready Expedited MODIS Data for Operational Land Surface Monitoring of Vegetation Condition. *Remote Sensing*, 7(12):16226–16240. Number: 12 Publisher: Multidisciplinary Digital Publishing Institute.

Brunner, M. I. (2023). Floods and droughts: a multivariate perspective. *Hydrology and Earth System Sciences*, 27(13):2479–2497. Publisher: Copernicus GmbH.

Canadell, J., Jackson, R. B., Ehleringer, J. B., Mooney, H. A., Sala, O. E., and Schulze, E.-D. (1996). Maximum rooting depth of vegetation types at the global scale. *Oecologia*, 108(4):583–595.

Cantor, D. J. (2023). Divergent dynamics: disasters and conflict as 'drivers' of internal displacement? *Disasters*, n/a(n/a). _eprint: https://onlinelibrary.wiley.com/doi/pdf/10.1111/disa.12589.

Cao, L., Xu, J., Chen, Y., Li, W., Yang, Y., Hong, Y., and Li, Z. (2013). Understanding the dynamic coupling between vegetation cover and climatic factors in a semiarid region—a case study of Inner Mongolia, China. *Ecohydrology*, 6(6):917–926. _eprint: https://onlinelibrary.wiley.com/doi/pdf/10.1002/eco.1245.

Ceola, S., Mård, J., and Di Baldassarre, G. (2023). Drought and Human Mobility in Africa. *Earth's Future*, 11(12):e2023EF003510. _eprint: https://onlinelibrary.wiley.com/doi/pdf/10.1029/2023EF003510.

Chae, Y. and Davidson, T. (2023). Large Language Models for Text Classification: From Zero-Shot Learning to Fine-Tuning. *Open Science Foundation*.

Chamaillé-Jammes, S. and Fritz, H. (2009). Precipitation–NDVI relationships in eastern and southern African savannas vary along a precipitation gradient. *International Journal of Remote Sensing*, 30(13):3409–3422. Publisher: Taylor & Francis _eprint: https://doi.org/10.1080/01431160802562206.

Chang, C.-W., Ushio, M., and Hsieh, C.-h. (2017). Empirical dynamic modeling for beginners. *Ecological Research*, 32(6):785–796.

Chen, C., He, B., Yuan, W., Guo, L., and Zhang, Y. (2019). Increasing interannual variability of global vegetation greenness. *Environmental Research Letters*, 14(12):124005. Publisher: IOP Publishing.

Chen, M., Tao, Z., Tang, W., Qin, T., Yang, R., and Zhu, C. (2023). Enhancing Emergency Decision-making with Knowledge Graphs and Large Language Models. arXiv:2311.08732 [cs].

Claassen, J. N., Ward, P. J., Daniell, J., Koks, E. E., Tiggeloven, T., and de Ruiter, M. C. (2023). A new method to compile global multi-hazard event sets. *Scientific Reports*, 13(1):13808. Publisher: Nature Publishing Group.

Clark, A. T., Ye, H., Isbell, F., Deyle, E. R., Cowles, J., Tilman, G. D., and Sugihara, G. (2015). Spatial convergent cross mapping to detect causal relationships from short time series. *Ecology*, 96(5):1174–1181. _eprint: https://onlinelibrary.wiley.com/doi/pdf/10.1890/14-1479.1.

Clement, V., Rigaud, K. K., de Sherbinin, A., Jones, B., Adamo, S., Schewe, J., Sadiq, N., and Shabahat, E. (2021). *Groundswell Part 2*. Other papers. World Bank.

Conway, D., Allison, E., Felstead, R., and Goulden, M. (2005). Rainfall variability in East Africa: implications for natural resources management and livelihoods. *Philosophical Transactions of the Royal Society A: Mathematical, Physical and Engineering Sciences*, 363(1826):49–54.

Cutter, S. L. (2018). Compound, Cascading, or Complex Disasters: What's in a Name? *Environment: Science and Policy for Sustainable Development*, 60(6):16–25. Publisher: Routledge _eprint: https://doi.org/10.1080/00139157.2018.1517518.

de Ruiter, M. C., Couasnon, A., van den Homberg, M. J. C., Daniell, J. E., Gill, J. C., and Ward, P. J. (2020). Why We Can No Longer Ignore Consecutive Disasters. *Earth's Future*, 8(3):e2019EF001425. _eprint: https://onlinelibrary.wiley.com/doi/pdf/10.1029/2019EF001425.

Defourny, P., Lamarche, C., Bontemps, S., De Maet, T., Van Bogaert, E., Moreau, I., Brockmann, C., Boettcher, M., Kirches, G., and Wevers, J. (2017). Land cover climate change initiative-product user guide v2. Issue 2.0. *ESA-UCLouvain-Geomatics, Louvain-la-Neuve, Belgium, Tech. Rep.*

Deyle, E. R., Fogarty, M., Hsieh, C.-h., Kaufman, L., MacCall, A. D., Munch, S. B., Perretti, C. T., Ye, H., and Sugihara, G. (2013). Predicting climate effects on Pacific sardine. *Proceedings of the National Academy of Sciences*, 110(16):6430–6435.

Deyle, E. R., Maher, M. C., Hernandez, R. D., Basu, S., and Sugihara, G. (2016). Global environmental drivers of influenza. *Proceedings of the National Academy of Sciences*, page 201607747.

D'Odorico, P., Caylor, K., Okin, G. S., and Scanlon, T. M. (2007). On soil moisture–vegetation feedbacks and their possible effects on the dynamics of dryland ecosystems. *Journal of Geophysical Research: Biogeosciences*, 112(G4). _eprint: https://agupubs.onlinelibrary.wiley.com/doi/pdf/10.1029/2006JG000379.

Earney, C. and Moreno Jimenez, R. (2019). Pioneering Predictive Analytics for Decision-Making in Forced Displacement Contexts. In Salah, A. A., Pentland, A., Lepri, B., and Letouzé, E., editors, *Guide to Mobile Data Analytics in Refugee Scenarios: The 'Data for Refugees Challenge' Study*, pages 101–119. Springer International Publishing, Cham.

Fanning, E. (2018). Drought, Displacement and Livelihoods in Somalia/Somaliland: Time for gender-sensitive and protection-focused approaches. Technical report, Concern Worldwide; Danish Refugee Council; Norwegian Refugee Council; Oxfam; Plan International; REACH; Save Somali Women and Children.

Fekih, S., Tamagnone, N., Minixhofer, B., Shrestha, R., Contla, X., Oglethorpe, E., and Rekabsaz, N. (2022). HumSet: Dataset of Multilingual Information Extraction and Classification for Humanitarian Crisis Response. arXiv:2210.04573 [cs].

FEWSNET (2015). Somalia Livelihoods Zones Map.

Floridi, L. and Chiriatti, M. (2020). GPT-3: Its Nature, Scope, Limits, and Consequences. *Minds and Machines*, 30(4):681–694.

Fogarty, M. J. and Collie, J. S. (2020). Empirical Dynamic Modeling. In Fogarty, M. J. and Collie, J. S., editors, *Fishery Ecosystem Dynamics*, page 0. Oxford University Press.

Freeman, L. (2017). Environmental Change, Migration, and Conflict in Africa: A Critical Examination of the Interconnections. *The Journal of Environment & Development*, 26(4):351–374. Publisher: SAGE Publications Inc.

Funk, C., Dettinger, M. D., Michaelsen, J. C., Verdin, J. P., Brown, M. E., Barlow, M., and Hoell, A. (2008). Warming of the Indian Ocean threatens eastern and southern African food security but could be mitigated by agricultural development. *Proceedings of the National Academy of Sciences*, 105(32):11081–11086. Publisher: National Academy of Sciences Section: Physical Sciences.

Funk, C., Peterson, P., Landsfeld, M., Pedreros, D., Verdin, J., Shukla, S., Husak, G., Rowland, J., Harrison, L., Hoell, A., and Michaelsen, J. (2015). The climate hazards infrared precipitation with stations—a new environmental record for monitoring extremes. *Scientific Data*, 2(1):150066. Number: 1 Publisher: Nature Publishing Group.

Funk, C., Peterson, P., Peterson, S., Shukla, S., Davenport, F., Michaelsen, J., Knapp, K. R., Landsfeld, M., Husak, G., Harrison, L., Rowland, J., Budde, M., Meiburg, A., Dinku, T., Pedreros, D., and Mata, N. (2019). A High-Resolution 1983–2016 T max Climate Data Record Based on Infrared Temperatures and Stations by the Climate Hazard Center. *Journal of Climate*, 32(17):5639–5658. Publisher: American Meteorological Society Section: Journal of Climate.

Funk, C. C. and Brown, M. E. (2006). Intra-seasonal NDVI change projections in semi-arid Africa. *Remote Sensing of Environment*, 101(2):249–256.

GADM (2015). Global ADMinistrative Areas.

Gao, Y., Xiong, Y., Gao, X., Jia, K., Pan, J., Bi, Y., Dai, Y., Sun, J., Wang, M., and Wang, H. (2024). Retrieval-Augmented Generation for Large Language Models: A Survey. arXiv:2312.10997 [cs].

Garcia, A. J., Pindolia, D. K., Lopiano, K. K., and Tatem, A. J. (2015). Modeling internal migration flows in sub-Saharan Africa using census microdata. *Migration Studies*, 3(1):89–110.

Gebrechorkos, S. H., Taye, M. T., Birhanu, B., Solomon, D., and Demissie, T. (2023). Future Changes in Climate and Hydroclimate Extremes in East Africa. *Earth's Future*, 11(2):e2022EF003011. _eprint: https://onlinelibrary.wiley.com/doi/pdf/10.1029/2022EF003011.

Gevaert, C. M., Carman, M., Rosman, B., Georgiadou, Y., and Soden, R. (2021). Fairness and accountability of AI in disaster risk management: Opportunities and challenges. *Patterns*, 2(11):100363.

Ghaffarian, S., Taghikhah, F. R., and Maier, H. R. (2023). Explainable artificial intelligence in disaster risk management: Achievements and prospective futures. *International Journal of Disaster Risk Reduction*, 98:104123.

Gherardi, L. A. and Sala, O. E. (2019). Effect of interannual precipitation variability on dryland productivity: A global synthesis. *Global Change Biology*, 25(1):269–276. _eprint: https://onlinelibrary.wiley.com/doi/pdf/10.1111/gcb.14480.

Ghosh, S., Maji, S., and Desarkar, M. S. (2022). GNoM: Graph Neural Network Enhanced Language Models for Disaster Related Multilingual Text Classification. In *Proceedings of the 14th ACM Web Science Conference 2022*, WebSci '22, pages 55–65, New York, NY, USA. Association for Computing Machinery.

Ginnetti, J. and Franck, T. (2014). Assessing Drought Displacement Risk for Kenyan, Ethiopian and Somali Pastoralists. Technical report, NRC, IDMC.

Goecks, V. G. and Waytowich, N. R. (2023). DisasterResponseGPT: Large Language Models for Accelerated Plan of Action Development in Disaster Response Scenarios. arXiv:2306.17271 [cs].

Greiner, C. and Sakdapolrak, P. (2013). Rural–urban migration, agrarian change, and the environment in Kenya: a critical review of the literature. *Population and Environment*, 34(4):524–553.

Griffith, D., Muneepeerakul, R., Guerry, G., Cabrero, A. C., Johnson, J. C., Munoz-Carpena, R., Puma, M., Lall, U., and Homayounfar, M. (2023). Migration and livelihood constellations: Assessing common themes in the face of environmental change in Somalia and among Agro-Pastoral peoples. *International Migration*, n/a(n/a). _eprint: https://onlinelibrary.wiley.com/doi/pdf/10.1111/imig.13122.

Groen, D. (2018). Development of a Multiscale Simulation Approach for Forced Migration. In Shi, Y., Fu, H., Tian, Y., Krzhizhanovskaya, V. V., Lees, M. H., Dongarra, J., and Sloot, P. M. A., editors, *Computational Science – ICCS 2018*, Lecture Notes in Computer Science, pages 869–875, Cham. Springer International Publishing.

Hao, Z., Hao, F., Singh, V. P., and Zhang, X. (2018). Changes in the severity of compound drought and hot extremes over global land areas. *Environmental Research Letters*, 13(12):124022. Publisher: IOP Publishing.

Hao, Z., Hao, F., Xia, Y., Feng, S., Sun, C., Zhang, X., Fu, Y., Hao, Y., Zhang, Y., and Meng, Y. (2022). Compound droughts and hot extremes: Characteristics, drivers, changes, and impacts. *Earth-Science Reviews*, 235:104241.

Hawinkel, P., Thiery, W., Lhermitte, S., Swinnen, E., Verbist, B., Van Orshoven, J., and Muys, B. (2016). Vegetation response to precipitation variability in East Africa controlled by biogeographical factors. *Journal of Geophysical Research: Biogeosciences*, 121(9):2422–2444. _eprint: https://onlinelibrary.wiley.com/doi/pdf/10.1002/2016JG003436.

Helman, D. and Zaitchik, B. F. (2020). Temperature anomalies affect violent conflicts in African and Middle Eastern warm regions. *Global Environmental Change*, 63:102118.

Hermans, K. and Garbe, L. (2019). Droughts, livelihoods, and human migration in northern Ethiopia. *Regional Environmental Change*, 19(4):1101–1111.

Hermans, K. and McLeman, R. (2021). Climate change, drought, land degradation and migration: exploring the linkages. *Current Opinion in Environmental Sustainability*, 50:236–244.

Hersbach, H., Bell, B., Berrisford, P., Hirahara, S., Horányi, A., Muñoz-Sabater, J., Nicolas, J., Peubey, C., Radu, R., Schepers, D., Simmons, A., Soci, C., Abdalla, S., Abellan, X., Balsamo, G., Bechtold, P., Biavati, G., Bidlot, J., Bonavita, M., De Chiara, G., Dahlgren, P., Dee, D., Diamantakis, M., Dragani, R., Flemming, J., Forbes, R., Fuentes, M., Geer, A., Haimberger, L., Healy, S., Hogan, R. J., Hólm, E., Janisková, M., Keeley, S., Laloyaux, P., Lopez, P., Lupu, C., Radnoti, G., de Rosnay, P., Rozum, I., Vamborg, F., Villaume, S., and Thépaut, J.-N. (2020). The ERA5 global reanalysis. *Quarterly Journal of the Royal Meteorological Society*, 146(730):1999–2049. _eprint: https://onlinelibrary.wiley.com/doi/pdf/10.1002/qj.3803.

Hesla, B. I., Tieszen, H. L., and Boutton, T. W. (1985). Seasonal water relations of savanna shrubs and grasses in Kenya, East Africa. *Journal of Arid Environments*, 8(1):15–31.

Hobbins, M., Dewes, C., McEvoy, D., Shukla, S., Harrison, L. S., Blakeley, S. L., McNally, A., and Verdin, J. P. (2018). A New Global Reference Evapotranspiration Reanalysis

Forced by MERRA2: Opportunities for Famine Early Warning, Drought Attribution, and Improving Drought Monitoring. AMS.

Hoffmann, R. (2022). Contextualizing Climate Change Impacts on Human Mobility in African Drylands. *Earth's Future*, 10(6):e2021EF002591. _eprint: https://onlinelibrary.wiley.com/doi/pdf/10.1029/2021EF002591.

Hoffmann, R., Dimitrova, A., Muttarak, R., Crespo Cuaresma, J., and Peisker, J. (2020). A meta-analysis of country-level studies on environmental change and migration. *Nature Climate Change*, 10(10):904–912. Number: 10 Publisher: Nature Publishing Group.

Hoffmann, R., Wiederkehr, C., Dimitrova, A., and Hermans, K. (2022). Agricultural livelihoods, adaptation, and environmental migration in sub-Saharan drylands: a meta-analytical review. *Environmental Research Letters*, 17(8):083003. Publisher: IOP Publishing.

Hoffmann, R., Šedová, B., and Vinke, K. (2021). Improving the evidence base: A methodological review of the quantitative climate migration literature. *Global Environmental Change*, 71:102367.

Hsu, J. S., Powell, J., and Adler, P. B. (2012). Sensitivity of mean annual primary production to precipitation. *Global Change Biology*, 18(7):2246–2255. _eprint: https://onlinelibrary.wiley.com/doi/pdf/10.1111/j.1365-2486.2012.02687.x.

Huang, J., Li, Y., Fu, C., Chen, F., Fu, Q., Dai, A., Shinoda, M., Ma, Z., Guo, W., Li, Z., Zhang, L., Liu, Y., Yu, H., He, Y., Xie, Y., Guan, X., Ji, M., Lin, L., Wang, S., Yan, H., and Wang, G. (2017). Dryland climate change: Recent progress and challenges. *Reviews of Geophysics*, 55(3):719–778. _eprint: https://onlinelibrary.wiley.com/doi/pdf/10.1002/2016RG000550.

Huang, S., Tang, L., Hupy, J. P., Wang, Y., and Shao, G. (2021). A commentary review on the use of normalized difference vegetation index (NDVI) in the era of popular remote sensing. *Journal of Forestry Research*, 32(1):1–6.

IDMC (2023a). Country Profile: Somalia.

IDMC (2023b). Global Report on Internal Displacement 2023. Technical report.

Imran, M., Ofli, F., Caragea, D., and Torralba, A. (2020). Using AI and Social Media Multimodal Content for Disaster Response and Management: Opportunities, Challenges, and Future Directions. *Information Processing & Management*, 57(5):102261.

Issa, R., Daalen, K. R. v., Faddoul, A., Collias, L., James, R., Chaudhry, U. A. R., Graef, V., Sullivan, A., Erasmus, P., Chesters, H., and Kelman, I. (2023a). Human migration on a heating planet: A scoping review. *PLOS Climate*, 2(5):e0000214. Publisher: Public Library of Science.

Issa, R., Sarsour, A., Cullip, T., Toma, S., Ruyssen, I., and Scheerens, C. (2023b). Gaps and opportunities in the climate change, migration and health nexus: Insights from a questionnaire based study of practitioners and researchers. *Journal of Migration and Health*, 7:100171.

Jiang, R., Xie, J., He, H., Kuo, C.-C., Zhu, J., and Yang, M. (2016). Spatiotemporal variability and predictability of Normalized Difference Vegetation Index (NDVI) in Alberta, Canada. *International Journal of Biometeorology*, 60(9):1389–1403.

Kabir, M. E., Serrao-Neumann, S., Davey, P., Hossain, M., and Alam, M. T. (2018). Drivers and temporality of internal migration in the context of slow-onset natural hazards: Insights from north-west rural Bangladesh. *International Journal of Disaster Risk Reduction*, 31:617–626.

Kaczan, D. J. and Orgill-Meyer, J. (2020). The impact of climate change on migration: a synthesis of recent empirical insights. *Climatic Change*, 158(3):281–300.

Kalisa, W., Igbawua, T., Henchiri, M., Ali, S., Zhang, S., Bai, Y., and Zhang, J. (2019). Assessment of climate impact on vegetation dynamics over East Africa from 1982 to 2015. *Scientific Reports*, 9(1):16865. Number: 1 Publisher: Nature Publishing Group.

Kelley, C. P., Mohtadi, S., Cane, M. A., Seager, R., and Kushnir, Y. (2015). Climate change in the Fertile Crescent and implications of the recent Syrian drought. *Proceedings of the National Academy of Sciences*, 112(11):3241–3246. Publisher: National Academy of Sciences Section: Physical Sciences.

Khalid, A., Babry, J. A., Vearey, J., and Zenner, D. (2023). Turning up the heat: A conceptual model for understanding the migration and health in the context of global climate change. *Journal of Migration and Health*, 7:100172.

Konings, A. G. and Gentine, P. (2017). Global variations in ecosystem-scale isohydricity. *Global Change Biology*, 23(2):891–905. _eprint: https://onlinelibrary.wiley.com/doi/pdf/10.1111/gcb.13389.

Konings, A. G., Williams, A. P., and Gentine, P. (2017). Sensitivity of grassland productivity to aridity controlled by stomatal and xylem regulation. *Nature Geoscience*, 10(4):284–288. Number: 4 Publisher: Nature Publishing Group.

Kreibich, H., Van Loon, A. F., Schröter, K., Ward, P. J., Mazzoleni, M., Sairam, N., Abeshu, G. W., Agafonova, S., AghaKouchak, A., Aksoy, H., Alvarez-Garreton, C., Aznar, B., Balkhi, L., Barendrecht, M. H., Biancamaria, S., Bos-Burgering, L., Bradley, C., Budiyono, Y., Buytaert, W., Capewell, L., Carlson, H., Cavus, Y., Couasnon, A., Coxon, G., Daliakopoulos, I., de Ruiter, M. C., Delus, C., Erfurt, M., Esposito, G., François, D., Frappart, F., Freer, J., Frolova, N., Gain, A. K., Grillakis, M., Grima, J. O., Guzmán, D. A., Huning, L. S., Ionita, M., Kharlamov, M., Khoi, D. N., Kieboom, N., Kireeva, M., Koutroulis, A., Lavado-Casimiro, W., Li, H.-Y., LLasat, M. C., Macdonald, D., Mård, J., Mathew-Richards, H., McKenzie, A., Mejia, A., Mendiondo, E. M., Mens, M., Mobini, S., Mohor, G. S., Nagavciuc, V., Ngo-Duc, T., Thao Nguyen Huynh, T., Nhi, P. T. T., Petrucci, O., Nguyen, H. Q., Quintana-Seguí, P., Razavi, S., Ridolfi, E., Riegel, J., Sadik, M. S., Savelli, E., Sazonov, A., Sharma, S., Sörensen, J., Arguello Souza, F. A., Stahl, K., Steinhausen, M., Stoelzle, M., Szalińska, W., Tang, Q., Tian, F., Tokarczyk, T., Tovar, C., Tran, T. V. T., Van Huijgevoort, M. H. J., van Vliet, M. T. H., Vorogushyn, S., Wagener, T., Wang, Y., Wendt, D. E., Wickham, E., Yang, L., Zambrano-Bigiarini, M., Blöschl, G., and Di Baldassarre, G. (2022). The challenge of unprecedented floods and droughts in risk management. *Nature*, 608(7921):80–86. Number: 7921 Publisher: Nature Publishing Group.

Krich, C., Runge, J., Miralles, D. G., Migliavacca, M., Perez-Priego, O., El-Madany, T., Carrara, A., and Mahecha, M. D. (2019). Causal networks of biosphere-atmosphere interactions. *EGU Biogeosciences*.

Kruczkiewicz, A., Klopp, J., Fisher, J., Mason, S., McClain, S., Sheekh, N. M., Moss, R., Parks, R. M., and Braneon, C. (2021). Compound risks and complex emergencies require new approaches to preparedness. *Proceedings of the National Academy of Sciences*, 118(19):e2106795118. Publisher: Proceedings of the National Academy of Sciences.

Lee, R., White, C. J., Adnan, M. S. G., Douglas, J., Mahecha, M. D., O'Loughlin, F. E., Patelli, E., Ramos, A. M., Roberts, M. J., Martius, O., Tubaldi, E., van den Hurk, B., Ward, P. J., and Zscheischler, J. (2024). Reclassifying historical disasters: From single to multi-hazards. *Science of The Total Environment*, 912:169120.

Lentz, E. C. and Maxwell, D. (2022). How do information problems constrain anticipating, mitigating, and responding to crises? *International Journal of Disaster Risk Reduction*, 81:103242.

Leonard, M., Westra, S., Phatak, A., Lambert, M., van den Hurk, B., McInnes, K., Risbey, J., Schuster, S., Jakob, D., and Stafford-Smith, M. (2014). A compound event framework for understanding extreme impacts. *WIREs Climate Change*, 5(1):113–128. _eprint: https://onlinelibrary.wiley.com/doi/pdf/10.1002/wcc.252.

Li, W., Pacheco-Labrador, J., Migliavacca, M., Miralles, D., Hoek van Dijke, A., Reichstein, M., Forkel, M., Zhang, W., Frankenberg, C., Panwar, A., Zhang, Q., Weber, U., Gentine, P., and Orth, R. (2023a). Widespread and complex drought effects on vegetation physiology inferred from space. *Nature Communications*, 14(1):4640. Number: 1 Publisher: Nature Publishing Group.

Li, X., Piao, S., Huntingford, C., Peñuelas, J., Yang, H., Xu, H., Chen, A., Friedlingstein, P., Keenan, T. F., Sitch, S., Wang, X., Zscheischler, J., and Mahecha, M. D. (2023b).

Global variations in critical drought thresholds that impact vegetation. *National Science Review*, 10(5):nwad049.

Lindley, A. (2010). The Early Morning Phonecall: Somali Refugees' Remittances. In *The Early Morning Phonecall*. Berghahn Books.

Lindley, A. (2011). Between a Protracted and a Crisis Situation: Policy Responses to Somali Refugees in Kenya. *Refugee Survey Quarterly*, 30(4):14–49.

Lindley, A. (2014). Questioning 'drought displacement': environment, politics and migration in Somalia. page 5.

Lwanga-Ntale, C. and Owino, B. O. (2020). Understanding vulnerability and resilience in Somalia. *Jàmbá : Journal of Disaster Risk Studies*, 12(1):856.

Lyon, B. and Vigaud, N. (2017). Unraveling East Africa's Climate Paradox. In *Climate Extremes*, pages 265–281. American Geophysical Union (AGU). Section: 16 _eprint: https://onlinelibrary.wiley.com/doi/pdf/10.1002/9781119068020.ch16.

Mach, K. J., Adger, W. N., Buhaug, H., Burke, M., Fearon, J. D., Field, C. B., Hendrix, C. S., Kraan, C. M., Maystadt, J.-F., O'Loughlin, J., Roessler, P., Scheffran, J., Schultz, K. A., and von Uexkull, N. (2020). Directions for Research on Climate and Conflict. *Earth's Future*, 8(7):e2020EF001532. _eprint: https://onlinelibrary.wiley.com/doi/pdf/10.1029/2020EF001532.

Mach, K. J., Kraan, C. M., Adger, W. N., Buhaug, H., Burke, M., Fearon, J. D., Field, C. B., Hendrix, C. S., Maystadt, J.-F., O'Loughlin, J., Roessler, P., Scheffran, J., Schultz, K. A., and von Uexkull, N. (2019). Climate as a risk factor for armed conflict. *Nature*, 571(7764):193–197. Number: 7764 Publisher: Nature Publishing Group.

Maestre, F. T., Benito, B. M., Berdugo, M., Concostrina-Zubiri, L., Delgado-Baquerizo, M., Eldridge, D. J., Guirado, E., Gross, N., Kéfi, S., Le Bagousse-Pinguet, Y., Ochoa-Hueso, R., and Soliveres, S. (2021). Biogeography of global drylands. *New Phytologist*, 231(2):540–558. _eprint: https://onlinelibrary.wiley.com/doi/pdf/10.1111/nph.17395.

Mangiarotti, S., Mazzega, P., Hiernaux, P., and Mougin, E. (2010). The vegetation cycle in West Africa from AVHRR–NDVI data: Horizons of predictability versus spatial scales. *Remote Sensing of Environment*, 114(9):2036–2047.

Mangiarotti, S., Mazzega, P., Hiernaux, P., and Mougin, E. (2012). Predictability of vegetation cycles over the semi-arid region of Gourma (Mali) from forecasts of AVHRR-NDVI signals. *Remote Sensing of Environment*, 123:246–257.

Maretti, M., Tontodimamma, A., and Biermann, P. (2019). Environmental and climate migrations: an overview of scientific literature using a bibliometric analysis. *International Review of Sociology*, 29(2):142–158. Publisher: Routledge _eprint: https://doi.org/10.1080/03906701.2019.1641270.

Martiny, N., Philippon, N., Richard, Y., Camberlin, P., and Reason, C. (2010). Predictability of NDVI in semi-arid African regions. *Theoretical and Applied Climatology*, 100(3):467–484.

Martínez-Zarzoso, I., Nowak-Lehmann, F., and Paschoaleto, R. D. L. (2023). Climate change, natural disasters, and international migration: A country-level analysis considering climatic zones. *Frontiers in Climate*, 4.

Mastrorillo, M., Licker, R., Bohra-Mishra, P., Fagiolo, G., D. Estes, L., and Oppenheimer, M. (2016). The influence of climate variability on internal migration flows in South Africa. *Global Environmental Change*, 39:155–169.

Maurer, G. E., Hallmark, A. J., Brown, R. F., Sala, O. E., and Collins, S. L. (2020). Sensitivity of primary production to precipitation across the United States. *Ecology Letters*, 23(3):527–536. _eprint: https://onlinelibrary.wiley.com/doi/pdf/10.1111/ele.13455.

Maxwell, D. and Fitzpatrick, M. (2012). The 2011 Somalia famine: Context, causes, and complications. *Global Food Security*, 1(1):5–12.

Maystadt, J.-F. and Ecker, O. (2014). Extreme Weather and Civil War: Does Drought Fuel Conflict in Somalia through Livestock Price Shocks? *American Journal of Agricultural Economics*, 96(4):1157–1182. _eprint: https://onlinelibrary.wiley.com/doi/pdf/10.1093/ajae/aau010.

McCreadie, R. and Buntain, C. (2023). CrisisFACTS: Buidling and Evaluating Crisis Timelines.

McGowan, J. A., Deyle, E. R., Ye, H., Carter, M. L., Perretti, C. T., Seger, K. D., Verneil, A. d., and Sugihara, G. (2017). Predicting coastal algal blooms in southern California. *Ecology*, 98(5):1419–1433.

McNally, A., Arsenault, K., Kumar, S., Shukla, S., Peterson, P., Wang, S., Funk, C., Peters-Lidard, C. D., and Verdin, J. P. (2017). A land data assimilation system for sub-Saharan Africa food and water security applications. *Scientific Data*, 4(1):170012. Number: 1 Publisher: Nature Publishing Group.

Measho, S., Chen, B., Trisurat, Y., Pellikka, P., Guo, L., Arunyawat, S., Tuankrua, V., Ogbazghi, W., and Yemane, T. (2019). Spatio-Temporal Analysis of Vegetation Dynamics as a Response to Climate Variability and Drought Patterns in the Semiarid Region, Eritrea. *Remote Sensing*, 11(6):724.

Mechiche-Alami, A. and Abdi, A. M. (2020). Agricultural productivity in relation to climate and cropland management in West Africa. *Scientific Reports*, 10(1):3393. Number: 1 Publisher: Nature Publishing Group.

Menkhaus, K. (2014). State Failure, State-Building, and Prospects for a "Functional Failed State" in Somalia. *The ANNALS of the American Academy of Political and Social Science*, 656(1):154–172. Publisher: SAGE Publications Inc.

Mishra, R. K. and Saini, K. (2014). Automatic detection of interlinked events for better disaster management. In *2014 IEEE International Advance Computing Conference (IACC)*, pages 595–600.

Mohamed, J. and Adam, M. B. (2022). Modeling of magnitude and frequency of extreme rainfall in Somalia. *Modeling Earth Systems and Environment*, 8(3):4277–4294.

Moitra, A., Wagenaar, D., Kalirai, M., Ahmed, S. I., and Soden, R. (2022). AI and Disaster Risk: A Practitioner Perspective. *Proceedings of the ACM on Human-Computer Interaction*, 6(CSCW2):1–20.

Morrissey, J. (2014). Environmental Change and Human Migration in Sub-Saharan Africa. In Piguet, E. and Laczko, F., editors, *People on the Move in a Changing Climate: The Regional Impact of Environmental Change on Migration*, Global Migration Issues, pages 81–109. Springer Netherlands, Dordrecht.

Mueller, V., Gray, C., and Kosec, K. (2014). Heat stress increases long-term human migration in rural Pakistan. *Nature Climate Change*, 4(3):182–185. Number: 3 Publisher: Nature Publishing Group.

Mukherjee, S. and Mishra, A. K. (2021). Increase in Compound Drought and Heatwaves in a Warming World. *Geophysical Research Letters*, 48(1):e2020GL090617. _eprint: https://onlinelibrary.wiley.com/doi/pdf/10.1029/2020GL090617.

Munawar, H. S., Mojtahedi, M., Hammad, A. W. A., Kouzani, A., and Mahmud, M. A. P. (2022). Disruptive technologies as a solution for disaster risk management: A review. *Science of The Total Environment*, 806:151351.

Munch, S. B., Brias, A., Sugihara, G., and Rogers, T. L. (2020). Frequently asked questions about nonlinear dynamics and empirical dynamic modelling. *ICES Journal of Marine Science*, 77(4):1463–1479.

Munch, S. B., Rogers, T. L., and Sugihara, G. (2023). Recent developments in empirical dynamic modelling. *Methods in Ecology and Evolution*, 14(3):732–745. _eprint: https://onlinelibrary.wiley.com/doi/pdf/10.1111/2041-210X.13983.

Nakayama, S.-I., Takasuka, A., Ichinokawa, M., and Okamura, H. (2018). Climate change and interspecific interactions drive species alternations between anchovy and sardine in the western North Pacific: Detection of causality by convergent cross mapping. *Fisheries Oceanography*, 27(4):312–322.

Natsukawa, H. and Koyamada, K. (2017). Visual analytics of brain effective connectivity using convergent cross mapping. In *SIGGRAPH Asia 2017 Symposium on Visualization*, SA '17, pages 1–9, New York, NY, USA. Association for Computing Machinery.

Nawrotzki, R. J. and DeWaard, J. (2018). Putting trapped populations into place: climate change and inter-district migration flows in Zambia. *Regional Environmental Change*, 18(2):533–546.

Nelson, E. L., Khan, S. A., Thorve, S., and Greenough, P. G. (2020). Modeling pastoralist movement in response to environmental variables and conflict in Somaliland: Combining agent-based modeling and geospatial data. *PloS One*, 15(12):e0244185.

Neumann, K., Sietz, D., Hilderink, H., Janssen, P., Kok, M., and van Dijk, H. (2015). Environmental drivers of human migration in drylands – A spatial picture. *Applied Geography*, 56:116–126.

Nguyen, T. H. and Rudra, K. (2022). Towards an Interpretable Approach to Classify and Summarize Crisis Events from Microblogs. In *Proceedings of the ACM Web Conference 2022*, pages 3641–3650, Virtual Event, Lyon France. ACM.

Nicholson, S. E., Davenport, M. L., and Malo, A. R. (1990). A comparison of the vegetation response to rainfall in the Sahel and East Africa, using normalized difference vegetation index from NOAA AVHRR. *Climatic Change*, 17(2):209–241.

Nova, N., Deyle, E. R., Shocket, M. S., MacDonald, A. J., Childs, M. L., Rypdal, M., Sugihara, G., and Mordecai, E. A. (2019). Empirical dynamic modeling reveals ecological drivers of dengue dynamics. preprint, Ecology.

Nova, N., Deyle, E. R., Shocket, M. S., MacDonald, A. J., Childs, M. L., Rypdal, M., Sugihara, G., and Mordecai, E. A. (2021). Susceptible host availability modulates climate effects on dengue dynamics. *Ecology Letters*, 24(3):415–425. _eprint: https://onlinelibrary.wiley.com/doi/pdf/10.1111/ele.13652.

Nugent, T., Petroni, F., Raman, N., Carstens, L., and Leidner, J. L. (2017). A comparison of classification models for natural disaster and critical event detection from news. In *2017 IEEE International Conference on Big Data (Big Data)*, pages 3750–3759.

Oakes, R., Van der Geest, K., Schraven, B., Adaawen, S., Ayeb-Karlsson, S., de Sherbinin, A., Etzold, B., Groth, J., Hermanns, K., Lakeman, S., Nawrotzki, R., Rademacher-Schulz, C., Romankiewic, C., Serraglio, D., Sterly, H., Thalheimer, L., Wiederkehr, C., and Williams, D. (2023). A future agenda for research on climate change and human mobility. *International Migration*, n/a(n/a). _eprint: https://onlinelibrary.wiley.com/doi/pdf/10.1111/imig.13169.

OCHA, U. (2023). Somalia: 2023 Deyr Season Floods Situation Report No. 5 (As of 24 December 2023) - Somalia | ReliefWeb.

Ogie, R. I. and Verstaevel, N. (2020). Disaster informatics: An overview. *Progress in Disaster Science*, 7:100111.

Oh, W. S., Muneepeerakul, R., Rubenstein, D., and Levin, S. (2024). Emergent network patterns of internal displacement in Somalia driven by natural disasters and conflicts. *Global Environmental Change*, 84:102793.

Olson, J. M., Alagarswamy, G., Andresen, J. A., Campbell, D. J., Davis, A. Y., Ge, J., Huebner, M., Lofgren, B. M., Lusch, D. P., Moore, N. J., Pijanowski, B. C., Qi, J., Thornton, P. K., Torbick, N. M., and Wang, J. (2008). Integrating diverse methods to understand climate–land interactions in East Africa. *Geoforum*, 39(2):898–911.

Ombadi, M., Nguyen, P., Sorooshian, S., and Hsu, K.-l. (2020). Evaluation of Methods for Causal Discovery in Hydrometeorological Systems. *Water Resources Research*, 56(7):e2020WR027251. _eprint: https://agupubs.onlinelibrary.wiley.com/doi/pdf/10.1029/2020WR027251.

Osman, A. A. and Abebe, G. K. (2023). Rural Displacement and Its Implications on Livelihoods and Food Insecurity: The Case of Inter-Riverine Communities in Somalia. *Agriculture*, 13(7):1444. Number: 7 Publisher: Multidisciplinary Digital Publishing Institute.

Osman, S. A. and Das, J. (2023). GIS-based flood risk assessment using multi-criteria decision analysis of Shebelle River Basin in southern Somalia. *SN Applied Sciences*, 5(5):134.

Owain, E. L. and Maslin, M. A. (2018). Assessing the relative contribution of economic, political and environmental factors on past conflict and the displacement of people in East Africa. *Palgrave Communications*, 4(1):1–9. Number: 1 Publisher: Palgrave.

Padhee, S., Saha, T. K., Tetreault, J., and Jaimes, A. (2020). Clustering of Social Media Messages for Humanitarian Aid Response during Crisis. arXiv:2007.11756 [cs].

Palmer, P. I., Wainwright, C. M., Dong, B., Maidment, R. I., Wheeler, K. G., Gedney, N., Hickman, J. E., Madani, N., Folwell, S. S., Abdo, G., Allan, R. P., Black, E. C. L., Feng, L., Gudoshava, M., Haines, K., Huntingford, C., Kilavi, M., Lunt, M. F., Shaaban, A., and Turner, A. G. (2023). Drivers and impacts of Eastern African rainfall variability. *Nature Reviews Earth & Environment*, pages 1–17. Publisher: Nature Publishing Group.

Papagiannopoulou, C., Gonzalez Miralles, D., Decubber, S., Demuzere, M., Verhoest, N., Dorigo, W. A., and Waegeman, W. (2017). A non-linear Granger-causality framework to investigate climate-vegetation dynamics. *GEOSCIENTIFIC MODEL DEVELOPMENT*, 10(5):1945–1960.

Pape, U. J. and Wollburg, P. R. (2019). Impact of Drought on Poverty in Somalia.

Pereira, J., Fidalgo, R., Lotufo, R., and Nogueira, R. (2023). *Crisis Event Social Media Summarization with GPT-3 and Neural Reranking.*

Petchey, O. (2016). Simplex projection walkthrough.

Petroni, F., Raman, N., Nugent, T., Nourbakhsh, A., Panić, , Shah, S., and Leidner, J. L. (2018). An Extensible Event Extraction System With Cross-Media Event Resolution. In *Proceedings of the 24th ACM SIGKDD International Conference on Knowledge Discovery & Data Mining*, KDD '18, pages 626–635, New York, NY, USA. Association for Computing Machinery.

Pfeifer, M., Platts, P. J., Burgess, N. D., Swetnam, R. D., Willcock, S., Lewis, S. L., and Marchant, R. (2013). Land use change and carbon fluxes in East Africa quantified using earth observation data and field measurements. *Environmental Conservation*, 40(3):241–252. Publisher: Cambridge University Press.

Pham, K. H. and Luengo-Oroz, M. (2022). Predictive modeling of movements of refugees and internally displaced people: Towards a computational framework. *arXiv:2201.08006 [cs]*. arXiv: 2201.08006.

Piguet, E. (2022). Linking climate change, environmental degradation, and migration: An update after 10 years. *WIREs Climate Change*, 13(1):e746. _eprint: https://onlinelibrary.wiley.com/doi/pdf/10.1002/wcc.746.

Pirani, E., Marino, M. F., and Petrucci, A. (2019). Correlates of Inter-Districts Migrations in Tanzania. A Gravity-Type Modeling Approach. *Statistica*, 79(2):201–221. Number: 2.

Pita Costa, J., Rei, L., Bezak, N., Mikoš, M., Massri, M. B., Novalija, I., and Leban, G. (2024). Towards improved knowledge about water-related extremes based on news media information captured using artificial intelligence. *International Journal of Disaster Risk Reduction*, 100:104172.

Pricope, N. G., Husak, G., Lopez-Carr, D., Funk, C., and Michaelsen, J. (2013). The climate-population nexus in the East African Horn: Emerging degradation trends in rangeland and pastoral livelihood zones. *Global Environmental Change*, 23(6):1525–1541.

Pringle, M. (2013). Robust prediction of time-integrated NDVI. *International Journal of Remote Sensing*, 34(13):4791–4811. Publisher: Taylor & Francis _eprint: https://doi.org/10.1080/01431161.2013.782117.

Prăvălie, R. (2016). Drylands extent and environmental issues. A global approach. *Earth-Science Reviews*, 161:259–278.

Pérez-Suay, A. and Camps-Valls, G. (2019). Causal Inference in Geoscience and Remote Sensing From Observational Data. *IEEE Transactions on Geoscience and Remote Sensing*, 57(3):1502–1513.

Raleigh, C. and Kniveton, D. (2012). Come rain or shine: An analysis of conflict and climate variability in East Africa. *Journal of Peace Research*, 49(1):51–64. Publisher: SAGE Publications Ltd.

Raleigh, C., Linke, r., Hegre, H., and Karlsen, J. (2010). Introducing ACLED: An Armed Conflict Location and Event Dataset. *Journal of Peace Research*, 47(5):651–660. Publisher: SAGE Publications Ltd.

Raymond, C., Horton, R. M., Zscheischler, J., Martius, O., AghaKouchak, A., Balch, J., Bowen, S. G., Camargo, S. J., Hess, J., Kornhuber, K., Oppenheimer, M., Ruane, A. C., Wahl, T., and White, K. (2020). Understanding and managing connected extreme events. *Nature Climate Change*, 10(7):611–621. Number: 7 Publisher: Nature Publishing Group.

Rezvani, R., RahimiMovaghar, M., Na, W., and Najafi, M. R. (2023). Accelerated lagged compound floods and droughts in northwest North America under 1.5 °C 4 °C global warming levels. *Journal of Hydrology*, 624:129906.

Rigaud, K. K., de Sherbinin, A., Jones, B., Bergmann, J., Clement, V., Ober, K., Schewe, J., Adamo, S., McCusker, B., Heuser, S., and Midgley, A. (2018). Groundswell: Preparing for Internal Climate Migration. Publisher: World Bank, Washington, DC.

Rishmawi, K., Prince, S. D., and Xue, Y. (2016). Vegetation Responses to Climate Variability in the Northern Arid to Sub-Humid Zones of Sub-Saharan Africa. *Remote Sensing*, 8(11):910. Number: 11 Publisher: Multidisciplinary Digital Publishing Institute.

Rocca, R., Tamagnone, N., Fekih, S., Contla, X., and Rekabsaz, N. (2023). Natural language processing for humanitarian action: Opportunities, challenges, and the path toward humanitarian NLP. *Frontiers in Big Data*, 6.

Ronco, M., Tárraga, J. M., Muñoz, J., Piles, M., Marco, E. S., Wang, Q., Espinosa, M. T. M., Ponserre, S., and Camps-Valls, G. (2023). Exploring interactions between socioeconomic context and natural hazards on human population displacement. *Nature Communications*, 14(1):8004. Number: 1 Publisher: Nature Publishing Group.

Rudra, K., Goyal, P., Ganguly, N., Mitra, P., and Imran, M. (2018). Identifying Subevents and Summarizing Disaster-Related Information from Microblogs. In *The 41st International ACM SIGIR Conference on Research & Development in Information Retrieval*, pages 265–274, Ann Arbor MI USA. ACM.

Runge, J., Bathiany, S., Bollt, E., Camps-Valls, G., Coumou, D., Deyle, E., Glymour, C., Kretschmer, M., Mahecha, M. D., Muñoz-Marí, J., Nes, E. H. v., Peters, J., Quax, R., Reichstein, M., Scheffer, M., Schölkopf, B., Spirtes, P., Sugihara, G., Sun, J., Zhang, K., and Zscheischler, J. (2019a). Inferring causation from time series in Earth system sciences. *Nature Communications*, 10(1):2553.

Runge, J., Nowack, P., Kretschmer, M., Flaxman, S., and Sejdinovic, D. (2019b). Detecting and quantifying causal associations in large nonlinear time series datasets. *Science Advances*, 5(11):eaau4996. Publisher: American Association for the Advancement of Science Section: Research Article.

Sakahira, F. and Hiroi, U. (2021). Designing cascading disaster networks by means of natural language processing. *International Journal of Disaster Risk Reduction*, 66:102623.

Sakdapolrak, P., Sterly, H., Borderon, M., Bunchuay-Peth, S., Naruchaikusol, S., Ober, K., Porst, L., and Rockenbauch, T. (2024). Translocal social resilience dimensions of migration as adaptation to environmental change. *Proceedings of the National Academy of Sciences*, 121(3):e2206185120. Publisher: Proceedings of the National Academy of Sciences.

Saldarriaga, J. F. and Hua, Y. (2019). A gravity model analysis of forced displacement in Colombia. *Cities*, 95:102407.

Sasaki, T., Collins, S. L., Rudgers, J. A., Batdelger, G., Baasandai, E., and Kinugasa, T. (2023). Dryland sensitivity to climate change and variability using nonlinear dynamics. *Proceedings of the National Academy of Sciences*, 120(35):e2305050120. Publisher: Proceedings of the National Academy of Sciences.

Scheffer, M., Bascompte, J., Brock, W. A., Brovkin, V., Carpenter, S. R., Dakos, V., Held, H., van Nes, E. H., Rietkerk, M., and Sugihara, G. (2009). Early-warning signals for critical transitions. *Nature*, 461(7260):53–59.

Schewel, K., Dickerson, S., Madson, B., and Nagle Alverio, G. (2024). How well can we predict climate migration? A review of forecasting models. *Frontiers in Climate*, 5.

Schiavina, M., Melchiorri, M., Pesaresi, M., Politis, P., Carneiro, F. S. M., Maffenini, L., Florio, P., Ehrlich, D., Goch, K., Carioli, A., Uhl, J., Tommasi, P., and Kemper, T. (2023). GHSL Data Package 2023. ISBN: 9789268023419.

Schiecke, K., Pester, B., Feucht, M., Leistritz, L., and Witte, H. (2015). Convergent Cross Mapping: Basic concept, influence of estimation parameters and practical application. In *2015 37th Annual International Conference of the IEEE Engineering in Medicine and Biology Society (EMBC)*, pages 7418–7421. ISSN: 1558-4615.

Schumacher, D. L., Keune, J., Dirmeyer, P., and Miralles, D. G. (2022). Drought self-propagation in drylands due to land–atmosphere feedbacks. *Nature Geoscience*, 15(4):262–268. Number: 4 Publisher: Nature Publishing Group.

Seal, A. and Bailey, R. (2013). The 2011 Famine in Somalia: lessons learnt from a failed response? *Conflict and Health*, 7(1):22.

Shi, H., Zhao, Y., Liu, S., Cai, H., and Zhou, Z. (2022). A New Perspective on Drought Propagation: Causality. *Geophysical Research Letters*, 49(2):e2021GL096758. _eprint: https://onlinelibrary.wiley.com/doi/pdf/10.1029/2021GL096758.

Sohoulande Djebou, D. C., Singh, V. P., and Frauenfeld, O. W. (2015). Vegetation response to precipitation across the aridity gradient of the southwestern United states. *Journal of Arid Environments*, 115:35–43.

Song, D., Vold, A., Madan, K., and Schilder, F. (2022). Multi-label legal document classification: A deep learning-based approach with label-attention and domain-specific pre-training. *Information Systems*, 106:101718.

Sugihara, G., May, R., Ye, H., Hsieh, C.-h., Deyle, E., Fogarty, M., and Munch, S. (2012). Detecting Causality in Complex Ecosystems. *Science*, 338(6106):496–500.

Sugihara, G. and May, R. M. (1990). Nonlinear forecasting as a way of distinguishing chaos from measurement error in time series. *Nature*, 344(6268):734.

Swets, D., Reed, B. C., Rowland, J., and Marko, S. E. (1999). A weighted least-squares approach to temporal NDVI smoothing.

Tadesse, T., Demisse, G. B., Zaitchik, B., and Dinku, T. (2014). Satellite-based hybrid drought monitoring tool for prediction of vegetation condition in Eastern Africa: A case study for Ethiopia. *Water Resources Research*, 50(3):2176–2190. _eprint: https://onlinelibrary.wiley.com/doi/pdf/10.1002/2013WR014281.

Takens, F. (1981). Detecting strange attractors in turbulence. In *Dynamical Systems and Turbulence, Warwick 1980*, volume 898, pages 366–381. Springer Berlin Heidelberg, Berlin, Heidelberg.

Tamagnone, N., Fekih, S., Contla, X., Orozco, N., and Rekabsaz, N. (2023). Leveraging Domain Knowledge for Inclusive and Bias-aware Humanitarian Response Entry Classification. arXiv:2305.16756 [cs].

Thalheimer, L., Gaupp, F., and Webersik, C. (2021a). Compound vulnerabilities exacerbate systemic risks of food security in Somalia. preprint, In Review.

Thalheimer, L., Gaupp, F., and Webersik, C. (2023a). Systemic risk and compound vulnerability impact pathways of food insecurity in Somalia. *Climate Risk Management*, 42:100570.

Thalheimer, L. and Oh, W. S. (2023). An inventory tool to assess displacement data in the context of weather and climate-related events. *Climate Risk Management*, 40:100509.

Thalheimer, L., Schwarz, M. P., and Pretis, F. (2023b). Large weather and conflict effects on internal displacement in Somalia with little evidence of feedback onto conflict. *Global Environmental Change*, 79:102641.

Thalheimer, L., Williams, D. S., van der Geest, K., and Otto, F. E. L. (2021b). Advancing the Evidence Base of Future Warming Impacts on Human Mobility in African Drylands. *Earth's Future*, 9(10):e2020EF001958. _eprint: https://onlinelibrary.wiley.com/doi/pdf/10.1029/2020EF001958.

Thoma, D. P., Munson, S. M., Irvine, K. M., Witwicki, D. L., and Bunting, E. L. (2016). Semi-arid vegetation response to antecedent climate and water balance windows. *Applied Vegetation Science*, 19(3):413–429.

Thomas, V. and López, R. (2015). Global Increase in Climate-Related Disasters.

Tian, S., Van Dijk, A. I. J. M., Tregoning, P., and Renzullo, L. J. (2019). Forecasting dryland vegetation condition months in advance through satellite data assimilation. *Nature Communications*, 10(1):469. Number: 1 Publisher: Nature Publishing Group.

Tietjen, B., Jeltsch, F., Zehe, E., Classen, N., Groengroeft, A., Schiffers, K., and Oldeland, J. (2010). Effects of climate change on the coupled dynamics of water and vegetation in drylands. *Ecohydrology*, 3(2):226–237. _eprint: https://onlinelibrary.wiley.com/doi/pdf/10.1002/eco.70.

Tounsi, A. and Temimi, M. (2023). A systematic review of natural language processing applications for hydrometeorological hazards assessment. *Natural Hazards*, 116(3):2819–2870.

Trabucco, A. and Zomer, R. J. (2019). Global Aridity Index and Potential Evapo-Transpiration (ET0) Climate Database v2.

Tripathy, K. P., Mukherjee, S., Mishra, A. K., Mann, M. E., and Williams, A. P. (2023). Climate change will accelerate the high-end risk of compound drought and heatwave events. *Proceedings of the National Academy of Sciences*, 120(28):e2219825120. Publisher: Proceedings of the National Academy of Sciences.

Tuholske, C., Di Landro, M. A., Anderson, W., van Duijne, R. J., and de Sherbinin, A. (2024). A framework to link climate change, food security, and migration: unpacking the agricultural pathway. *Population and Environment*, 46(1):8.

Tuttle, S. and Salvucci, G. (2016). Empirical evidence of contrasting soil moisture–precipitation feedbacks across the United States. *Science*, 352(6287):825–828.

Tuttle, S. E. and Salvucci, G. D. (2017). Confounding factors in determining causal soil moisture-precipitation feedback. *Water Resources Research*, 53(7):5531–5544.

UNDRR (2016). Report of the open-ended intergovernmental expert working group on indicators and terminology relating to disaster risk reduction.

UNHCR (2022). Global Trends Report 2022. Technical report.

UNHCR, S. (2017). Protection & Return Monitoring Network (PRMN)-Notes on methodology. pages 626–634.

van den Hurk, B. J., White, C. J., Ramos, A. M., Ward, P. J., Martius, O., Olbert, I., Roscoe, K., Goulart, H. M., and Zscheischler, J. (2023). Consideration of compound drivers and impacts in the disaster risk reduction cycle. *iScience*, 26(3):106030.

van Nes, E. H., Scheffer, M., Brovkin, V., Lenton, T. M., Ye, H., Deyle, E., and Sugihara, G. (2015). Causal feedbacks in climate change. *Nature Climate Change*, 5(5):445–448.

Velev, D. and Zlateva, P. (2023). CHALLENGES OF ARTIFICIAL INTELLIGENCE APPLICATION FOR DISASTER RISK MANAGEMENT. *The International Archives of the Photogrammetry, Remote Sensing and Spatial Information Sciences*, XLVIII-M-1-2023:387–394. Conference Name: 39th International Symposium on Remote Sensing of Environment (ISRSE-39) "From Human needs to SDGs" - 24–28 April 2023, Antalya, Türkiye Publisher: Copernicus GmbH.

Verma, S., Vieweg, S., Corvey, W., Palen, L., Martin, J., Palmer, M., Schram, A., and Anderson, K. (2021). Natural Language Processing to the Rescue? Extracting "Situational Awareness" Tweets During Mass Emergency. *Proceedings of the International AAAI Conference on Web and Social Media*, 5(1):385–392.

Vermiglio, C., Noto, G., Rodríguez, B. M. P., and Zarone, V. (2021). Disaster management and emerging technologies: a performance-based perspective. *Meditari Accountancy Research*, 30(4):1093–1117. Publisher: Emerald Publishing Limited.

Vesco, P., Kovacic, M., Mistry, M., and Croicu, M. (2021). Climate variability, crop and conflict: Exploring the impacts of spatial concentration in agricultural production. *Journal of Peace Research*, 58(1):98–113. Publisher: SAGE Publications Ltd.

Wakabi, W. (2009). Fighting and drought worsen Somalia's humanitarian crisis. *The Lancet*, 374(9695):1051–1052. Publisher: Elsevier.

Walker, D. P., Marsham, J. H., Birch, C. E., Scaife, A. A., and Finney, D. L. (2020). Common Mechanism for Interannual and Decadal Variability in the East African Long Rains. *Geophysical Research Letters*, 47(22):e2020GL089182. _eprint: https://onlinelibrary.wiley.com/doi/pdf/10.1029/2020GL089182.

Walsh, R. P. D. and Lawler, D. M. (1981). Rainfall Seasonality: Description, Spatial Patterns and Change Through Time. *Weather*, 36(7):201–208. _eprint: https://onlinelibrary.wiley.com/doi/pdf/10.1002/j.1477-8696.1981.tb05400.x.

Wan, Z. (2014). New refinements and validation of the collection-6 MODIS land-surface temperature/emissivity product. *Remote Sensing of Environment*, 140:36–45.

Wang, C., Li, Z., Chen, Y., Ouyang, L., Li, Y., Sun, F., Liu, Y., and Zhu, J. (2023). Drought-heatwave compound events are stronger in drylands. *Weather and Climate Extremes*, page 100632.

Wang, Y., Yang, J., Chen, Y., Maeyer, P. D., Li, Z., and Duan, W. (2018). Detecting the Causal Effect of Soil Moisture on Precipitation Using Convergent Cross Mapping. *Scientific Reports*, 8(1):1–8.

Warner, K., Hamza, M., Oliver-Smith, A., Renaud, F., and Julca, A. (2010). Climate change, environmental degradation and migration. *Natural Hazards*, 55(3):689–715.

Warsame, A., Frison, S., and Checchi, F. (2023). Drought, armed conflict and population mortality in Somalia, 2014–2018: A statistical analysis. *PLOS Global Public Health*, 3(4):e0001136. Publisher: Public Library of Science.

Warsame, A. A., Sheik-Ali, I. A., Ali, A. O., and Sarkodie, S. A. (2021). Climate change and crop production nexus in Somalia: an empirical evidence from ARDL technique. *Environmental Science and Pollution Research*, 28(16):19838–19850.

Warsame, A. A., Sheik-Ali, I. A., Hassan, A. A., and Sarkodie, S. A. (2022). Extreme climatic effects hamper livestock production in Somalia. *Environmental Science and Pollution Research*, 29(27):40755–40767.

Wei, F., Wang, S., Fu, B., Pan, N., Feng, X., Zhao, W., and Wang, C. (2018). Vegetation dynamic trends and the main drivers detected using the ensemble empirical mode decomposition method in East Africa. *Land Degradation & Development*, 29(8):2542–2553. _eprint: https://onlinelibrary.wiley.com/doi/pdf/10.1002/ldr.3017.

White, R. W. (2023). Advancing the Search Frontier with AI Agents.

Willett, J. and Sears, J. (2018). Complicating our understanding of environmental migration and displacement: The case of drought-related human movement in Kenya. *International Social Work*, page 0020872818799431.

Wu, D., Zhao, X., Liang, S., Zhou, T., Huang, K., Tang, B., and Zhao, W. (2015). Time-lag effects of global vegetation responses to climate change. *Global Change Biology*, 21(9):3520–3531.

Wu, G. and Zhu, J. (2020). Multi-label classification: do Hamming loss and subset accuracy really conflict with each other? In *Advances in Neural Information Processing Systems*, volume 33, pages 3130–3140. Curran Associates, Inc.

Ye, H., Beamish, R. J., Glaser, S. M., Grant, S. C. H., Hsieh, C.-h., Richards, L. J., Schnute, J. T., and Sugihara, G. (2015). Equation-free mechanistic ecosystem forecasting using empirical dynamic modeling. *Proceedings of the National Academy of Sciences*, 112(13):E1569–E1576.

Yela-Bello, J. P., Oglethorpe, E., and Rekabsaz, N. (2021). MultiHumES: Multilingual Humanitarian Dataset for Extractive Summarization. In *Proceedings of the 16th Conference of the European Chapter of the Association for Computational Linguistics: Main Volume*, pages 1713–1717, Online. Association for Computational Linguistics.

Yuen, A., Warsame, A., and Checchi, F. (2022). Exploring the temporal patterns and crisis-related risk factors for population displacement in Somalia (2016-2018). *Journal of Migration and Health*, 5:100095.

Zeng, X. (2001). Global Vegetation Root Distribution for Land Modeling. *Journal of Hydrometeorology*, 2(5):525–530. Publisher: American Meteorological Society Section: Journal of Hydrometeorology.

Zhou, H., Liu, Y., and Liu, Y. (2019). An Approach to Tracking Meteorological Drought Migration. *Water Resources Research*, 55(4):3266–3284.

Zickgraf, C. (2019). Keeping People in Place: Political Factors of (Im)mobility and Climate Change. *Social Sciences*, 8(8):228. Number: 8 Publisher: Multidisciplinary Digital Publishing Institute.

Zickgraf, C. (2021). Climate change, slow onset events and human mobility: reviewing the evidence. *Current Opinion in Environmental Sustainability*, 50:21–30.

Zscheischler, J., Martius, O., Westra, S., Bevacqua, E., Raymond, C., Horton, R. M., van den Hurk, B., AghaKouchak, A., Jézéquel, A., Mahecha, M. D., Maraun, D., Ramos, A. M., Ridder, N. N., Thiery, W., and Vignotto, E. (2020). A typology of compound weather and climate events. *Nature Reviews Earth & Environment*, 1(7):333–347. Number: 7 Publisher: Nature Publishing Group.